UNIVERSITY OF SOUTHERN CALIFORNIA
DEPARTMENT OF CIVIL ENGINEERING

AUTOMATIC DIGITIZATION AND PROCESSING OF ACCELEROGRAMS USING PC

by

Vincent W. Lee and Mihailo D. Trifunac

Report No. 90-03

Los Angeles, California
April, 1990

ABSTRACT

This report presents the current data reduction and analysis procedures on a PC in the routine processing of strong-motion accelerograms. It presents a new generation of computer programs and various hardware and software developments relative to and following our previous report on this subject in 1979 (Trifunac and Lee, 1979).

The first part of this report (Part I) describes the new hardware for automatic digitization of analog traces on a personnal computer. The second part describes the latest version of our software in the procedures used in data processing of the digitized accelerograms.

TABLE OF CONTENTS

PART I:

AUTOMATIC DIGITIZATION USING PC AND SCANNER

Table of Contents (for Part I)

*I*1 The Automatic Digitization System

*I*1.1 Introduction

The need for availability and efficient dissemination of digitized strong motion accelerograph data is recognized by engineers, seismologists, and geologists throughout the world. Analysis and interpretations of this data are found in the works of earthquake engineers concerned with the development of earthquake resistant structural design, of geophysicists and seismologists dealing with the understanding of earthquake source mechanism, and of social scientists and public officials responsible for public safety and disaster response and mitigation.

A study made for the Office of Science and Technology of the Executive Office of the President of the United States concludes that:

> "... effort must be devoted to ... the collection of records after destructive earthquakes, analyzing the motions to derive various engineering characteristics, and making the original data and analyses available shortly after the earthquake. The fundamental aspect of all dynamic research in earthquake engineering is the ground motion to which the structure is subjected in a major earthquake..."

Some twenty years ago, the only digitization process available was the manual, hand digitization (Trifunac and Lee, 1973). Before digitizing, the film record, or its enlargement, had to be placed on the digitizing table with the horizontal axis lined up by eye to an estimated zero axis. Each line was then digitized by placing the crosshair manually on successive points of the trace. The digitizer converted the coordinates to numbers which were directly punched on cards or recorded on tape. A set of computer programs were then used to read and to plot the data to the same scale as that of the original digitized record. This plot was then checked against the digitized record. Any errors found had to be corrected manually. Any portion that was digitized improperly had to be redigitized and rechecked until the final plot agreed well with the digitized record. The raw data was then ready for routine computer processing (Trifunac and Lee, 1973).

*I*1.2 The Original Automatic Digitization System

Digitization of a record by the old manual method and data verification and preparation, took up to several days to complete one record. With the development of image processing techniques in the 60's and 70's, Trifunac and Lee (1979) developed an automatic digitization system for strong-motion accelerograms. Under this system, up to four 10 inch-sections of the accelerogram record could be reproduced on a 10 inch $\times$ 10 inch negative film, which was then put into the drum of the photodensitometar for scanning. A scanning program, 'FILM' available for the NOVA-3 Data General mini-computer, was used to control the densitometer and to store the data read by it onto a disk. A filtering program, 'TRACE', was used to read through the raw data and to locate the coordinates of all the traces found. The user then ran the editing program, 'TV' to read the traces,

display them graphically on the Tektronix terminal, and perform editing and correcting operations on the traces. Finally, the edited traces were plotted on a plotter and written onto a disk file by the output program 'SCRIBE'.

In contrast to the manual systems, of the late 1960's and the early 1970's, the automatic system on NOVA-3 computer took only two to three hours to digitize a typical record and to get it ready for data processing. Another important difference between the manual and the automatic digitization was in the average number of digitized points per second of the record. The old manual digitizing method resulted in at most 30 to 50 digitized points per second, as compared to 200 and more points per second for the automatic digitization method.

In the 70's, several manufacturers of strong-motion recording instruments also developed digital instruments for a commercial sale. The advantage of these digital instruments, when compared to their analog counterparts, is that the analog-to-digital conversion is built-in, so that data is available in digital form, thus eliminating the need for digitization. It might have been expected by some that in the 80's, these digital instruments would outsell and gradually replace the analog instruments. This decade came and passed by, but analog instruments continue to be available and are still used at most recording stations. In fact, the majority of the recordings of the 1987 Whittier-Narrows Earthquake and of the 1989 Loma Prieta Earthquake in California are on analog records. This may be due to the fact that (1) many of the existing instruments still in use are analog instruments, (2) the purchase price of new digital accelerographs is still high compared to the analog ones, and (3) the electronic chips used in digital instruments are outdated rapidly with the ongoing development in solid state physics, so that it is not clear what might be their useful life. It is, of course, expected that digital instruments will eventually replace the analog ones. But it is also clear that the analog instruments and, hence, digitization of their records, is here to stay for a long time.

*I*1.3 The New Automatic Digitization System

With new developments in personal computer hardware, the automatic digitization systems of 15 years ago (Trifunac and Lee, 1979), can now be modernized. The digitization system which we developed in 1975 employed a photodensitometer which at that time had a value of over $30,000. It had to be interfaced with a minicomputer, which was costly to acquire ($150,000) and expensive to maintain ($15,000 per year in 1976 and $7,000 per year in 1989). It used the Tektronix terminal ($12,000 in 1975), which used to be one of the best high-resolution Graphics terminals some 10 years ago.

The development of inexpensive high-speed personal computers (PC's) interfaced with desktop digital scanners in the 80's now enables the automatic digitization system to be available to users at an affordable price. This report illustrates such new capabilities via a Hewlett-Packard digital Scanjet, interfaced with an IBM or compatible PC, with 286, 386 or 486 Intel processor. Our new and updated software package, consisting of the programs SCAN, FILM, TRACE, TV, and SCRIBE, now runs on a PC interfaced with an

enhanced graphics (EGA or VGA) terminal, and can perform the same functions of the digitization process as before. With the development of better scanners, these programs will continuously be updated and improved.

We note that the hardware and software presented in this report are in no way limited to digitization and time series analysis operations on strong motion earthquake accelerograms only. We will present all aspects of digitization and processing of accelerograms, because this is in the area of our specialty, and because that subject has motivated us so far to develop systems for the required data analysis. From the material in this work, it should be clear that our programs are able to analyze virtually any analog trace, a contour map or a line chart, directly or after only minor modifications.

*I*1.4 Hardware Components

The elements of the new automatic digitization system are shown schematically in Figure $I1-1$. The reading of an 8.5×11 inch film positive is performed by the Hewlett-Packard HP9195A (or HP9190A) Desktop digital Scanner, also called "Scanjet Plus". It is interfaced with the IBM PC or compatible, with 286, 386 or 486 Intel processor, via the HP88295A (or HP88290A) interface card. The PC is equipped with a 100 (a minimum of 40 Mb) hard disc, a 1.2 Mb $5\frac{1}{4}''$, or a 1.5 Mb $3\frac{1}{2}''$, floppy disk drive, and with 640K (RAM) memory. The automatic digitization system will require the disk operating system "DOS" version 3.0 or higher. (At present, it is running on DOS 5.0). A VGA (or EGA) graphics display terminal is interfaced with the PC via Enhanced Graphics Adapter (EGA) card. An HP Laserjet Series III (or II, IIp, and IIIp) laser printer with graphics data memory of at least 512K (preferably 1.5 Mbyte) is also recommended to be connected to the PC.

A typical strong-motion accelerogram record usually lasts for tens of seconds. Sometimes, if the complete length of useful recording is considered, many such records may approach the duration of a minute or even longer. Then, considering a typical SMA-1 70 mm wide film record, one would have to digitize a rectangular area of 70 mm (2.75 in) wide and up to, say, 80 sec (80 cm, 31.5 in) long. The Scanjet is designed to scan a regular size paper 8.5×11 inches. It is thus useful to expand and augment a 2.75×31.5 inch rectangular area into a 8.5×11 inch area, to avoid wasting information, without creating undue complications in the software required to reconstruct the original record.

Figure $I1-2$ shows the solution which we developed in 1976 for use with Optronics densitometer. It can be adopted again, at present, using a photocopy machine, to produce the resolution comparable with that of the Optronics scanner (300 dpi or higher). In this approach, a transparency with fiducial marks (as shown Figure $I1-2a$) is used with the original accelerograph record. This is a profile with three pairs of fiducial marks corresponding to three consecutive sections (zones) of the 70mm record. By carefully positioning the first portion (zone 1) of the record with the top pair of fiducial marks (step 1 of Figure $I1-2b$), it can be photocopied onto an 8.5×11 inch paper. This paper is then put back into the auto feeder of the photocopying machine and the next portion (zone 2) of the record is positioned with the middle pair of fiducial marks (step 2 of Figure $I1-2b$).

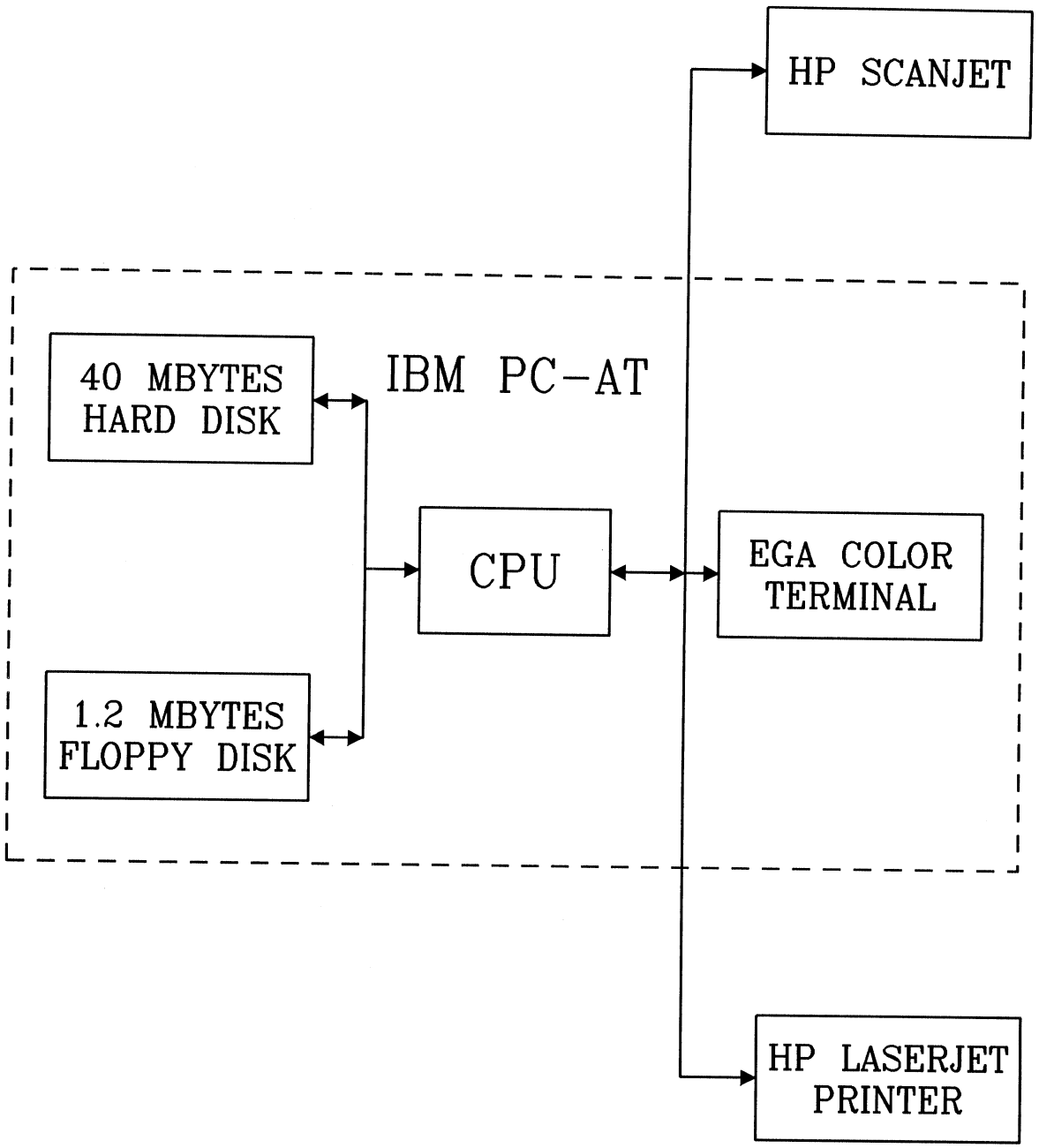

Figure I1 - 1 Hardware components of the automatic digitization and data processing system.

(a) Transparency

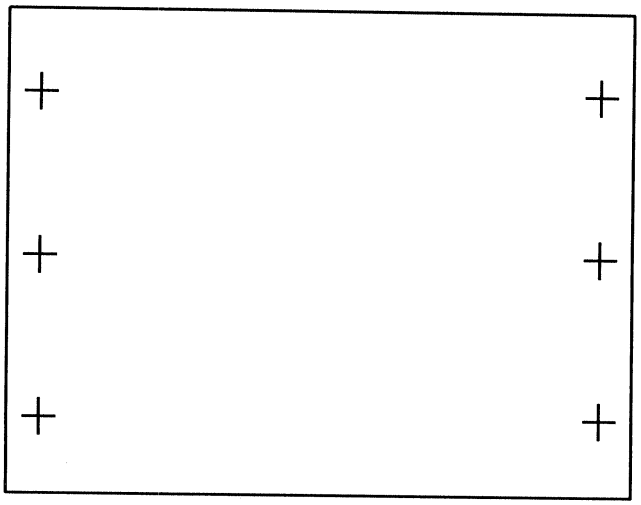

(b) Film Duplication onto Transparency

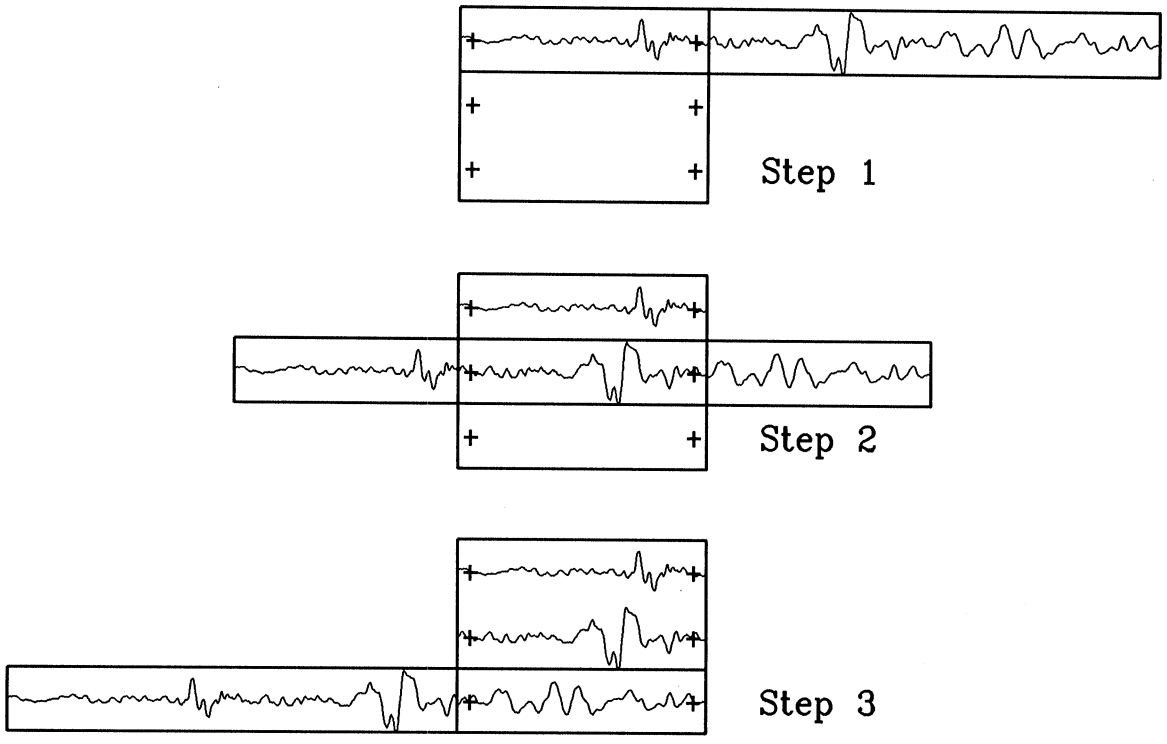

Figure I1 - 2

This process may be repeated for the third portion (zone 3) of the record with the bottom pair of fiducial marks (steps 3 of Figure $I1-2b$). Care must be taken that the left fiducial mark of the current zone is at the same point of the record as the right fiducial mark of the previous zone. The end result is that three consecutive sections of the original record, one below another, are photocopied onto an 8.5×11 inch paper, with consecutive sections marked with corresponding fiducial marks to facilitate subsequent software reconstruction of the original records.

In some cases, when the half-second timing marks are present in both the top and in bottom portions of the 70mm record (and only one of them is needed), only 50mm of the 70mm width of the record may be photocopied. Four consecutive portions of the record, totalling over 100 seconds, can be photocopied onto the single 8.5×11 inch paper.

In another simpler approach, instead of photocopying, consecutive portions of a record, together with the pairs of fiducial marks on a transparency, only one segment can be scanned by the scanjet and written onto the successive disk files. A program can then read all the successive files and assemble them into one continuous disk file. This file will correspond to the one from scanning the photocopy with consecutive sections of the original record, one below another, all with the corresponding fiducial marks. It is seen that this procedure enables one to digitize very long accelerograph records essentially without any limitations on the record duration. The HP Scanjet can also scan metric size paper (A4 format). The above procedures of photocopying the record and all the subsequent digitization programs can also be run for digitization using A4 paper, without any major changes. Alternatively, a 12-in record (wide film with 13 or more components of accelertion) can also be scanned from top to bottom (instead of from left to wright). A program can then switch the data back to be from left to right.

*I*1.5 Noise Characteristics of the New System

The Response and Fourier amplitude spectra of digitization noise, representing the overall automatic digitization process, are next evaluated. This will describe the amplitude and frequency range in which the digitized accelerograms will provide accurate representation of the recorded motions. In general, the amplitude of this noise may depend on the resolution of the scanner, but for this, as for the optical scanner we described in 1979, it will depend mostly on the thickness of the acceleration trace on the film, and on the length of the record. With the old digitization methods, in comparing the recordings on acceleration and displacement tranducers (Trifunac and Lee, 1974), it was found that typical digitization noise may result in "ground displacement" amplitudes of up to several centimeters.

In dealing with semi-automatic hand digitization (Trifunac and Lee, 1973), the resolution (in terms of the number of digitized points per physical length on the record) of digitization plays an important role in the noise characteristics of the system. In automatic digitization this physical resolution of the system (in pixels per mm) can be chosen sufficiently small not to affect the noise amplitudes. For the automatic digitization system

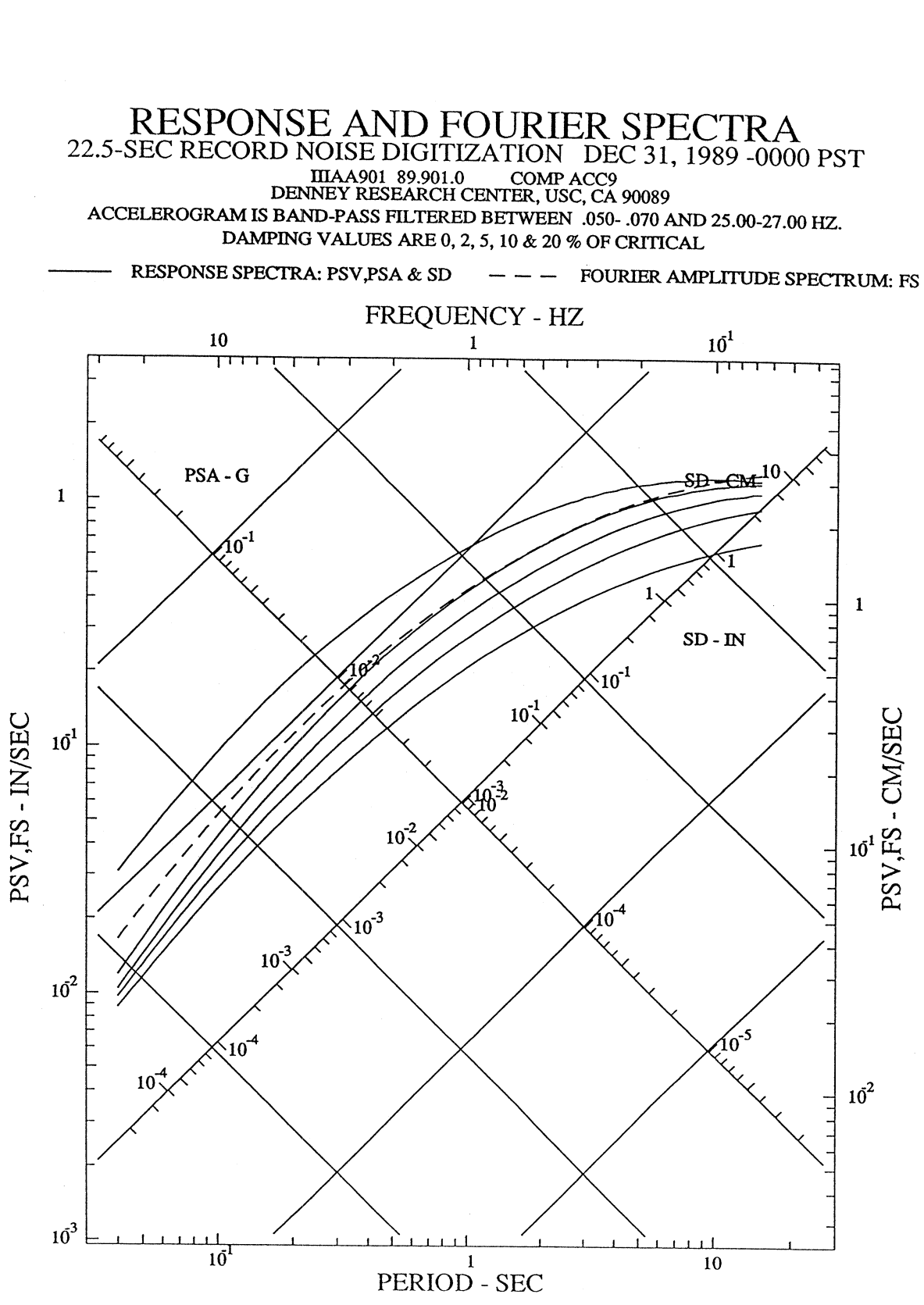

Figure I1 - 3 Noise spectra of a 22.5-sec. record.

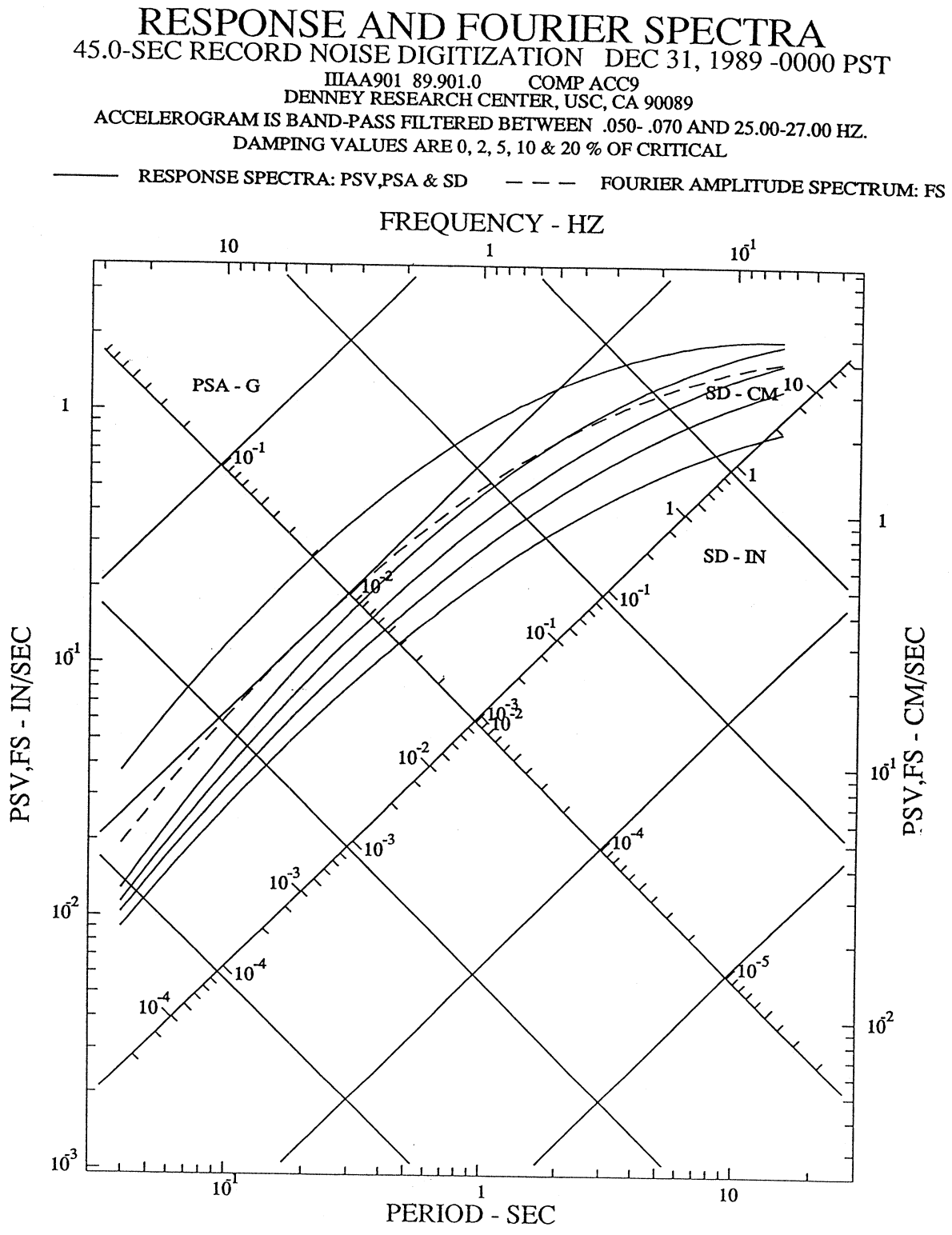

Figure I1 - 4 Noise spectra of a 45.0-sec. record.

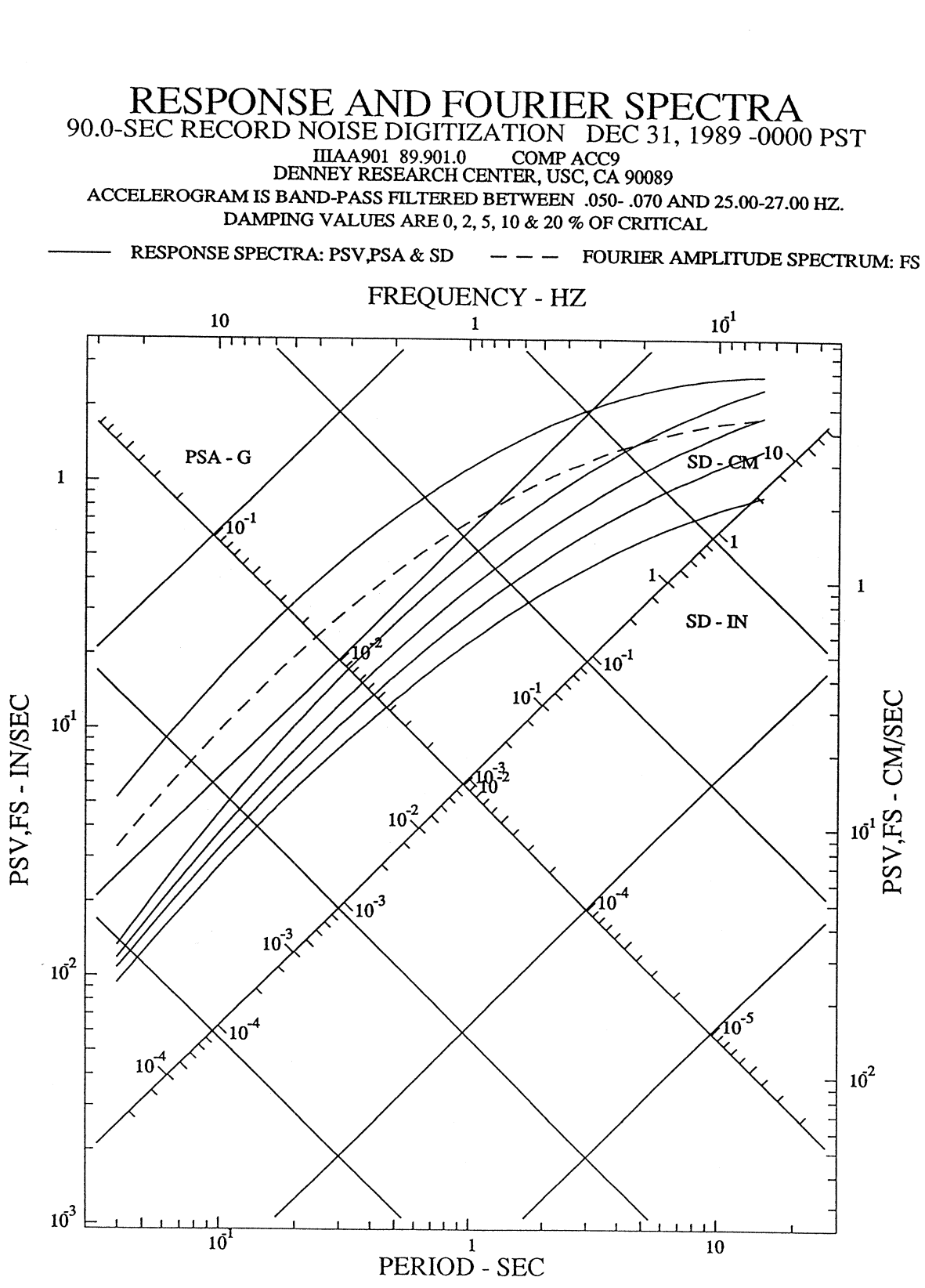

Figure I1 - 5 Noise spectra of a 90.0-sec. record.

using photodensitometer (Trifunac and Lee, 1979), a resolution of 200 points/cm is sufficient (pixels $50\mu \times 50\mu$). The noise amplitudes, then, are dependent more on the thickness of the traces of the record to be scanned. In the new automatic digitization system, a typical resolution is 600 points/inch (dpi). For a record with a time scale of 1 cm/sec, 600 dpi corresponds to 236 points/sec and, hence, to a Nyquist frequency of 118 Hz, which is more than sufficient.

To create "noise acceleration traces," several SMA-1 accelerograms were selected. For each record, the pair of baselines was then digitized, one as a "zero" acceleration trace and the other as a zero baseline. Together with the time trace, all were scaled, and instrument and baseline corrected. The final acceleration data were band pass filtered in the frequency range from .07 to 25 Hz. Response and Fourier amplitude spectra were then calculated. Figures $I1-3$ through $I1-5$ show the smoothed average spectral amplitudes for records 22.5, 45 and 90 seconds long respectively. It can be concluded from these figures that the overall spectrum amplitudes are similar to those for the automatic digitization system on NOVA-3 computer (Trifunac and Lee, 1979), with the present long period noise amplitudes lower than before.

$I1.6$ Use of Numeric Keys for Crosshair Cursor Control

It is assumed here that the user is familiar with the functions of the numeric keys on the right-hand side of the typical keyboard. Figure $I1-6$ shows a diagram of these keys. The Num-Lock key can be pressed to have the Num-Lock light either on or off. When the crosshair cursor appears on the screen, it can be moved in all eight directions, as illustrated by the arrows in the numeric keys 1-9 in this figure. Thus, to go to the right ($\rightarrow$), the user should press the key 6. The crosshair cursor will advance to the right for one small step. The user may keep the right ($\rightarrow$) key down to continue moving the crosshair further to the right, until it gets to the desired position. Each time the user wants to change direction, the corresponding key should be pressed, keeping it down continuously, as desired. To define a point on the screen occupied by the crosshair curser, the user should press the enter key or, if the Num-lock light is on, either the OK[5] or the enter key. The (+) and (-) keys are used for changing the size of the crosshair cursor.

The next four chapters will describe the programs used for automatic digitization of accelerograms: SCAN, FILM, TRACE, TV, and SCRIBE. Old versions of these programs have been discussed in some detail, and the overall process of automatic digitization was presented in our first report on this subject (Trifunac and Lee, 1979). Many ideas, procedures and operator tasks have changed little or not at all in this transition to a personal computer hardware. Numerous new software and algorithm improvements will not be obvious to a new–comer to this subject. Also, many steps and procedures have evolved from our experience in working with the old automatic accelerogram digitization system. For brevity we will not explain or justify all such steps and inovations here, but suggest that the interested reader peruse our 1973 and 1979 reports. At the time when this report is going into print, new options and other updated version of the programs are continuously

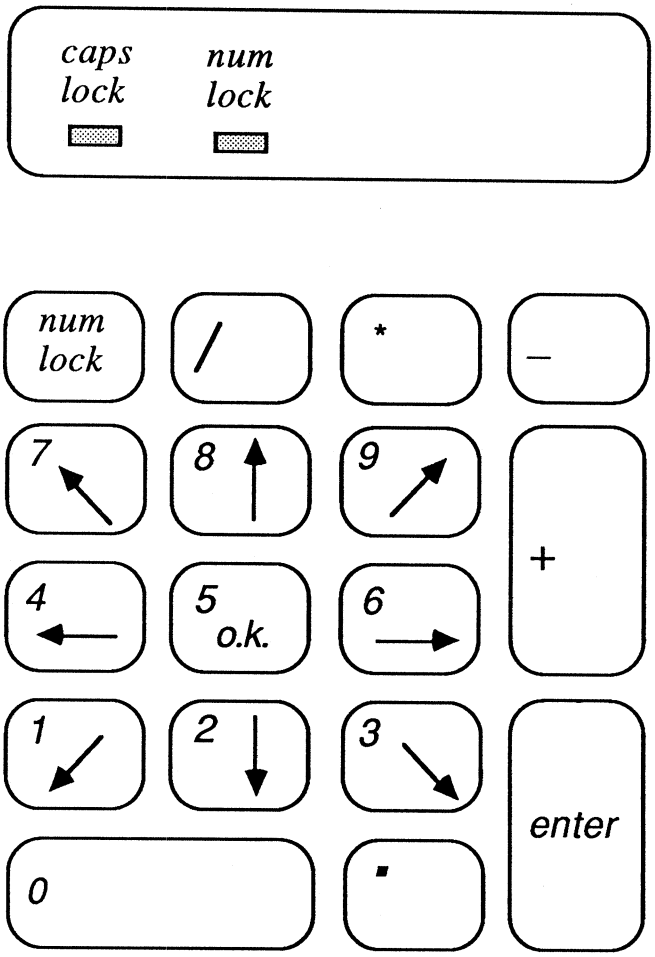

Figure I1 - 6 Numeric keypads used for crosshair cursor control.

being developed. Therefore the following chapters will describe the most recent (current) version of these programs.

*I*2 SCAN and FILM

*I*2.1 Introduction

Instructions on connecting the scanner with the PC by the HP 88290A (or HP88295A) interface card are well documented in the Hewlett-Packard User's Guide and will not be repeated here. It is assumed that the user can read this guide and is familiar with the manual before proceeding. Once the 8.5 × 11 inch positive or paper copy of the film is made, it is placed face down onto the Scanner's flat surface, so that the beginning of the record is at the lower edge of the scanner.

The program SCAN will be used to scan the record image and store it onto a disk file. Under normal circumstances, the record will be scanned at normal intensity without shades of Gray/Color at a resolution of 600 dpi, or for thick traces with low recorded frequencies with 300 dpi. In all cases, 100% of the paper (8.5 inch by 11 inch) will be scanned. With the 300 dpi option, the image file will consist of just over one Mbytes and can be stored onto a high density floppy disk.

The scanning process, will take several minutes. The program FILM will next be used to define the reference points and the lines of the record. There are 3 types of reference lines: "Time-Hacks", "Half-second" lines and "Baselines". Reference points include fiducials, common edges between adjacent sections of the record, and upper and lower limits. All these points and lines, if present, have to be defined (Trifunac and Lee, 1979).

It is important to identify correctly the reference lines. If the trace identification program (TRACE) misses or never receives information on the starting points for a base-line (the solid straight line), this line will be considered as an acceleration trace and the program's ability to deal with intersections between acceleration traces and baselines will be reduced. If a dashed reference line (time-hacks or half-second marks) is missed, each separate dash will be stored on disk as a separate line segment. The user will have to concatenate them, one by one, by the editor program, TV. There can be as many as 75 such broken segments, resulting in considerable and unnecessary work.

As program TRACE (next chapter) reads through the raw data file, it announces on screen how many of the reference lines remained to be identified. If it fails to identify all, the user should stop the program TRACE and go back to FILM to find out why. It is probably so because the reference coordinate was not defined correctly. It might also be because a fiducial mark or common-edge was misidentified as being a reference line, for example.

*I*2.2 Program Flow of FILM

*I*2.2.1 Initialization

The user has just scanned the record using the program SCAN, and is ready to run the program FILM. A special reference file, REFS.DAT, will be created and updated during 'FILM'. When FILM starts, it will first inquire if the user desires to (1) create a new REFS.DAT file for a NEW SCAN, or (2) edit the old REFS.DAT file of an OLD SCAN. Option 1 is for a user who has just scanned a record and is running FILM for that record for the first time. Option 2 is for one who wants to change and edit a previously defined REFS.DAT file from previous runs of FILM.

FILM will clear the screen and the raw data of the beginning portion of the record will begin to appear.

*I*2.2.2 Options (Figure *I*2 – 1)

FILM then gives the user the following options:

MORE ^"R"AW Data
"Q"UIT, ^"B"LOWUP
OR "M"EASURE?

"R" (Raw data) will activate the crosshairs, expecting the coordinates of two opposite corners of a rectangular region to be defined. FILM will then display the RAW DATA within the rectangle outlined by the user. "^R" will result in the RAW DATA in the whole screen window to be displayed.

"Q" (Quit) will allow the user to exit from FILM after the reference points have been defined. The file REFS.DAT will contain the coordinates and types of all reference points or lines defined.

"B" (Blow-up) will activate the crosshairs, expecting the coordinates of two opposite (diagonal) corners of a smaller rectangular window to be defined by the user. FILM software will then reset and rescale the screen, and the region defined will now be enlarged to fill the whole graphic screen with the raw data of the window just defined above.

"^B" will result in the screen cleared and an initial portion of the raw data in the screen replotted at the same scale.

"M" (measure) allows the user to define coordinates of seven types of reference points or lines:

(1) "B"ASELINE: beginning of a solid "zero" baseline.

(2) "H"ALF-SECONDS: beginning of dashed or square-wave half-second ticks.

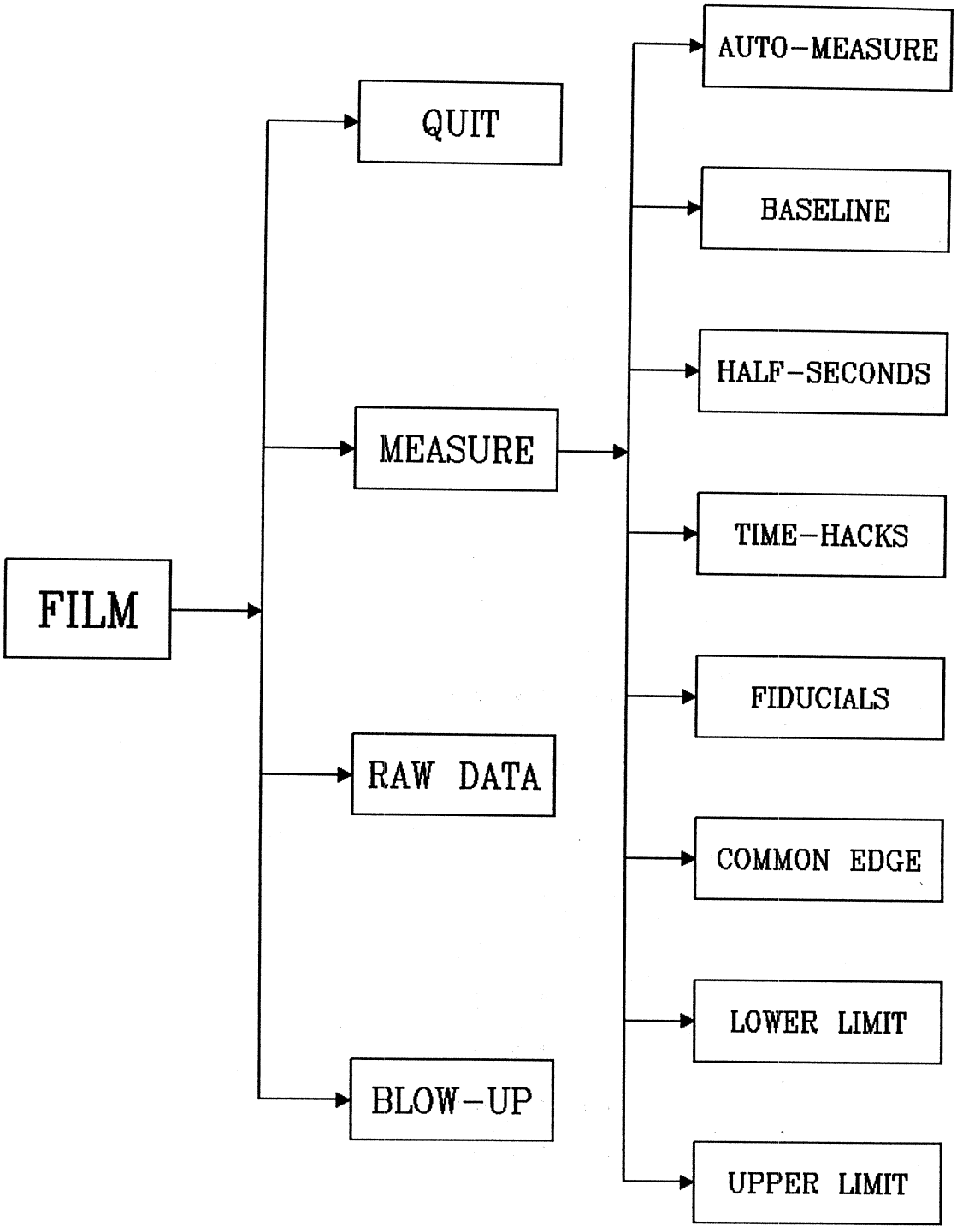

Figure I2 - 1 Flow-chart of program FILM.

(3) "T"IME-HACKS: beginning of a dashed line of a clock time-hacks.

(4) "F"IDUCIALS: the fiducial reference points of different sections.

(5) "C"OMMON edge: a point or a horizontal line marking the common edge between neighboring sections.

(6) "L"OWER edge: lower limit in Y to be considered by program TRACE.

(7) "U"PPER edge: upper limit in Y to be considered by program TRACE.

The option "A" for auto-measurement will allow all the above baseline, half-seconds, time hacks and fiducials (respectively "types" 1 to 4) in a given vertical section to be measured. A vertical crosshair line will first come on. Using keypad keys, the crosshair line can be moved to an appropriate cross-section and the point can be defined.

FILM then indicates on the screen

TYPE n: 0-4, 0 to
IGNORE, -n to DEL

All the raw data traces that intersect the vertical crosshair will be marked and a request made for type # identification:

TYPE #:

acceleration traces are of "type 0" and are ignored. A previously defined point of type n can also be deleted by typing in -n, with n the corresponding type number of the previously defined point.

*I*2.2.3 Methods of "Measurement"

Having specified "M", as explained in the previous section, FILM responds with:

AUTO-MEASURE = (1) "B"ASELINE (2) "H"ALF-SEC (3) "T"IME- HACK
(4) "F"IDUCIAL "C"OMMON-EDGE "U"PPER or "L"OWER LIMITS?
"B", "H", "T", "F",
"C", "U", "L", OR
"A"UTO MEASURE?

"B", "H", "T", "F","C", "U", and "L" will correspond to one of the seven types of reference points or lines described above. Picking any one of these (except "A", which has been described) will result in a little crosshair '+' appearing in the middle of the screen. Using keypad keys, the crosshair can be moved to the desired location and a point defined. FILM will then reply with the question:

"A"DD, "D"EL OR "I"GNORE

"A" will "accept" the measurement, and FILM will then draw an arrow labeled with the corresponding letter identifying its type. "D" is used to delete an earlier measurement. To delete an earlier measurement, the user can call "M"EASURE, center onto a previously defined point, at the tip of the arrow, define the "new" point where the earlier measurement was made, and when the message "A"DD, "D"EL or "I"GNORE? : comes on, type D. The previous measurement will then be deleted as indicated by a box enclosing the coordinate being drawn. Answering "I" will simply ignore the current measurement made.

*I*2.3 Sample Session

In what follows, the user has a record photocopied in sections onto an 8.5 × 11 in paper which is to be scanned by the HP Scanner with resolution of 300 dpi (points/inch). The scanner image file, with this resolution, will be ~ 1 Mbytes and the user may store it onto a high density floppy disk in drive A.

In this sample session:

[Brackets indicate computer activity]
(Explanations are given in parenthesis)
User keyboard entries are underlined.
↩ denotes carriage return or ENTER

*I*2.3.1 Task 1 : Scanning

Step # Transaction/Explanation

1. A:↩
   (User inserts an empty formatted high-density floppy disk into drive A)

2. C: SCAN ↩
   (User runs the program SCAN in drive C to scan the page of a record; the scanner should be on with the record page facing down, and the beginning of the record at the bottom edge of the scanner).

3. (SCAN will first ask the user for the scan image filename, and under normal circumstances, will scan the full page at 300 dpi. The whole process will take about 10 to 15 minutes.)

*I*2.3.2 Task 2: running FILM

Step# Transaction/Explanation

1. FILM ↩
   (To execute the program FILM)

2. [Screen erase]

   ```
   ************
   *  FILM    *
   ************
   ```

   FILM VERSION 3.0

3. Filename of Scan Image (A20) [____ .RAW]: A:IMAGE.RAW ↩
   (User inputs scan filename)

4. (1) CREATE NEW REFS.DAT FILE FOR NEW SCAN, OR
   (2) EDIT OLD REFS.DAT FILE OF OLD SCAN? (1/2): 1 ↩

   (User is to define the file REFS.DAT from scratch for the image file of the record just scanned).

5. Starting Graphics Mode of the EGA Terminal,...
   PAUSE
   Hit return to continue... ↩

   (reminds user to check that the Num-Lock and Caps-Lock keys are on).

6. SCANNER UNITS USED, PTS/IN, DPI[300]: 300 ↩

   (300 dpi is the resolution used in this example of scanning the record).

7. [Screen is erased; after a few seconds, raw data of the beginning portion of the record will begin to appear on screen].
   MORE ^"R"AW DATA
   "Q"UIT, ^"B"LOWUP
   or "M"EASURE? B

   (User wants to blowup an area to be defined using the crosshairs).

   [crosshairs come on]

   (Using keypad keys, user enters the coordinates at 2 opposite corners of a rectangular area).

[defined rectangle is drawn on screen]

CONFIRM, Y/N: Y

(User confirms it)

[Screen erased; raw data of the beginning portion within the window are displayed in a scale such that the window area now takes up the whole screen].

8. MORE ^"R"AW data
"Q"UIT, ^"B"LOWUP
or "M"EASURE? M

(User wishes to perform reference measurement routine)

AUTO-MEASURE: (1) "B"ASELINE, (2) "H"ALF–SEC (3) "T"IME- HACK
(4) "FIDUCIAL "C"OMMON-EDGE "U"PPER or "L"OWER LIMITS?
"B", "H", "T", "F",
"C", "U", "L", or
"A"UTO MEASURE: A

(User requests FILM to perform automatic reference measurements).

[Vertical crosshair line comes on]

(Using keypad keys, user can move the crosshair line to an appropriate x-value and press ENTER)

TYPE n:0-4, 0 TO
IGNORE, -n TO DEL
(All raw data that intersect the vertical crosshair will be marked and the type number will be requested from the user)

TYPE # :3

(The first raw data marked is a time-hack trace (type 3); other traces that may be marked are half-second (type 2), baseline (type 1) or acceleration (type 0) traces; this question will be repeated until all raw data of the section are marked.)

9. "B", "H", "T", "F"
"C", "U", "L", or
"A" UTO MEASURE F

(User now wants to define a fiducial mark directly; a little crosshair will appear in the middle of the screen; using keypad keys, user will move the crosshair to the center of the fiducial mark and press ENTER.)

"A"DD "D"EL or
"I"GNORE? A

(User types "A" to add this point to the list of reference points defined; an arrow with initial F is drawn, marking that the coordinate is taken.)

10. "B", "H", "T", "F"
"C", "U", "L", or
"A"UTO MEASURE:↩

(User is ready to rap up after defining all the reference points.)

MORE ^"R"AW DATA
"Q"UIT, ^"B"LOWUP
OR "M"EASURE? Q

(User orders FILM to Quit.)
[screen erased]

FILM VERSION 3.0

[Program Stops]

(All reference points and lines have been defined and storted in the file REFS.DAT. User is now ready for the next program: TRACE.)

*I*3 TRACE

*I*3.1 Introduction

Program TRACE reads through the RAW DATA file "IMAGE.RAW" locating groups of 'shades of gray' (black dots) along the y-axis that may represent the cross-section of a trace on the film. Initially, a trace segment is begun with every group of gray levels it encounters, and, subsequently, as TRACE moves along the x-axis, further groups of gray in the y-direction are associated with earlier groups, if they are 'close enough' according to certain empirically chosen criteria. In this way, continuous segments are built up, while scratchy segments caused by various imperfactions in the image are discarded if they do not accumulate a required minimum number of 'points'.

Eventually, ambiguous situations are encountered. When this happens, TRACE will examine the problem in greater detail, trying to resolve any confusion resulting from the intersection of segments, or from the presence of scratch marks among the segments. In general, properly identified reference lines will always be pulled through, and intersections with them of the adjacent acceleration traces, if at a sufficiently steep angle, will be resolved correctly. Difficulties arise when traces merge over a substantial length, when traces disappear (gaps), or when two or more traces simultaneously intersect a reference line. When TRACE cannot resolve a problem, the new "pulse" will be used to create a new segment, and earlier disjointed segments will eventually be closed out. Note that TRACE does not 'look ahead'. It deals only with the "pulses" currently in buffer, and attempts to associate them with segments already in existence, the building ends of which lie in the immediate vicinty of the pulses.

As segements are built up, they are each stored on disk as a y-coordinte file SCxxx.DAT, where xxx is a numerical suffix, from 001, 002, 003,... All other information on the segment is stored on a corresponding record in the parameter file PARAMS.

*I*3.2 Program Flow of TRACE (Figure *I*3 – 1)

*I*3.2.1 Initialization

When TRACE begins, it initializes the various parameters created by the previous run of FILM. It then requests the user to provide the leftmost and the rightmost limits, in x scanner units, to begin and to end the scan. For an 8.5×11 inch paper scanned by FILM with a resolution of 300 dpi, the scanner units in the x-direction will range from 5 to 3300. The user may set the leftmost beginning x to some scanner unit ≥ 5, but which is less than the minimum x-coordinate of any of the traces on the paper. One may set the rightmost ending x-value to anything beyond 3300. TRACE will then read the file 'REFS.DAT', created by FILM, containing the coordinates and types of the reference lines and points defined earlier.

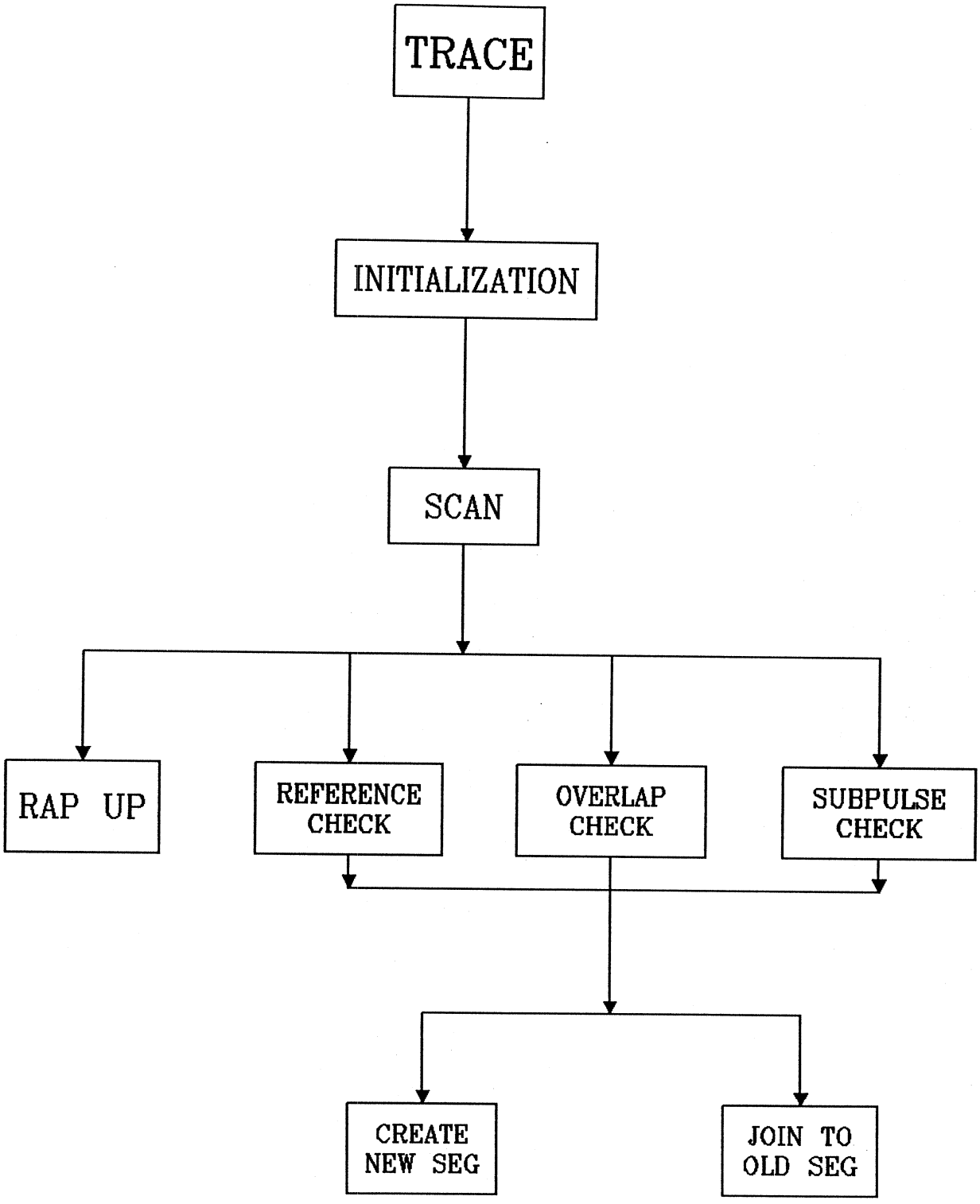

Figure I3 - 1 Flow-chart of program TRACE.

*I*3.2.2 Scanning

With initialization complete, TRACE begins to read the digitized RAW DATA file 'IMAGE.RAW', skipping through the blank area at the beginning, until the starting x-values of one or more traces are encountered. TRACE will then loop through the input buffer looking for distinct groups of densities in the y-direction. Each such grouping, which might represent the cross-section of a trace, is put into a pulse buffer in memory, consisting of a group of densities contiguous in y, together with the pulse width and the bottom y-coordinate.

*I*3.2.3 Reference-Line Check

First, TRACE checks to see if the pulse found is part of any existing reference line segment. The required condition is to be sure that the y-coordinate of the center of the pulse matches closely with the center of the end of any of the reference lines in memory. If this criterion is met, the pulse is associated with the corresponding reference line segment.

*I*3.2.4 Overlap check

If it fails the above reference test, but follows consecutively after the last pulse of other existing segment, with the pulse's center lying within the expected projected direction the given segment is 'pointing', and if there is no overlap with any other segment, the pulse is associated with that segment. If more than one segment overlap the pulse, the pulse will be looked at in a greater detail.

*I*3.2.5 Subpulse check.

TRACE examines the pulse for 'subpulse' that can occur when two or more segments are intersecting. TRACE will try to create subpulses that can be associated with the overlapping segments according to an empirically adopted scoring system.

*I*3.2.6 Creating a New Segment

Any pulse that fails to be associated with any existing segment will eventually be defined as a new segment. When a segment is created, a new segment number is assigned and all known and necessary information about the segment will be stored and updated periodically in an array in the memory. Up to a maximum of 50 segments are in active memory. When there is no room, segments whose ends were left far behind, and whose lengths are insufficient to warrant keeping, are removed and destroyed. Segments that are long enough, but which are now too far away in the x-direction to consider, will be closed and written onto the disc to make room in memory for new segments.

*I*3.2.7 Adding to an Existing Segment

The center y-coordinate of each pulse that can be associated with an existing segment is put into an array in memory. Each array has room for 64 coordinates for up to 128 segments. When they are full, they are written to the SCxxx.DAT file of each corresponding segment, where xxx ranges from 001 to 999.

*I*3.2.8 RAPUP

Once the entire image file has been read, the segments in core are written onto disk and closed. A summary file, 'SUMUP.DAT' is written, containing the maximum x- and y-values found in the segments, and the total number of segments found. The user is now ready to run the next program, TV.

*I*4 TV

*I*4.1 Introduction

Once the program, TRACE, has finished, the trace segments created are stored in disk files. The file PARAMS.DAT contains stored information on each segment, including the file name suffix where the y-coordinates can be found, the first x-coordinate, file type (0, 1, 2 or 3), etc.. The y-coordinate files are named SCxxx.DAT, suffixed with xxx a 3-digit number, 001, 002, 003,..., 999. The total number of such files for each record digitized will vary, depending on its size and quality.

With TV, the next program, the user can access the segments, display them on the screen, and perform required editing functions. It is important to note that the SC-files and the file PARAMS are not altered after any editing session. Any editing performed is stored by means of a map file MPxx.DAT which is created by TV. The suffix of the files MPxx.DAT can range from 01, 02, 03, to 99, thus allowing a total of up to 99 editing sessions, which is probably more than enough. As the editing progresses, the operator, through editing, will create single traces running continuously from the left side of the scanned image to the right.

A typical editing session involves examining the segments in each zone section by section. Initially, the operator may request all segments of all zones to be displayed on the screen, so as to be able to mark down all those segment numbers starting from the left margin that do not go all the way to the right margin. Then, using the crosshair cursor, the trouble spots may, one by one, be blown-up to a higher resolution for editing.

The editing involves truncation, splitting, filling-in, deleting and creating of segments. All these changes are recorded on the map file MPxx.DAT. The final phase of the digitizing process, performed by the program SCRIBE, will then read the map file to plot and write onto disk the full-length traces.

The first editing session, after running TRACE, begins by creating the map file from scratch. TV does this by reading the PARAMS.DAT file and the SCxxx.DAT files and puts the information onto the map file MP00.DAT. This is the original, uneditted version that should be retained for possible reference. The user should instruct TV to record all subsequent editing changes on other map files, say MP01, MP02,..., up to MP99.

*I*4.2 Program Flow of TV (Figure *I*4 – 1)

*I*4.2.1 Initialization

When TV starts, it initializes the various parameters of each segment created earlier by TRACE. It then reads the file 'REFS.DAT', consisting of coordinates of the reference points and traces defined by FILM. TV will next request from the user the map file suffix MPxx, where the serial number and filename SCxxx of the traces are available. A zone

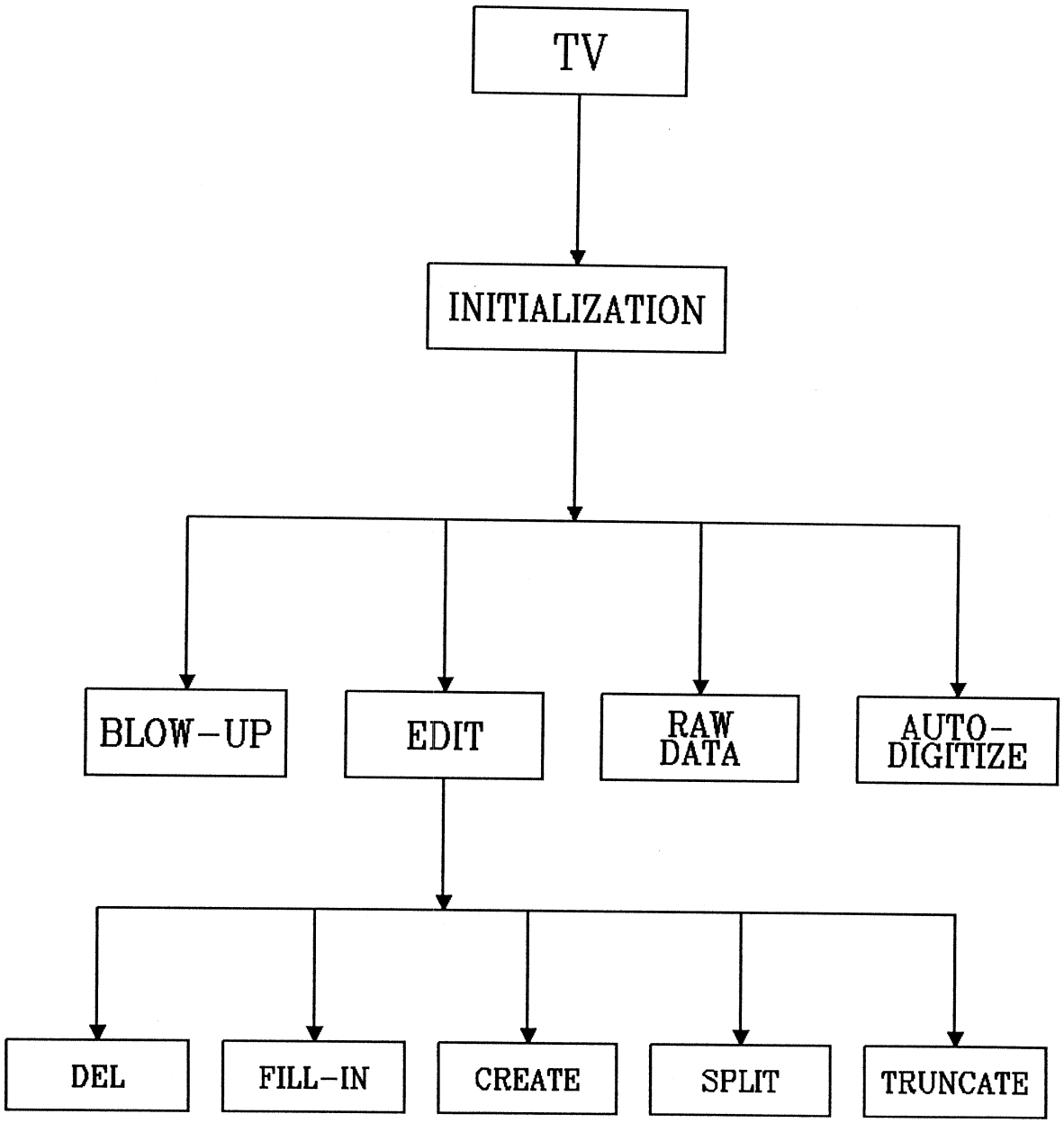

Figure I4 - 1 Flow-chart of program TV.

(film section) number is also assigned to each segment of the traces. This is to speed up the searches of segments when they are to be displayed on the screen. The screen is then reset and cleared. The coordinates of the reference points and traces are displayed as arrows, labelled with their corresponding types on the screen.

*I*4.2.2 Plot Request

TV then requests from the user information on whether to display all or some of the segments, to go on to the next step, or to quit and exit from TV:

"Q"UIT, OR PLOT
"N"ONE, "S"OME
OR "A"LL SEG?

A response of "A" (all segments) will be followed by another question:

ZONE: 0 1 2 3
4 5 6
7 :

Zones 0 though 3 correspond respectively to the bottom through top zones of the film. Zone 4 corresponds to zones 0 and 1, 5 corresponds to 1 and 2, 6 to 2 and 3, and 7 corresponds to all the zones.

A response of "S" (some segments) will result in the question from TV:

SEG:

where the 3-digit serial numbers of up to 5 segments are to be input by the user. If less than 5 segments are to be input, the user can simply hit carriage return (or the enter key) once after the last serial number. A response of "N" will instruct TV to go on to the next step of the program. A "no" response (carriage return) will set TV to get ready to quit.

*I*4.2.3 Menu

With the response of "A" or "S" in the above step, TV will display the requested segments on the graphic screen. Only those segments that are within the current screen window will be plotted. Each segment is labelled with its serial number. If the end of the segment is also within the window, the end will be shown by a small triangle.

After the segments are all displayed on the screen, TV requests from the user directions for the next step with the following list of MENU:

"A"UTO DIGITIZE
^"B"LOWUP "E"DIT

OR ^"R"AW DATA?

"B"(blowup) will activate the crosshair, expecting the coordinates of two diagonally opposite corners of a (smaller) region to be defined by the user. TV will then reset and rescale the screen and the region defined will now be enlarged to fill the whole screen with all the segments in that region displayed.

^"B" will result in all the segments in the current screen windows to be replotted in the same scale.

"E" (Edit) will result in sending the control to the editing routine.

"R" (Raw data) will also activate the crosshairs, expecting the coordinates of two diagonally opposite corners of a rectangular region to be defined. TV will then display the RAW DATA within the rectangle outlined by the user. Note that the size and scale of the current window is unchanged.

^"R" will result in the RAW DATA in the whole screen to be displayed.

"A" (Auto digitize) will again activate the crosshairs, expecting the coordinates of two opposite corners of a rectangular region to be defined. TV will then digitize the RAW DATA within the region resulting in defining a new segment.

A no response (↩) will clear, reset and rescale the screen to the area of the full size record and will then go back to step 4.2.2 above.

*I*4.2.4 Edit

This is the step in TV that controls the editing functions. TV responds with the following list of options.

"D"EL "F"ILL-IN
"C"REATE "S"PLIT
"T"RUNCATE:

"D" (Del) is used to delete (up to a maximum of five) segments. It will result in the question from TV:

SEG :

where the 3-digit serial numbers of up to 5 segments are to be input by the user. Each of the segments input will be deleted one by one on the screen and confirmation for each segment requested:

CONFIRM,(Y/N):

If confirmation is "Y" (Yes), the segment will be deleted from the list of active segments on the map file. If it is "N" (No), the segment will be redrawn on the screen and its deletion is cancelled.

"F" (Fill-in) is to "fill in" a sequence of (up to five) segments. TV will request the user to input from two to as many as five serial numbers. The segments must be entered in the same order as they appear on the screen from left to right. The last point of a preceding segment must be at least one scanner x-unit less than the first point of the next segment following in the list. If this condition is satisfied, TV will connect them with a straight line joining the end points. The joining line will be a solid line if the end points are exactly one x-unit apart, otherwise it will appear as a dotted line on the screen. TV will then request confirmation from the user. If it is confirmed, the two segments will become one with the serial number same as that of the preceding segment, while the serial number of the right segment will disappear from the screen. This process will be repeated for the current segment and for the next segment on the input list.

"C" (Create) is to create a segment manually by the user. TV will activate the little crosshair, expecting up to 20 coordinates to be entered, with the last coordinates entered by pressing the key with period "." instead of Enter (or OK [5]) (see section I1.6). With all the points entered, TV will first rearrange the points in increasing values of x. For each integer value of x (in scanner units) between the first (leftmost) and last (rightmost) points defined, TV will calculate the corresponding values of y, using straight line interpolation between successive points entered by the user. A segment is then defined and displayed on the screen with a serial number assigned by the program.

"S" (split) is to split a segment. TV will request from the user a serial number:

SEG:

The user responds with a three-digit serial number, corresponding to that of the segment to be split followed by two carriage returns. Next TV activates a vertical crosshair, expecting the user to locate the appropriate x-coordinate of the point on the segment to be split. After this, a small crosshair will appear at the chosen point on the segment and the following request will appear:

OK? OR ELSE MOVE
↑ OR ↓ THE SEG?

The user can use the numeric keypad keys to further move the crosshair left or right along the segment and then press Enter or 'OK'. The segment will be split in two, resulting in a new segment with a new serial number to appear left of the point chosen. The original segment will end at the chosen point.

"T" (Truncate) is to truncate the tail (right) end of a segment. This proceeds the same way as the option "S" (SPLIT) above, with the exception that, at the end, no new

segment to the right of the point will be created, but will be deleted, after confirmation from the user.

*I*4.3 Sample Session

[Brackets indicate computer activity]
(Explanations are given in parentheses)
User keyboard entries are underlined.

Step # Transaction/Explanation

1. TV ↩
   (To execute the program TV)

2. [Screen erase]

   TV VERSION 3.0

3. FILENAME OF SCAN IMAGE (A20) [___ .RAW]: A:IMAGE.RAW ↩
   (User inputs the scan filename)

4. Starting Graphics Mode of the EGA Terminal,...
   PAUSE
   Hit return to continue... ↩
   (reminds user to check that the Num-Lock and Caps-Lock keys are on)

5. [Screen erased]

   ****
   * TV *
   ****

   MP##: MP ↩
   (User wants a new map file.)
   [computer process for 5 to 10 seconds]

6. [screen erased]
   [reference coordinates are displayed by arrows on white background]

7. PLOT "N"O, "S"OME
   OR "A"LL SEG A

   ZONE: 0 1 2 3
   4 5 6
   7:
   7

   (User wants all segments of all zones to be plotted)

[segments of all zones and their labels come on to the screen]

8. "A"UTO-DIGITIZE
^"B"LOWUP "E"DIT
or ^"R"AW DATA: B

(User wants to examine in detail an area to be defined using the crosshairs)
[crosshairs come on]
(Using keypad keys, the user enters the coordinates at two diagonally opposite corners of the rectangular area of interest)
[the rectangle defined is drawn on the screen]
CONFIRM, Y/N:Y

(User confirms it)

9. [Screen erased]

[All segments within the window are displayed in the full screen; they are labeled at their beginning and/or where they enter the window; their ends are marked with a small triangle, but not where they exit to the right end of the window (Figure $I4-2$)]

10. "A"UTO - DIGITIZE
^"B"LOWUP "E"DIT
OR ^"R"AW DATA: R

(User wants to see the raw data in an area to be specified)

[crosshair's come on]

[rectangle defined drawn on screen]

(As in step #8, a rectangular area is defined and confirmed by the user. The user wants to analyse an area surrounding a discontinuity of trace 002. After inspection of the original acceleration traces, the user will perform the following steps to split, old segments, create new segments, delete segments which are not required and, finally, to merge the remaining sements into continuous traces.)

CONFIRM, Y/N: Y:

[Raw data comes on within the rectangle (Figure $I4-3$)]

11. "A"UTO - DIGITIZE
^"B"LOWUP "E"DIT
OR ^"R"AW DATA: E

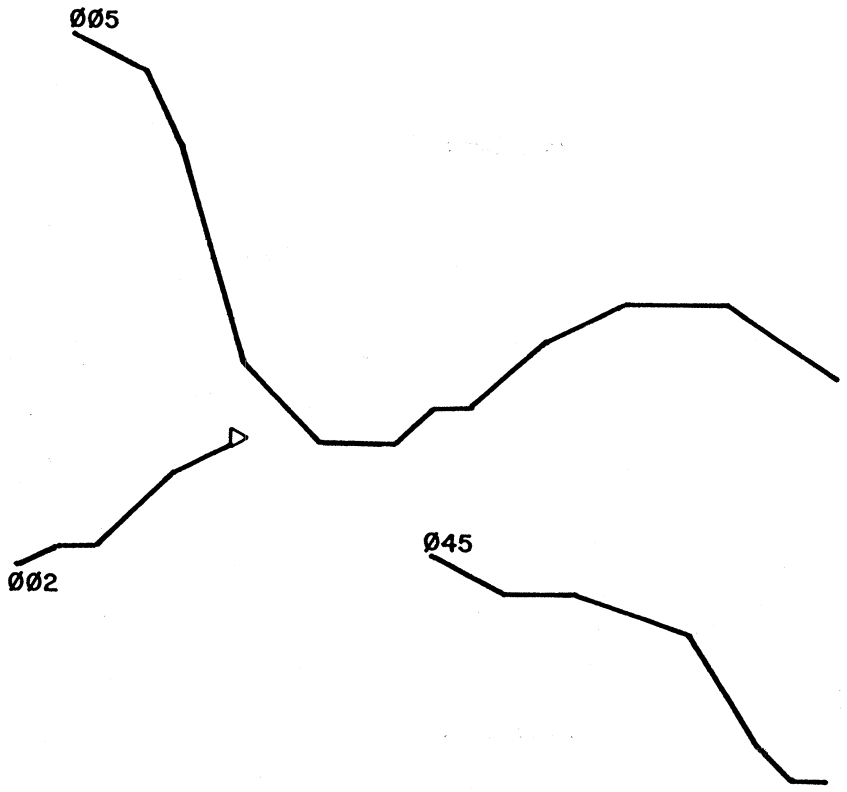

Figure I4 - 2 Screen as it appears after the execution of step 9. Only segment 002 actually ends within the window.

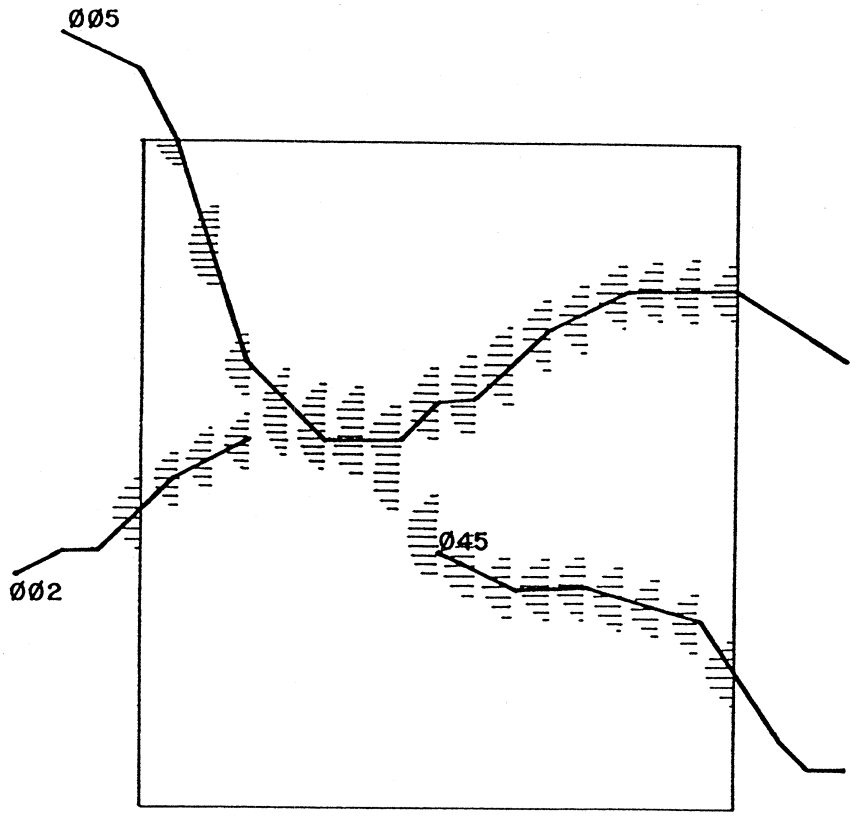

Figure I4 - 3 Screen as it appears after the execution of step 10, and when 16 or 256 density levels have been employed. With only two density levels all data points would be shown with lines of constant lenght.

(User wants to perform some editing on the segments now on screen)

12. "D"EL "F"ILL-IN
"C"REATE "S"PLIT
"T"RUNCATE: S

(User wants to split a segment in two)

SEG:005
SEG: ↩

(User enters the serial number of the segment to be split. User could have entered a new number if 005 was wrong; there was no error, so user hits ↩)

13. [Vertical line comes on] (Figure *I*4 – 4)
(User moves the vertical crosshair to the vicinity of x where split is desired and hits return. A small '+' will appear at a point on the segment where the vertical crosshair intersects)

14. OK? OR ELSE MOVE
↑OR ↓ THE SEG?

(User can now use the keypad keys to move the '+' crosshair up and down the segment to the precise point to split and hit OK [5 ↩]; SEG 005 is now split in two and a new serial number, e.g. 254, is created for the right half of the segment).

15. "D"EL "F"ILL-IN
"C"REATE "S"PLIT
"T"RUNCATE: C

(User wishes to create a segment manually)

[The '+' (crosshair) comes on.]

(With the keypad keys, the user defines each point, entering the last point with ↩; if only one point is entered, a 1-point segment is defined; if more than one point is entered, a segment is defined with straight lines connecting the points.) (Figure *I*4 – 5)

SEG 255 CREATED.

16. "D"EL "F"ILL-IN
"C"REATE "S"PLIT
"T"RUNCATE : F

(User wants to connect (fill-in) segment 005, the newly created segment 255 and segment 045.)

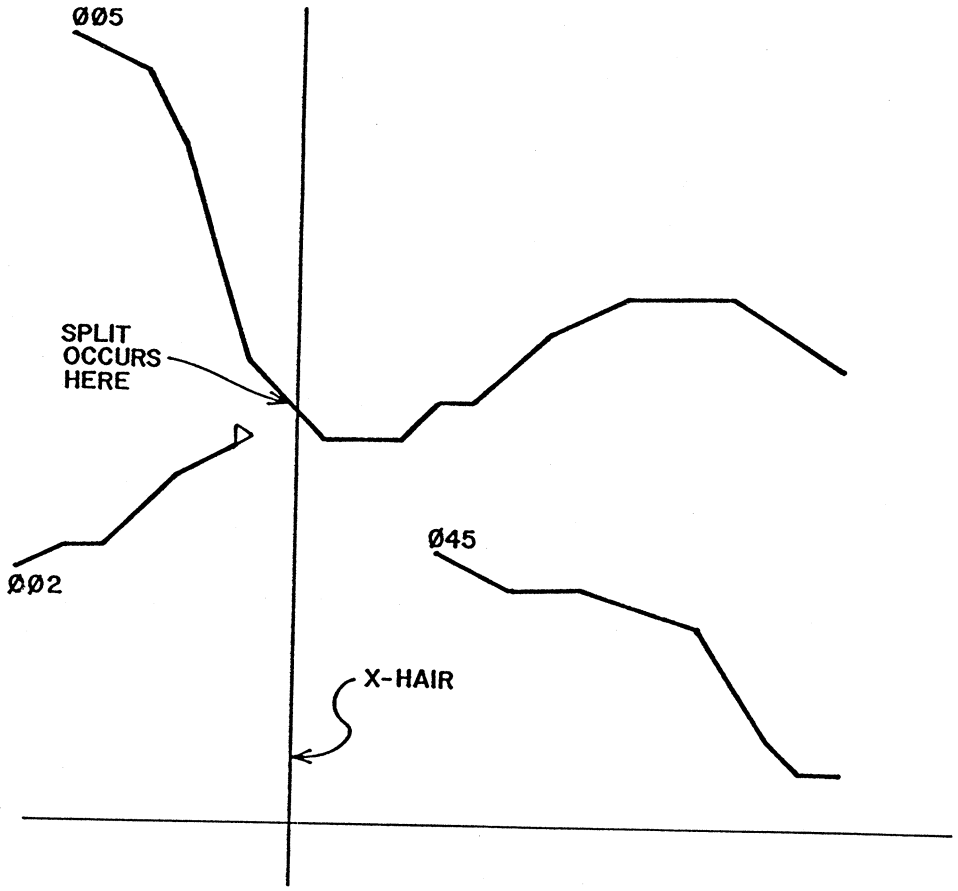

Figure I4 - 4 Appearance of the screen during the execution of step 13. The vertical crosshair is used to define the cutoff. The raw data amplitudes, shown in Figure I4-3 have been omitted here.

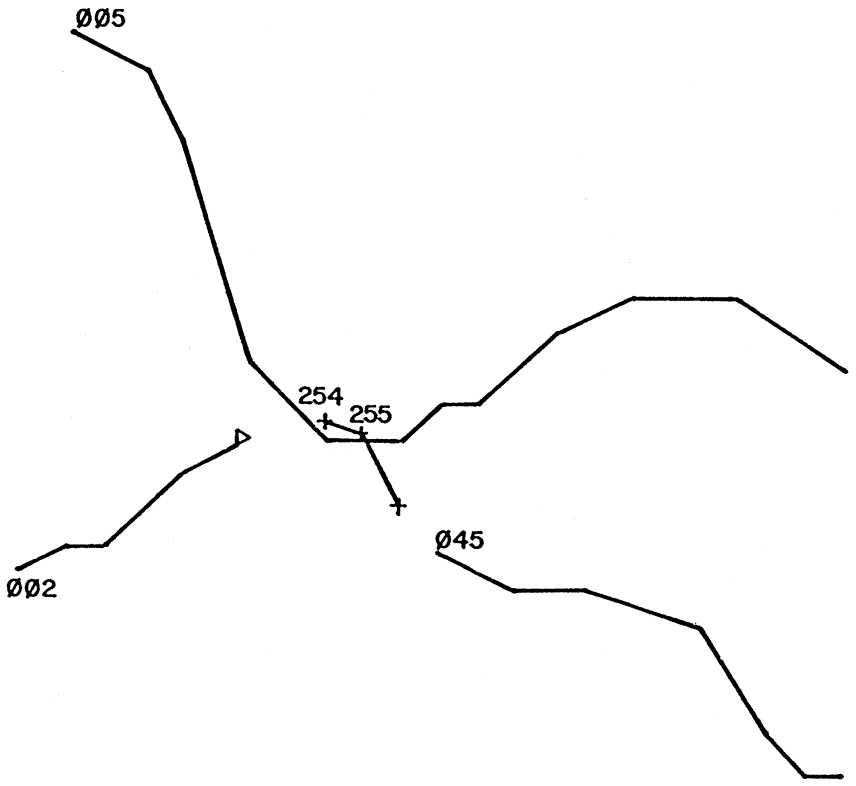

Figure I4 - 5 The segments as they appear just prior to performing "F" ILL-IN in step 15. As in Figure I4-4, the raw data amplitudes shown in Figure I4-3 have been omitted here.

SEG : 005
SEG : 255
SEG : 045
SEG : ↩

(A line will be drawn from the end of segment 255 to the beginning of segment 045)

CONFIRM, Y/N:Y

(User again confirms it; the label 045 will disappear as segment 045 is now part of segment 255; a line will next connect segments 005 and 255);

CONFIRM, (Y/N): Y

(User again confirms it; the label 255 will disappear and it is now a part of segment 005 (Figure *I*4 – 6).)

17. "D"EL "F"ILL-IN
"C"REATE "S"PLIT
"T"RUNCATE: F

(User now wants to fill-in segments 002 and 254)

SEG : 002
SEG : 254
SEG : ↩

[segments 002 and 254 are connected]

CONFIRM, (Y/N):Y

(User conforms it; the label 254 disappears as this trace is now a part of segment 002 (Figure *I*4 – 7)).

18. "D"EL "F"ILL-IN
"C"REATE "S"PLIT
"T"RUNCATE:↩

(User is now done with editing in this window)

"A"UTO - DIGITIZE
^"B"LOWUP "E"DIT
OR ^"R"AW DATA? R

(User wants to see on the screen raw data in another area of missing segments to be outlined with crosshairs)

[same as step 10]

(A rectangular area is defined and confirmed by the user, Figure *I*4 – 8.)

19. "A"UTO - DIGITIZE

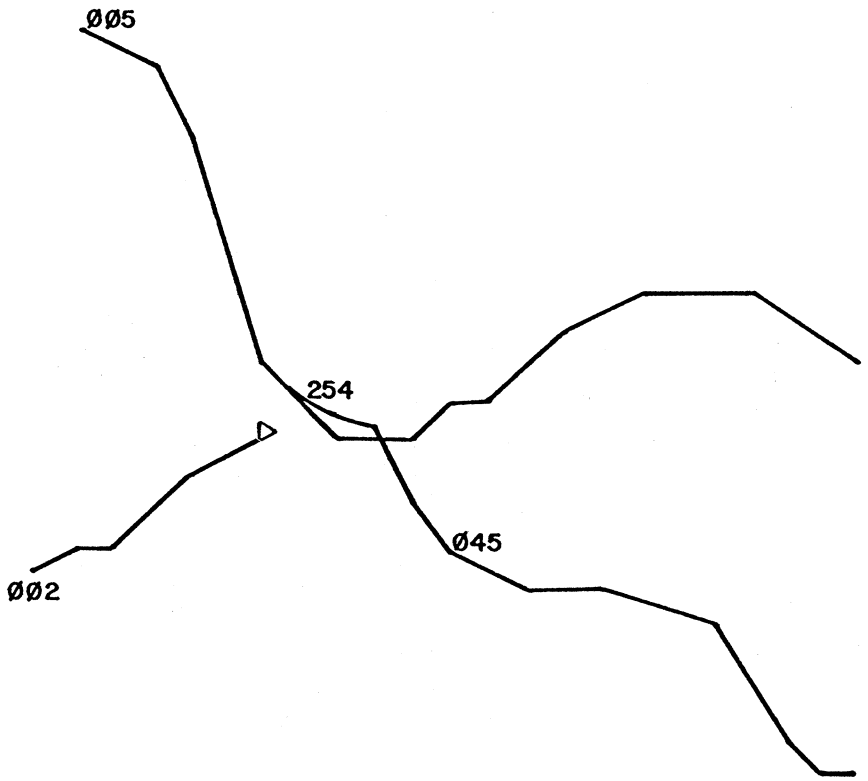

Figure I4 - 6 The segments as they appear after performing FILL-IN in step 15. Note that seg # 254 refers to the segment created earlier by the splitting of seg # 005.

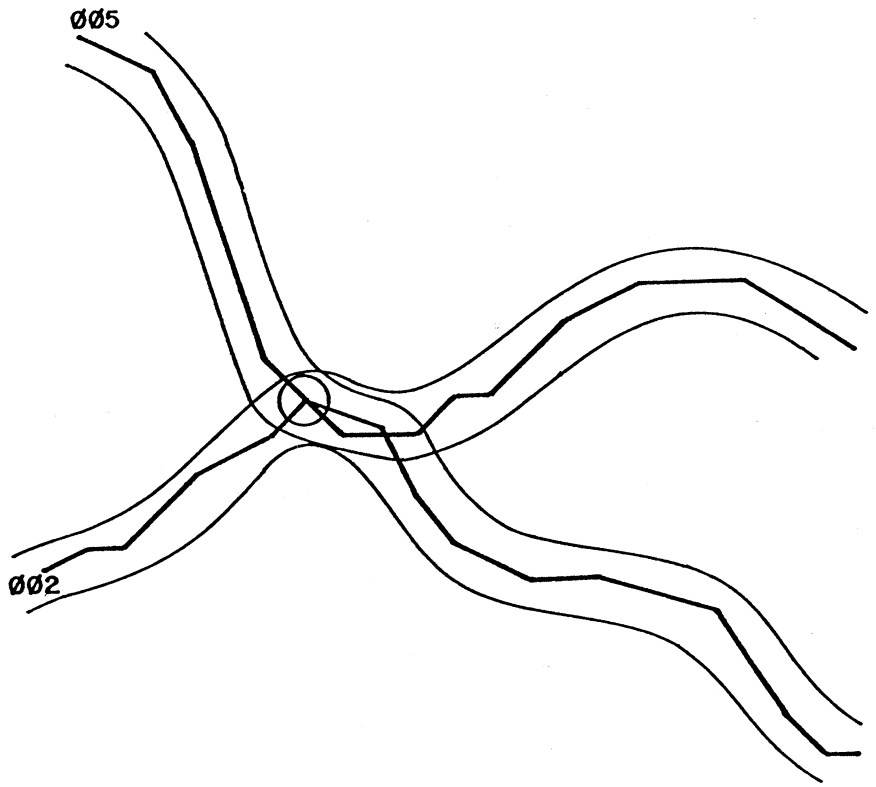

Figure I4 - 7 After editing, one may erase the screen and replot the same window. This is how the edited segments would appear (heavy, piecewise straight, lines). Note that the point circled is shared by the 2 segments. Light smooth lines outline the areas corresponding to the traces and filled with raw data.

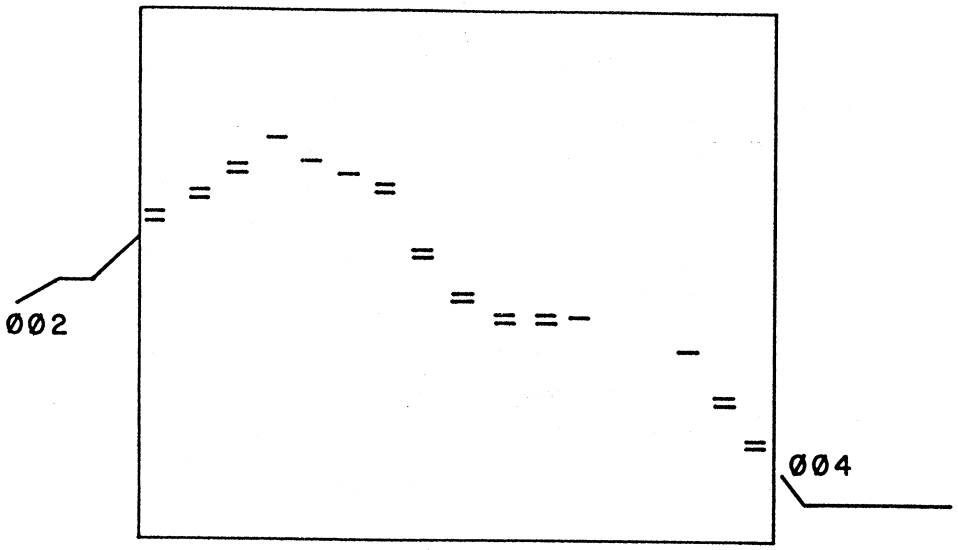

Figure I4 - 8

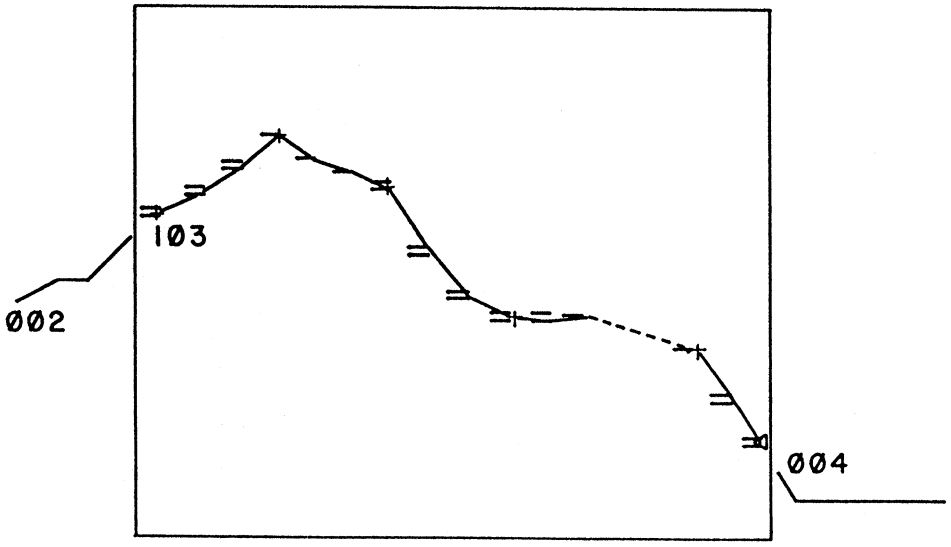

Figure I4 - 9

^"B"LOWUP "E"DIT
or ^"R"AW DATA? ↩

(User wants the program TV to automatically digitize a segment of the raw data displayed)

[crosshairs come on]
(As in step #8, a rectangular area is defined and confirmed by the user)

CONFIRM, Y/N: Y

[a '+' (crosshair) will move along the digitized path. Depending on the total number of points digitized, one or more segments are defined and eventually connected together as one segment. The assigned serial number, e.g. 103, will then appear, Figure *I*4 – 9)

20. "A"UTO - DIGITIZE
^"B" LOWUP "EDIT
or ^"R"AW DATA? ↩

(User is ready to finish)

[screen erased, and rescaled to that of the full record on the screen; reference coordinates are displayed by arrows]

"Q"UIT, OR PLOT
"N"ONE, "S"OME
OR "A"LL SEG? Q
MP##: MP01

(User saves the current map in file MP01.DAT; other files written will be SC901.DAT containing the coordinates of the segments that were created, and TPFD01.DAT, with information for the next phase of the system (SCRIBE))
[screen erased]

```
**********
*   TV   *
**********
```

"C"ONTINUE OR "Q"UIT: Q

TV VERSION 3.0

[Program stops].

*I*5 SCRIBE

*I*5.1 Introduction

With editing completed, the trace segments are ready to be plotted and/or written onto a disk file. Initially, SCRIBE requests for options to plot, write onto disk or both:

"P"LOT, "D"ISK, or "B"OTH:

Next, the output file name is requested (if disk file is to be created):

FILENAME FOR OUTPUT RAW DATA ON DISK (A2O): V0X0001.DAT ↩

SCRIBE then asks for the mapfile suffix created by TV:

ENTER MAPFILE SUFFIX: MP01 ↩

The map file MP01.DAT is open, and its first record read. SCRIBE is now ready to plot and/or write onto disk all types of curves found. Recall that the curve types are defined as follow:

Type	Description
3	time-clock marks
2	half-second time marks
1	fixed traces (baselines)
0	acceleration traces

SCRIBE has one additional question:

INCLUDE REFERENCE LINES? (Y/N): Y ↩

Here reference lines include lines of type 1, 2 and 3. For each type, starting with type 3, SCRIBE goes through an inner loop searching for a segment of that type in zone 1 (top zone). The serial and type numbers of any such segment found are written onto the screen with a question:

THIS SEGMENT TO BE PLOTTED? (Y/N):

If the segment is to be plotted, SCRIBE will proceed to read the points from the disk files and plot them and/or write them onto the disk. When the end of the segment in the top zone is reached, and if there are more zones, SCRIBE will first identify the matching segment in the next zone. It then proceeds to plot and/or write data to disk, after making the necessary corrections to each coordinate to recreate the original, a continuous curve out of the corresponding segments in two or more zones. SCRIBE will repeat this for each segment until all the zones are read.

If dashed reference lines are present (type 3 radio clock time-hack traces, type 2 crystal clock time or half-second traces), they are written to file in two formats: an all point version followed by the 'abbreviated', dash end-points-only version.

*I*5.2 Transformation Correction

When more than 1 zone (sections) of the record are included, as consecutive sections, one below the other, all photocopied onto the 8.5×11 inch paper, these sections need to be assembled together to recreate the original continuous record. Each zone has an associated pair of fiducials at the left and right ends. The points in each zone will be rotated so that the resulting fiducial pairs are perfectly horizontal. They are then translated so that the left fiducial of the zone will correspond to the right fiducial of the previous zone. This is summarized in the following set of transformation equations (Figure $I5-1$):

For Section i, let

$$
\begin{aligned}
(XL_i, YL_i) &= \text{Coordinate of the left fiducial in zone i,} \\
(XR_i, YR_i) &= \text{Coordinate of the right fiducial in zone i,} \\
D_i &= \text{Distance between the left and right fiducials in zone i} \\
D_i &= \sqrt{(XR_i - XL_i)^2 + (YR_i - YL_i)^2} \qquad \text{(I5.1)} \\
\alpha_i &= \text{angle in zone i to be rotated so that the} \\
&\qquad \text{fiducial pair is horizontal} \\
\alpha_i &= \tan^{-1}\left(\frac{YR_i - YL_i}{XR_i - XL_i}\right) \qquad \text{(I5.2)}
\end{aligned}
$$

Then, for (X,Y) the coordinates of a point in zone i, the rotation by an angle α_i results in

$$
\begin{aligned}
\text{Rotated } X &= (X - XL_i)\cos\alpha_i + (Y - YL_i)\sin\alpha_i \\
\text{Rotated } Y &= (Y - YL_i)\cos\alpha_i - (X - XL_i)\sin\alpha_i \ . \qquad (I5.3)
\end{aligned}
$$

Let

(XT_i, YT_i)= translated coordinates for points in zone i, then

$$
\begin{aligned}
XT_i &= XT_{i-1} + D_{i-1} \\
YT_i &= YT_{i-1} \quad (YT_1 = YL_1) \qquad (I5.4)
\end{aligned}
$$

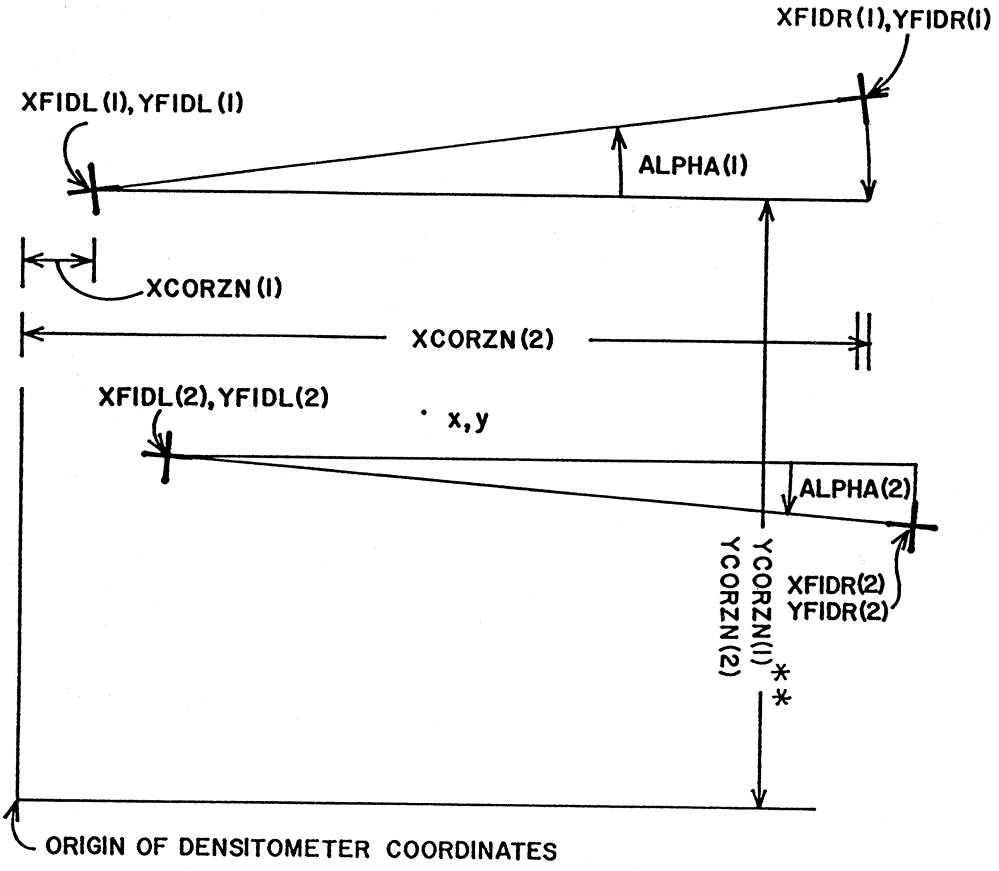

Figure I5 - 1 Correction constants.

so that

$$\begin{aligned} CORRECTED\ X &= XT_i + \text{Rotated } X \\ &= XT_i + (X - XL_i)\cos\alpha_i + (Y - YL_i)\sin\alpha_i \\ CORRECTED\ Y &= YT_i + \text{Rotated } Y \\ &= YT_i + (Y - YL_i)\cos\alpha_i - (X - XL_i)\sin\alpha_i\ . \end{aligned} \qquad (I5.5)$$

Such transformation correction is applied by SCRIBE to every point of every segment in every zone and will result in the recreation of the original record.

$I5.3$ Program Flow of SCRIBE (Figure $I5-2$)

Steps # ACTIVITY

1. Initialization
   SCRIBE initially asks for the map file suffix, opens the file MPxx.DAT, where xx is the suffix input by the user. SCRIBE reads the first record of the map file. It then opens the corresponding file, TPFDxx.DAT and reads the whole file containing information on the fiducial coordinates, on the serial number, type, initial y-coordinate and zone numbers of the segments.

2. Correction Constants
   SCRIBE calculates from the fiducial coordinates the transformation correction constants used later to transform the coordinates of every point of every segment in every zone, so as to recreate the original record.

3. LOOP
   SCRIBE begins looping on the curve types, starting from type 3 (Time Hack), followed by types 2 (Half-second), 1 (baselines) and 0 (acceleration). For each type, an inner loop searches for a segment of that type in zone 1.

4. Segment Address
   SCRIBE finds the segment serial number in the map file and identifies the file name suffixes of the SCxxx.DAT file containing the y-coordinates of the segment, the beginning and ending addresses within the SCxxx.DAT files, and the first x-coordinate of each piece of the segment. SCRIBE reads in blocks of y-coordinates, and computes the corresponding x-coordinate for each y.

5. Transformation Correction
   SCRIBE "rotates" the points around the left fiducial of the zone containing the point to eliminate the fiducial skew (equation $I5.3$), and the "rotated" coordinates are then added to the translational terms (equation $I5.5$) to recreate the original continuous curve.

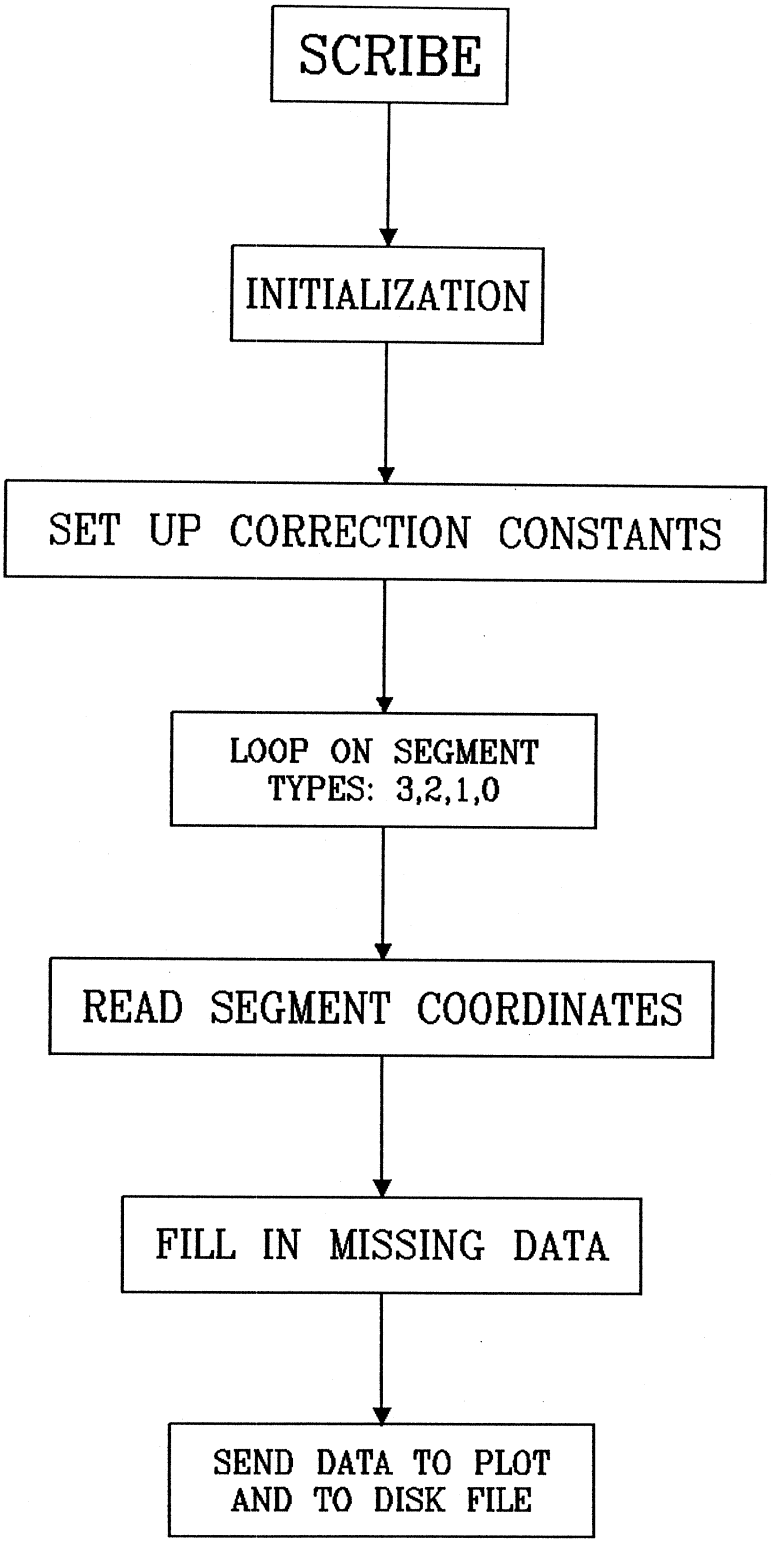

Figure I5 - 2 Flow-chart of program SCRIBE.

6. Fill-in Missing Data
   'Missing' data is defined as empty gaps lying between two successive points of the segment. Those are stored as 0 y-coordinates in the data files. They exist in segments at area of missing raw data or are created by 'FILLIN' during TV editing. SCRIBE assumes that the curve is a straight line joining the two points to the left and right of the missing data.

7. Output: to Plot and to File
   When the points of a segment are transformed, they are sent by SCRIBE to the plotter and/or the disk file. The disk file will now be called the file of unscaled RAW DATA.

*I*5.4 Input/Output files from Digitization

The following is a summary of the list of all files created during digitizations, starting from SCAN, through FILM, TRACE, TV and SCRIBE.

1. IMAGE.RAW This is the file created by the scanning program SCAN. It is the image file resulting from scanning the 8.5×11 inch paper containing the record to be digitized.

2. REFS.DAT This file is created by FILM containing the coordinates and types of the reference lines and points. It is read by TRACE and TV.

3. PARMS.DAT This file is written by TRACE, containing parameters associated with each record of the segments written on to disk. It contains information on the filename SCxxx.DAT of the record, segment type, zone number and the first x-value of the segment, etc.

4. SCxxx.DAT Files of this name are written by TRACE. Each such file contains the y-coordinates of the segments. xxx ranges from 001 to 999. Files SC001.DAT to SC899.DAT are created by TRACE to be read by TV and SCRIBE. The more complicated is the record, more of these will be used. Files SC900.DAT to SC999.DAT are created by TV during editing, to be read by SCRIBE.

5. SUMUP.DAT This file is written by TRACE. It contains the maximum x and y scanner units found for the segments and the total number of segments found.

6. TPFDxx.DAT Files of this name are written by TV. Those contain a list of the segment serial numbers, the y-coordinates of their first point, segment type and film zone. Those files also contain the fiducial coordinates in descending order. TPFDxx.DAT is created at the end of editing TV. The number xx corresponds to the map file MPxx.DAT, where xx ranges from 00 to 99. This file is to be read by SCRIBE.

7. MPxx.DAT Files of this type are written by TV. The map file contains information on all given segments created or edited by TV. A segment, after editing, might consist

of points stored in several different SCxxx.DAT files, or in different parts of a single SCxxx.DAT file. Information on the address of each group of these points are contained in the map file MPxx.DAT, created at the end of editing version number xx by TV, where xx ranges from 00 to 99. This file is to be read by SCRIBE.

8. Unscaled RAW DATA FILE: V0X0001.DAT This is the final file written by SCRIBE containing the unscaled coordinates of the Raw Data of the digitized record.

Having completed the digitization of an accelerogram record, with the unscaled RAW DATA file V0X0001.DAT, part II of this report will describe the data processing of the strong-motion record.

PART II:

DATA PROCESSING USING PC

Table of Contents (for Part II)

*II*1 The Original Data Processing System

*II*1.1 Introduction: Previous Work

Data Processing of the strong-motion accelerograms evolved alongside with digitization of analog records, after the first earthquake accelerogram was recorded on March 10, 1933, during the Long Beach earthquake in California. This remarkable event, which triggered numerous pioneering accomplishments in strong motion instrumentation, was commemorated during the 50th anniversary of strong-motion seismology in Los Angeles (Hudson, 1984). Through the 1940's and 1950's, there were only a dozen or so recorded "significant" strong motion accelerograms (Alford et al., 1951). The accelerograph data processing then required lengthy manual calculations (Housner, 1947) or the use of analog computers (Biot, 1941). The 1960's marked the beginning of the rapid growth of the number of recordings and of the development and use of digital computers. With these, new methods associated with digital data processing slowly gained in speed, accuracy, access and popularity (Brady, 1966). In the early 1970's after the San Fernando earthquake (1971) in California, the large number of recorded accelerograms, and the need of many investigators to compare their results on a common basis, finally resulted in the need for a systematic development of routine data processing of strong-motion accelerograms.

The systematic development of routine computer programs for processing strong-motion earthquake accelerograms was completed in the early part of the 1970's (Trifunac and Lee, 1973). Almost all of the records then were in analog form and were digitized manually. In fact all of the records from the 1971 San Fernando earthquake have been digitized this way (Hudson et al., 1971). The routine data processing software was then developed for the manual digitization scheme. Our programs (Trifunac and Lee, 1973) were first written for the IBM 7094 and 360 computers. These programs involved the following steps:

(I) Volume I Processing:

The half-second timing marks were first checked for "evenness" of spacing, and then smoothed by the 1/4, 1/2, 1/4 running average. The x-coordinates of each trace were then scaled to units of time in seconds. Each fixed trace (baseline) was next smoothed and subtracted from the corresponding acceleration trace, with the y-coordinates subsequently scaled to units of g/10, (where g = 9.81 m /sec^2).

(II) Volume II Processing:

The scaled uncorrected Vol. I acceleration data was next corrected for instrument response and baseline adjustment. The data were first low-pass filtered with an Ormsby filter having a cutoff frequency $f_c = 25$ Hz and a roll-off termination frequency $f_t = 27$ Hz. Instrument correction was next performed using the instrument constants. These constants are the natural frequency and ratio of critical damping of the instrument, considered as

a single-degree-of-freedom system. These were determined from calibration tests for each accelerograph transducer. The data were then baseline corrected by a highpass Ormsby filter. The cutoff and roll-off frequencies of the filter were usually determined from the signal-to-noise ratio of each component (Trifunac and Lee, 1978). The acceleration data were then integrated twice to get the velocity and displacement data. To avoid long period errors resulting from the uncertainties involved in estimating the initial values of velocity and displacement, the computed velocity and displacement data were high-pass filtered at each stage of integration, using the Ormsby filter with the same cutoff and roll-off frequencies as for the corrected accelerogram.

(III) Volume III Processing:

Using an approach based on the exact analytical solution of the Duhamel integral for successive linear segments of excitation, this state consisted of calculating the Response and Fourier Spectra for up to 91 periods and 5 damping ratios. From the Vol. II corrected accelerogram data, the times of maximum response for all periods and damping ratios were also recorded.

Following early developments of the Automatic Routine Digitization System (Trifunac and Lee, 1979), the above computer processing programs were all modified to run on the Data General mini computers. This new approach which took advantage of image processing techniques increased the speed of overall data processing by one order of magnitude.

*II*1.2 The Updated System

In general, the principles and the requirements governing the routine data processing of strong-motion records have changed little, if any, since the early 1970's. However, since then, we have witnessed a remarkable progress in digital signal processing techniques, in their accuracy, efficiency, speed and in the major reduction of the cost of the required hardware. These improvements have been incorporated into the routine data processing of strong-motion accelerograms (Lee and Trifunac, 1984).

With the present development of the new automatic digitization system using a digital scanner interfaced with a PC, the new and improved version of all routine data processing software for strong-motion accelerograms is now running on a PC. Together with the digitization software, this then becomes a complete software package for desktop digitization and processing of accelerograms. The following six chapters will describe the new version of the programs used for routine data processing of accelerograms: *VOLUME* 1 (Chapter *II*.2), *VOLUME* 2 (Chapters *II*3,4,5,6) and *VOLUME* 3 (Chapter *II*.7). These chapters will discuss the following steps in data processing:

(i) Volume 1 Scaled Uncorrected Acceleration Data

This step of processing remains essentially same as before. The data are scaled to units of seconds and g/10. No filtering or any corrections are made, so that the data can be considered as close a representation of the original raw information as it is feasible to achieve with digitization.

(ii) Volume II Low-pass Filtering

Low-pass filtering is performed to eliminate the high frequency digitization errors. The problem associated with the design of a low-pass filter will be discussed first. Different types of low-pass filters that have been used for accelerograms will be reexamined. Guidelines for the design of low-pass filters for use with accelerograms will be presented, followed by an example of a low-pass filter.

(iii) Volume II Instrument Correction

Numerical differentiation is required for instrument correction. Instrument correction represents the step of the transformation from the digitized relative displacement of a transducer x(t) to the true input ground acceleration a(t). The ideal differentiating filter will be examined first, and the problems associated with its design will be discussed. Different types of differentiating filters available are examined and their performance evaluated. The guidelines for the design of the filter for instrument correction in earthquake engineering will be considered, and followed by the presentation of a differentiation filter designed within the proposed guidelines.

(iv) Volume II Baseline Correction

Since the frequencies, where the long period errors dominate in digitized data, represent a small fraction of the whole frequency band of the data, this becomes the problem of narrow band filtering or of narrow band rejection. An efficient algorithm for the design of narrow band filtering involving multi-stage decimation and interpolation will be adopted. The procedure for decimation and interpolation of data involving the design and use of appropriate low-pass filters will be discussed also.

(v) Automatic Determination of the Frequency Band of the Data with Acceptable Signal-to-Noise Ratio

A frequency band from .07 to 25 Hz has been considered in routine processing of acceleration data some twenty years ago. However, this frequency band actually varies from record to record, and sometimes even from component to component, depending

upon the signal-to-noise ratio of the data. A new subroutine in the data processing software has been developed which, for each input component of the acceleration data, determines the appropriate frequency limits for band-pass filtering in the above steps, so that the resulting data in the band is as free from noise as desirable. This procedure has been introduced to control uniformly the signal-to-noise ratio of the data.

(vi) Calculation of Velocity and Displacement Data

With the acceleration data instrument corrected and band-pass filtered, digital integration is performed twice to get the velocity and displacement data. The ideal integration filter is first derived and the problem involved in its implementation examined. The trapezoidal rule of integration originally used together with selected available algorithms will be examined and their performances compared. A guideline for the design of the appropriate integration filter will be considered. Criteria for the use of the trapezoidal rule of integration within the guideline are examined, together with examples of possible new integration filters.

(vii) New Volume III Data Processing

Efficient algorithm for the calculation of the relative displacement, velocity and acceleration of the response of a single-degree-of-freedom-system oscillator to earthquake excitation has been used in the calculation of Response and Fourier Spectra for specified natural periods and damping ratios (Volume III data). Compared to our old algorithm, the new algorithm results in a saving of as much as 56% of computer time.

*II*2 Data Processing for Volume I: Scaled Uncorrected Acceleration Data

II.2.1 Input

The Volume I data consists of scaled digitized acceleration data of earthquake strong-motion record obtained from strong-motion instruments. No band-pass filtering, instrument corrections or adjustments of any type have been made so that the data may be regarded as scaled "uncorrected" data. The scaled digitized data is thus considered to be as close as possible a representation of the original raw data.

The file, V0X001.DAT, in our examples, from the program SCRIBE of the digitization package, contains the RAW DATA coordinates of the digitized record. The program *VOLUME*1 will read the coordinates of all the traces in the file, starting from the time-hack (type 3) traces, followed by the half-second timing marks (type 2), the baselines (type 1) and finally all the acceleration traces(type 0). Information about the earthquake, the recording station and the instrument, and the record file itself are also read.

The information on the earthquake to be supplied by the user includes:

(1) published name of the earthquake,

(2) date and time of the earthquake,

(3) epicentral coordinates of the earthquake (latitude and longitude),

(4) published magnitude (including magnitude definition) and maximum intensity (Modified Mercalli, Medvedev-Karnik-Sponheuer, etc...) of the earthquake, and

(5) focal depth of the earthquake in km.

Information on the recording station and instrument includes:

(1) address identifying the location of the station,

(2) station coordinates (latitude and longitude)

(3) modified Mercalli Intensity (or other applicable scale) at the site, and

(4) station identification name and/or instrument serial number,

Information on the record file includes:

(1) record reference name (like AA001),

(2) record log number (like 71.001), (e.g., see Lee and Trifunac, 1982)

(3) the component direction and name, the transducer sensitivity (cm/g) and its natural period and damping ratio, for each component of recorded acceleration.

II.2.2 Program Flow

II.2.2.1 Scaling the Half-Second Timing Marks

From the RAW DATA file, the abbreviated version of the half-second timing trace is read in. This is the version present in the file where only the end-point coordinates of each timing marks are written. The program $VOLUME1$ will first check that the timing coordinates, taken to be the mid-points of the timing marks, are in increasing order, and are even in spacing. Those are then smoothed by the 1/4, 1/2, 1/4 running average. The smoothed timing marks are then checked for even spacing. Timing marks which are "unusual" in spacing are typed out on the screen with a warning.

*II*2.2.2 Scaling the Baseline (Fixed Trace)

The baseline coordinates are next read in. Those are digitized at the same resolution as the acceleration traces, which is normally with 300 or 600 points/inch. Most of the records have two or more such fixed traces, produced by 'fixed' mirrors rigidly attached to the accelerograph frame (Trifunac and Hudson, 1970). Occasionally, these traces may depart measurably from straight lines, usually in cases involving long-period motions ascribed to film distortion, motion of the film in the drive mechanism, etc.. The digitized fixed trace is first averaged over intervals of one-quarter second, or to four points per second, and then smoothed by the 1/4, 1/2, 1/4 running average.

*II*2.2.3 Scaling the Acceleration Traces

The acceleration trace is next scaled and a horizontal line is fixed at the zero mean level, as described in the following. To fix the particular values of the digitized coordinates, some more-or-less arbitrary decisions must be made as to the position of a straight reference line. When the record is placed into the scanner, it is lined up with the horizontal axis of the glass, as closely as can be judged by eye. For this purpose, the fixed traces serve as useful guides, as do the zero trace sections at the beginning of the record before the triggering of the instrument. It must be realized, however, that small shifts of the axis in translation or rotation can lead to large deviations in the displacement curves. Therefore, some technique which assures a uniform result is needed. For this purpose, the following procedures have been adopted. If the corresponding sections of the record traces and the fixed mirror traces have been digitized simultaneously, then the subtraction of the two traces will correct for any slight rotation of the record on the instrument, so that only a translation of the zero line is required. The zero axis is translated until the integral of the digitized acceleration curve over the length of the record is zero. This is, same as making the mean zero, or making the sum of the squares of the deviations from the zero line a minimum. Physically, this means that the change in ground velocity from beginning to end of the record is zero. For any individual earthquake record, this assumption cannot be justified, but it is nevertheless the most practical choice on which to base the first step in a standard procedure.

For those records for which fixed traces are not available, or for which there are more than one section to be digitized, the baseline is not only translated to make the mean zero as above, but a very small rotation is introduced to make the sum of the squares of the deviations from the straight line a minimum. This removes slight rotational misalignment without interfering with the basic data. In all the cases, the minimum RMS acceleration values are recorded as a significant parameter of the record. It should be noted that this is always the RMS value calculated over the entire length of the digitized record, which may be considerably longer than the strong-motion portion of the record.

It is believed that the above data processing steps represent the minimum interference with the basic data, and that the digitized data so obtained may legitimately be referred to as the basic "uncorrected" data.

*II*2.3 The Volume I Output File: *V1X0001.DAT*

At the end, the scaled data are written onto a file, '*V1X0001.DAT*' on disk. Each component of the acceleration data is accompanied by its heading data containing all pertinent information on the station, the earthquake, and the instrument characteristics. The heading data are read, reproduced, and later augmented by the programs of Volume II and III. For this reason, ample space in various arrays of the heading data is left unused to allow the addition of significant information during the later stages of processing or analysis. The set-up of a Volume I disk file is as follows:

Volume I disk file, '*V1X0001.DAT*' (one file per acceleration component) has:

1) Heading data of alphanumeric type
2) Heading data of integer type
3) Heading data of floating point type
4) Scaled data sequence (time, acceleration)
5) EOF (end of file)

The detailed description and a sample of the heading data set are given in the following:

Volume I Heading Data

Line Number	Heading Data Array (CORTIL(I),I=Il,I2) used in Volume I MAIN Program Il-I2	Format (40A2)	Description*
1	1-40	"	File identification
2	41-80	"	Name of the earthquake
3	81-120	"	Date & time of the earthquake

4	121-160	"	Volume reference and log nomber of the accelerogram
5	161-200	"	Station No. & coordinates of the accelerograph station
6	201-240	"	Location of the station
7	241-280	"	Component direction (pendulum motion for the upward deflection of trace on the record)
8	281-320	"	Full title of the earthquake
9	321-360	"	Epicenter of the earthquake
10	361-400	"	Natural period; damping & sensitivity of the instrument
11	401-440	"	No. of points & duration of data
12	441-480	"	Units of data (g=981 cm/sec^2)
13	481-520	"	RMS of data

* The alphanumeric information on each line above ranges from columns 1 to 72. Integers in columns 73 and 74 from the fourth line on dictate the number of letters in each line.

*II*3 Data Processing for Volume II: (A) Low-Pass Filtering

*II*3.1 Introduction

The scaled uncorrected acceleration data, obtained from the first stage of processing next needs to be corrected. The processing for corrected accelerograms involves low-pass filtering, instrument correction and baseline correction. Low-pass filtering is applied to remove the high frequency errors present in the accelerograms (Trifunac et al., 1971, 1973). Those may be present in the original record, or may result from digitization by the scanner.

In the processing routines originally developed for manually digitized data (Trifunac and Lee, 1973), the hand digitized data was available at only 30 to 50 points/sec. Those were first interpolated to equally-spaced data at 200 points/sec using straight line interpolation. Later, in automatic digitization (Trifunac and Lee, 1979), the digitized data became available at 200 or more points/sec for analog records on film at 1cm/sec. Now, with digitization using presently available digital scanners interfaced with a PC, the data can be digitized with 300 to 600 points/in. In all cases, the data are first generated by interpolation or by decimation to equally spiced 200 points/sec. The data are then low-pass filtered at a standard cutoff frequency of 25 Hz.

Low-pass filters, like the high-pass and band-pass filters, have an amplitude response of unity within the pass band and zero elsewhere (the stop band) in the frequency domain. The pass bands for low-, high- and band-pass filters are illustrated in Fig. $II3-1$. The frequencies ω_L and ω_H are called the cutoff frequencies. The response functions in this figure are those of the ideal filters, and will be simulated numerically.

*II*3.2 Lowpass Filter: Ideal Unit Impulse Response Function

An ideal low-pass filter in the frequency domain passes all low frequencies, $|\omega| \leq \omega_L$, without any change, and blocks all high frequencies $|\omega| > \omega_L$. Its transferfunction $H(\omega)$ is

$$H(\omega) = \begin{cases} 1 & |\omega| \leq \omega_L \\ 0 & |\omega| > \omega_L \end{cases}. \qquad (II3.2.1)$$

The unit impulse response, $h(t)$, and $H(\omega)$ form a Fourier Transformed pair, so that:

$$h(t) = \frac{1}{2\pi}\int_{-\omega_L}^{\omega_L} H(\omega)e^{i\omega t}d\omega = \frac{\omega_L}{\pi}\frac{\sin\omega_L t}{\omega_L t} \qquad (II3.2.2)$$

For an arbitrary time function, $x(t)$, acting as the filter input, the output time function, $y(t)$, is given by the convolution integral of $x(t)$ with $h(t)$,

$$y(t) = \int_{-\infty}^{\infty} h(\tau)x(t-\tau)d\tau. \qquad (II3.2.3)$$

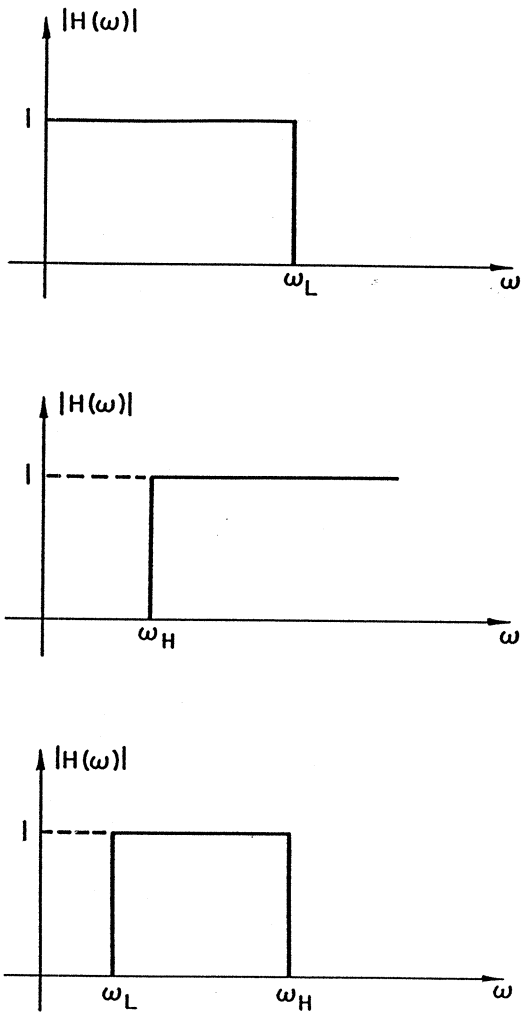

Figure II3 - 1 Ideal low-pass (top), high-pass (center) and band-pass (bottom) filters.

For digital data sampled at equally spaced intervals of T seconds, the Nyquist (folding) frequency of the input data is given by:

$$\omega_N = \pi/T. \qquad (II3.2.4)$$

Assume that the cutoff frequency is less than the Nyquist Frequency ($\omega_L < \omega_N$). In the discrete time domain, the ideal low-pass filter can be expressed as complex Fourier Series:

$$H(\omega) = \sum_{-\infty}^{\infty} h[k] e^{-ik\omega T} \quad \text{for} \quad -\omega_N \leq \omega \leq \omega_N \qquad (II3.2.5)$$

and the corresponding impulse-invariant filter weights $h[k]$, are

$$h[k] = \frac{\omega_L T}{\pi} \frac{\sin k\omega_L T}{k\omega_L T} \qquad (II3.2.6)$$

for k = ...,-2,-1,0,1,2,... from $-\infty$ to ∞. Given the equally spaced set of input data, $(x[n])$, the output data $(y[n])$ will then be given by

$$y[n] = \sum_{n} h[k] x[n-k] \qquad (II3.2.7)$$

for k = ...,-2,-1,0,1,2,....

An exact realization of an ideal low-pass filter given by (*II*3.2.1) thus requires an infinitely long sequence $(h[k])$ which extends to infinity in the direction of both positive and negative time.

Several interesting properties of the filter follow directly from Eq. (*II*3.2.7). Due to the non-zero values with positive and negative time indices, it represents a noncausal system. The response sequence in Eq. (*II*3.2.7) consists of both anticipation ($k < 0$) as well as memory ($k > 0$) terms. Consequently, the output values are influenced by past, present and future input. This requires that the input signal be available in a stored form. For data processing carried out by a computer, this requirement will not create any difficulties.

The impulse response terms in Eq. (*II*3.2.6) form an even time sequence, with $h[-k] = h[k]$, so that the memory and anticipation (past and future) terms are mirror images of each other. The ideal filter is therefore a symmetric one. Consequently,

$$H(\omega) = h[0] + 2\sum_{k=1}^{\infty} h[k] \cos(k\omega T), \qquad (II3.2.8)$$

so that the transfer function is real. The ideal low-pass filter thus has zero-phase characteristics, and a system described by Eq. (*II*3.2.8) will perform a phase-distortionless

transmission, a property which is required and essential in most Earthquake Engineering Data Processing applications.

A low-pass filter with impulse response function defined by ($II3.2.7$) thus performs an ideal separation of the desired frequency components from the unwanted high frequencies. However, since infinitely long signals cannot be processed by digital computers, the sequence ($h[k]$) has to be truncated. Unfortunately, the convergence of the sequence is slow and large number of terms are often needed to get to the sufficiently small coefficients $h[k]$.

Taking a finite number of terms in Eq. ($II3.2.8$), will give:

$$H(\omega) = h[0] + 2\sum_{1}^{N} h[k]\cos(k\omega T) \qquad (II3.2.9)$$

Truncation will introduce errors not only in the vicinity of the cutoff frequency, a phenomenon known as Gibbs effect. This effect may be reduced by increasing the length of the impulse response. Further, this can be improved be a smoothing technique, known as windowing, in the time domain. Take, for example, Hanning window:

$$w(t) = \frac{1}{2}(1 + \cos\frac{t\pi}{NT}). \qquad (II3.2.10)$$

Taking $w[k] = w(kT)$, the "windowed" coefficients become

$$b[k] = h[k]w[k] = \frac{(1 + \cos(k\pi/N))\sin k\omega_L T}{2k\pi} \qquad (II3.2.11)$$

and ($II3.2.7$) then becomes

$$y[n] = \sum_{-N}^{N} h[k]w[k]x[n-k] = \sum_{-N}^{N} b[k]x[n-k]. \qquad (II3.2.12)$$

For example, the transfer function amplitudes for the case of $N = 30$, $\omega_L = 2\pi/T$, or the cutoff frequency being $1/5$ that of the Nyquist frequency, is given in Fig. $II3-2$. Since the filter weights are symmetric, Eq. ($II3.2.12$) can be written as

$$y[n] = b[0]x[n] + \sum_{k} b[k](x[n-k] + x[n+k]). \qquad (II3.2.13)$$

Another procedure for better and smoother approximations of the discontinuity at the cutoff frequency is to introduce a transition frequency band within which the pass-band

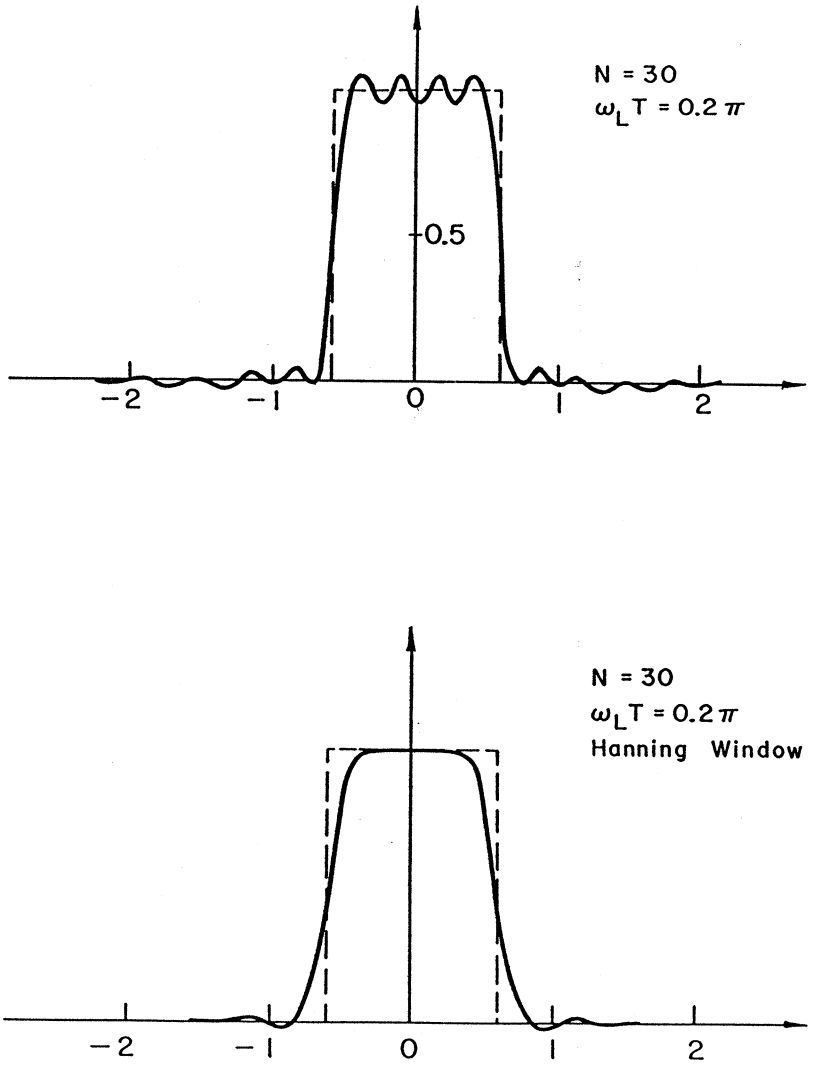

Figure II3 - 2 Transfer function amplitudes, for digital filters with $N = 30$ and $\omega_L T = 0.2\pi$, without (top) and with (bottom) Hanning window.

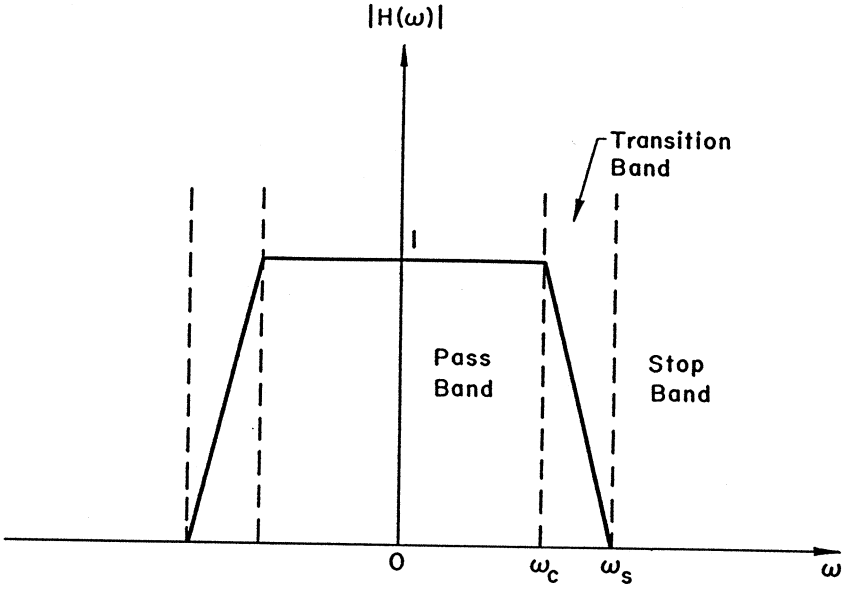

Figure II3 - 3 Low-pass transfer function with transition bands

amplitude will gradually decrease or roll off to the stop-band amplitude (Fig. $II3-3$). The fine details will depend upon the particular filter design.

A number of methods available for constructing finite-length low-pass filters have been proposed and used for Earthquake Engineering Data Processing. Some of these methods are briefly outlined in the following.

$II3.3$ The Ormsby and Elliptic-Type Filters

Anders et al. (1964) proposed the following frequency response function (Fig. $II3-3$) with a first-order roll-off:

$$H(\omega) = \begin{cases} 1 & |\omega| \leq \omega_c \\ 0 & |\omega| > \omega_s \\ (\omega + \omega_s)/\Delta\omega & -\omega_s \leq \omega < -\omega_c \\ (\omega_s - \omega)/\Delta\omega & \omega_c \leq \omega < \omega_s \end{cases} \qquad (II3.3.1)$$

where (ω_c, ω_s) is the transition band, $\Delta\omega = \omega_s - \omega_c$. The corresponding impulse response $h(t)$ is given by:

$$h(t) = \frac{\cos\omega_c t - \cos\omega_s t}{2\pi^2 t^2 \Delta\omega}. \qquad (II3.3.2)$$

The impulse response filter weights for discrete data are again obtained by quantizing $h(t)$ at equal time intervals of kT, for $-\infty < k < \infty$ giving

$$h[k] = h(kT) = \frac{\cos\omega_c kT - \cos\omega_s kT}{2\pi^2 k^2 T^2 \Delta\omega} \qquad (II3.3.3)$$

Since the amplitude response $|H(\omega)|$ is now continuous, without a step jump, (Fig. $II3-3$), the sequence of weights $(h[k])$ in Eq. $(II3.3.3)$ will approximate well the behavior of $H(\omega)$ for sufficiently large k. The filter weights are again symmetric about $k = 0$, with $h(-k) = h(k)$, so that the filter performs a perfect phase-distortionless transmission.

Figs. $II3-4$ (top and bottom) show a plot of the truncated Ormsby-type transfer function on linear and logarithmic amplitude scales. The cutoff frequency and roll-off frequency intervals are 25 and 2 Hz, respectively. The Ormsby filter was first used in routine data processing of strong-motion accelerograms in 1971 (Trifunac 1971, 1972).

The same windowing technique can be used for the Ormsby filter to minimize Gibbs effect in the vicinity of the transition frequency that will result from truncation of the infinite series. With $w[k] = w(kT)$, Eq. $(II3.2.10)$ the "windowed" Ormsby coefficients become, (from Eq. $II3.3.3$)

$$\begin{aligned} b[k] &= h[k]w[k] \\ &= \frac{(1 + \cos(k\pi/N))(\cos\omega_c kT - \cos\omega_s kT)}{4\pi^2 k^2 T^2 \Delta\omega} \end{aligned} \qquad (II3.3.4)$$

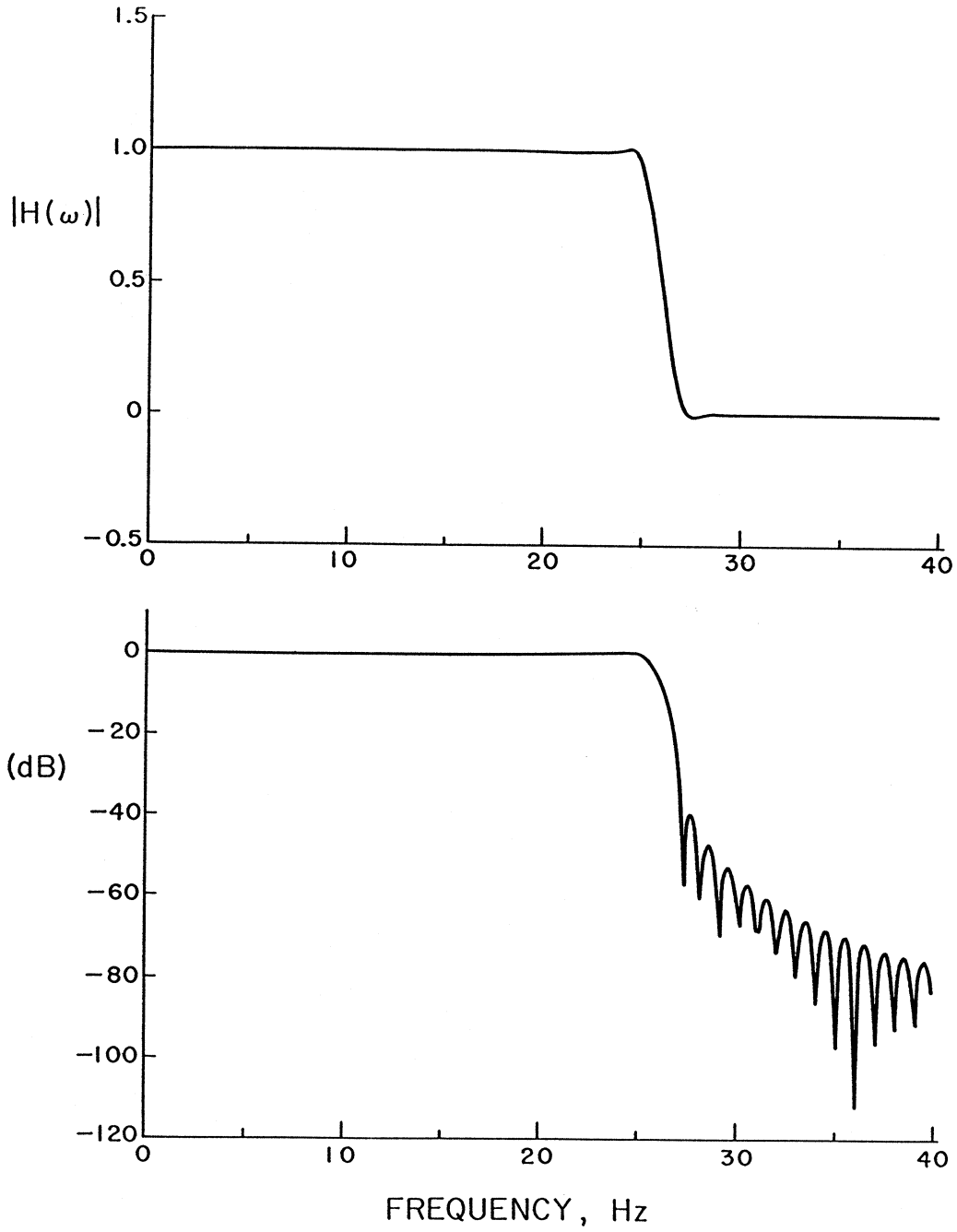

Figure II3 - 4 Ormsby low-pass filter. (Top: linear amplitude scale, bottom: db amplitude scale).

Another type of a filter which has been suggested and studied in detail is the type (elliptic) used by Chebyshev and Butterworth (Oppenheim and Schafer, 1975).

The design of this type of (elliptic) filter involves the approximation of the desired frequency response amplitude by a rational function of the form:

$$H(\omega) = \frac{\sum_k b[k] \exp(-ik\omega T)}{1 + \sum_k a[k] \exp(-ik\omega T)} \qquad (II3.3.5)$$

where the summation for $b[k]$ is from $k = 0$ to K, and that for $a[k]$ is from $k = 1$ to L, for some given K and L. The coefficients of the rational function are determined by an appropriate set of specifications on the digital filter. In the case of a low-pass filter, this often takes the form of a tolerance scheme, as shown in Fig. $II3 - 5$. The dashed line region represents the magnitude of the frequency response of a filter that meets the following specifications:

(1) For a given pass-band cutoff frequency, ω_c, and a stop-band cutoff frequency, ω_s, a transition band of nonzero width, $|\omega_s - \omega_c|$, is assumed in which the magnitude of the response drops continuously from the pass-band to the stop-band.

(2) Within the pass-band, $|\omega| \leq \omega_c$, the magnitude of the response must approximate unity to within an error of $\pm\varepsilon_1$:

$$1 - \varepsilon_1 \leq H(\omega) \leq 1 + \varepsilon_1 \qquad (II3.3.6)$$

(3) Within the stop-band, $|\omega|$, the magnitude of the response must approximate zero to within an error of $\pm\varepsilon_2$:

$$|h(\omega)| \leq \varepsilon_2 \qquad (II3.3.7)$$

For the case of elliptic and other similar filters, like Butterworth filters, there is usually no constraint on the phase response. Often such a filter is determined only in terms of the above magnitude approximation, and the phase of the resulting filter is usually disregarded.

Starting from the equally-spaced input sequence $(x[n])$, the filter output sequence $(y[n])$ is given by:

$$y[n] = \sum_k b[k]x[n-k] - \sum_k a[k]y[n-k] \qquad (II3.3.8)$$

where the summation for b[k] is from k = 0 to K, and that for a[k] is from k = 1 to L.

Note that, in general, the output values are determined in terms of the past and present input plus the past output. Filters with this causal characteristic are useful when the outputs need to be available concurrently with input. A digital filter is completely defined by the sequence $(a[k])$ and $(b[k])$, so that designing such a digital filter means finding the constants $a[k]$ and $b[k]$ which will satisfy the given specifications. Elliptic filters

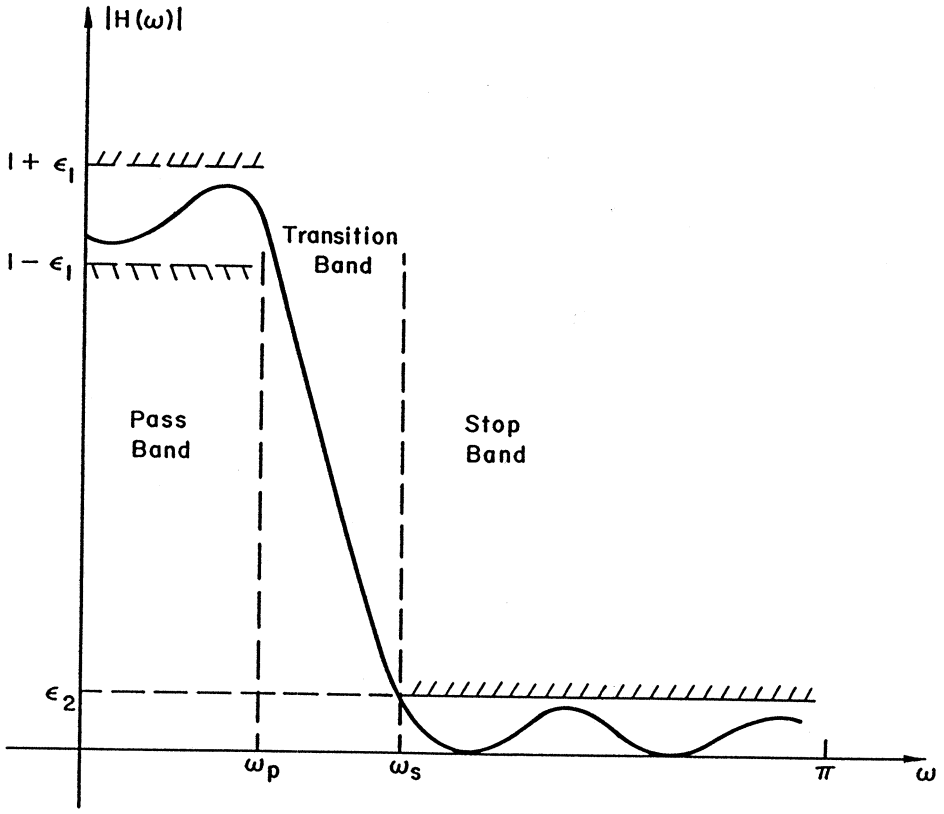

Figure II3 - 5 Tolerance scheme in pass-, transition- and stop-bands.

are characterized by a magnitude response that is equally rippled in both the passband and the stopband. The frequency response of a low-pass elliptic filter takes the form:

$$H(\omega) = \frac{1}{1 + \varepsilon^2 U^2(N, \omega)} \qquad (II3.3.9)$$

where $U(N, \omega)$ is a Jacobian elliptic function. A detailed discussion of the design of such a filter is described in Gold and Radar (1975). The phase $Ph(\omega)$ is given by

$$Ph(\omega) = \tan^{-1}\left(\frac{\text{Imag}(H(\omega))}{\text{Real}(H(\omega))}\right) \qquad (II3.3.10)$$

where Imag$(\cdot)$ and Real$(\cdot)$ are the imaginary and real parts of a complex function. Eq. $(II3.3.5)$ shows that $Ph(\omega)$ is nonlinear in ω. This means that, in general, the filter cannot attain a zero or linear phase characteristics, so that the filter will provide a phase-distorted output. In typical Earthquake Engineering Data Processing, signal distortions due to phase characteristics are not desirable and should be eliminated. To eliminate the phase distortion for a filter of this kind, the original filter may be replaced by the corresponding magnitude-squared filter, using a time reversal transformation (Gold and Radar, 1975).

Fig. $II3-6$ gives a plot of a typical elliptic filter in linear and logarithmic scales, in the top and bottom respectively. The pass-band and stop-band frequencies used are 12 to 18 Hz, respectively. Fig. $II3-7$ gives a plot of the phase of the same elliptic filter to illustrate its nonlinear characteristics.

With all the input data available in a stored form in a computer before the computation starts, the requirements that the filter be casual (physically realizable) is not essential. This means that the filter used does not have to be recursive, i.e. that the outputs depend only on past and present inputs and past outputs. In other words, with the input data in stored form, the filter used can have both memory and anticipation terms so that the outputs are dependent on both past, present and future inputs. This results in two important characteristics. First, the impulse response terms $(h[k])$ can be chosen to form an even time sequence with

$$h[k] = h[-k], \qquad (II3.3.11)$$

i.e. with anticipation and memory terms being mirror images of each other. This will result in a filter which will perform a perfect phase-distortionless transmission, an important property in earthquake engineering data processing (Section $II3.2$).

Secondly, a filter having both memory past and present and anticipation (future) terms, as compared to one with just memory terms, will mean that it uses more information available about the inputs to produce the outputs. The significance of this is best illustrated in the next two sets of figures. Fig. $II3-8$ shows plots of exponentially decaying input cosine functions versus time and the corresponding output functions (dashed lines) filtered by the Ormsby filter, with a cutoff frequency of 25 Hz and a transition frequency of 2 Hz. The frequencies of the input functions in this figure are respectively 8, 16, 24, 28, 32 and

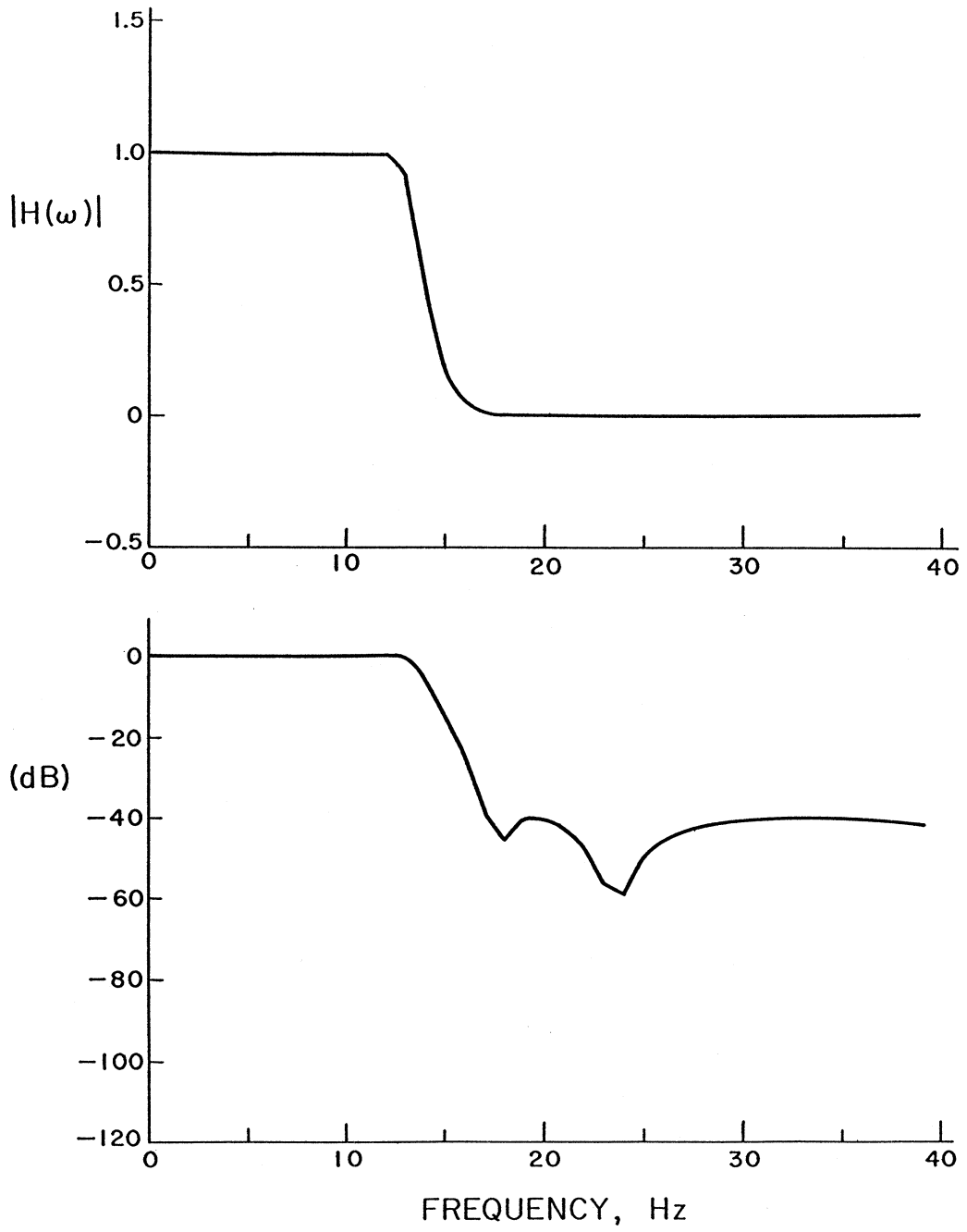

Figure II3 - 6 Elliptic low-pass filter. (Top: linear amplitude scale, bottom: db amplitude scale).

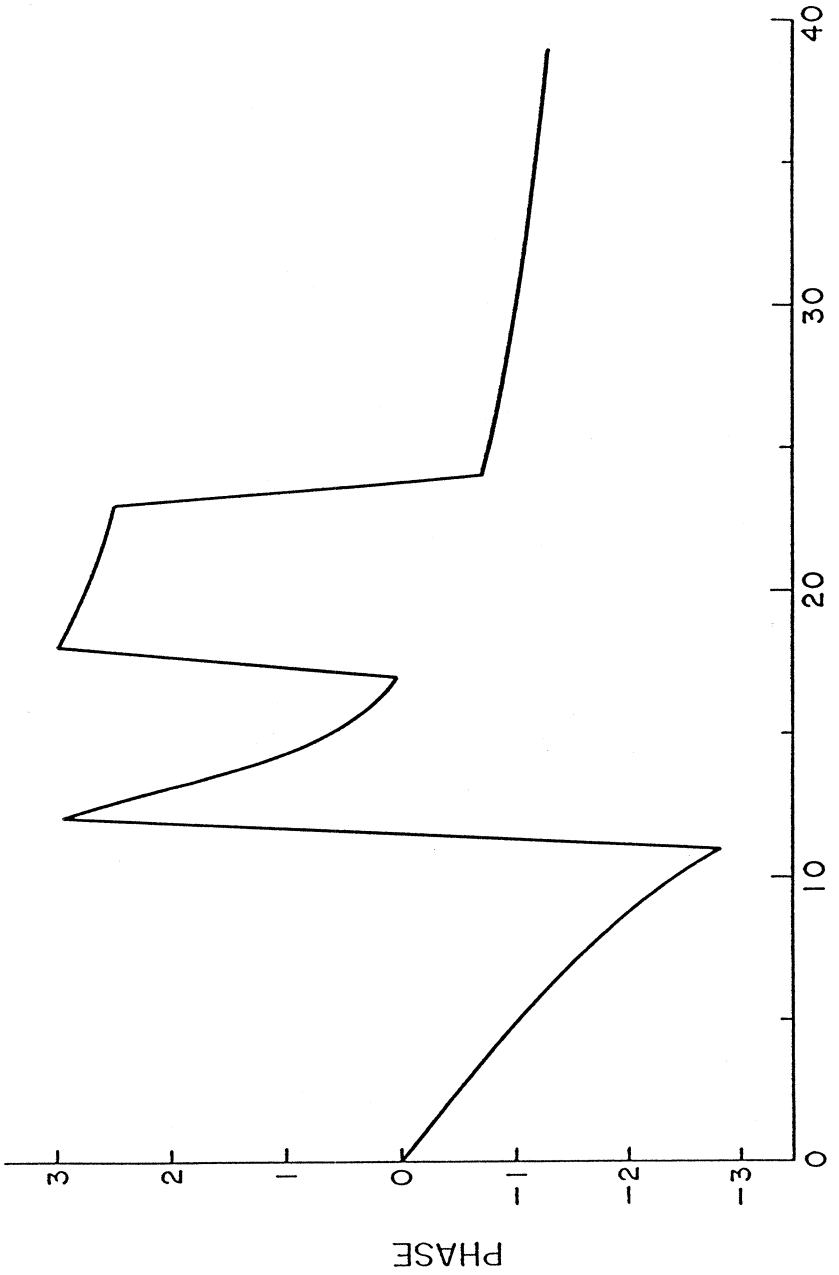

Figure II3 - 7 Phase of the elliptic filter in Figure II3 - 6.

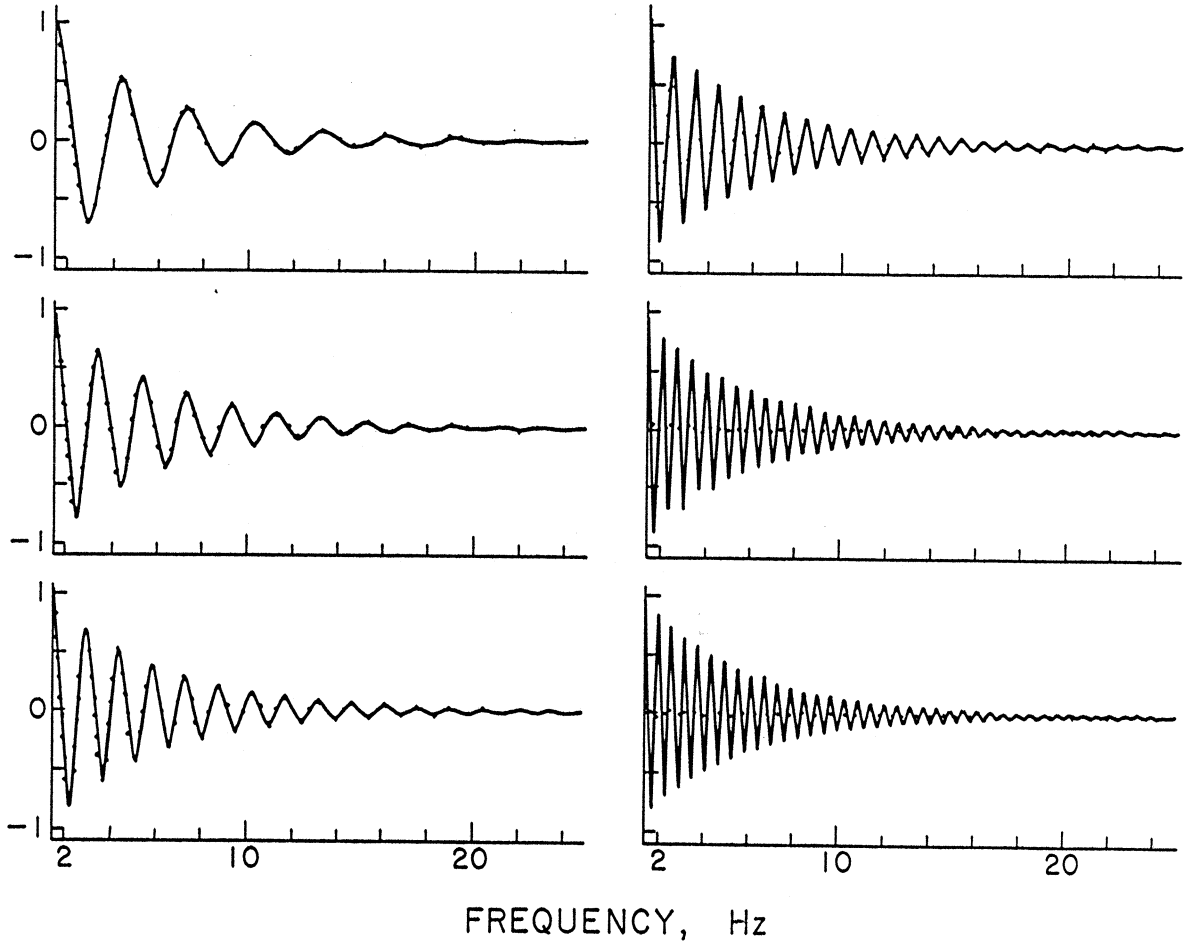

Figure II3 - 8 Input (solid lines) and output (dotted lines) decaying cosine functions, filtered by the Ormsby filter.

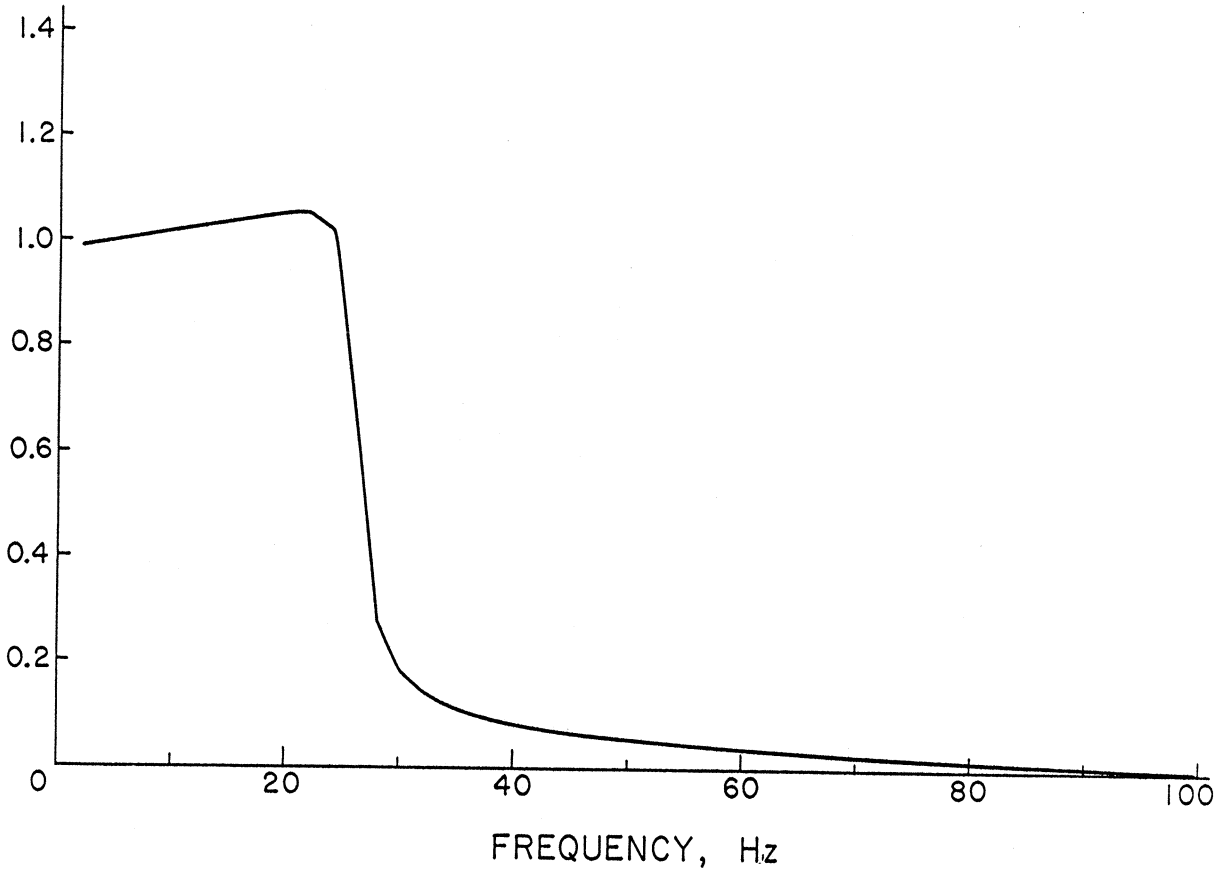

Figure II3 - 9 Transfer function amplitudes of Ormsby filter.

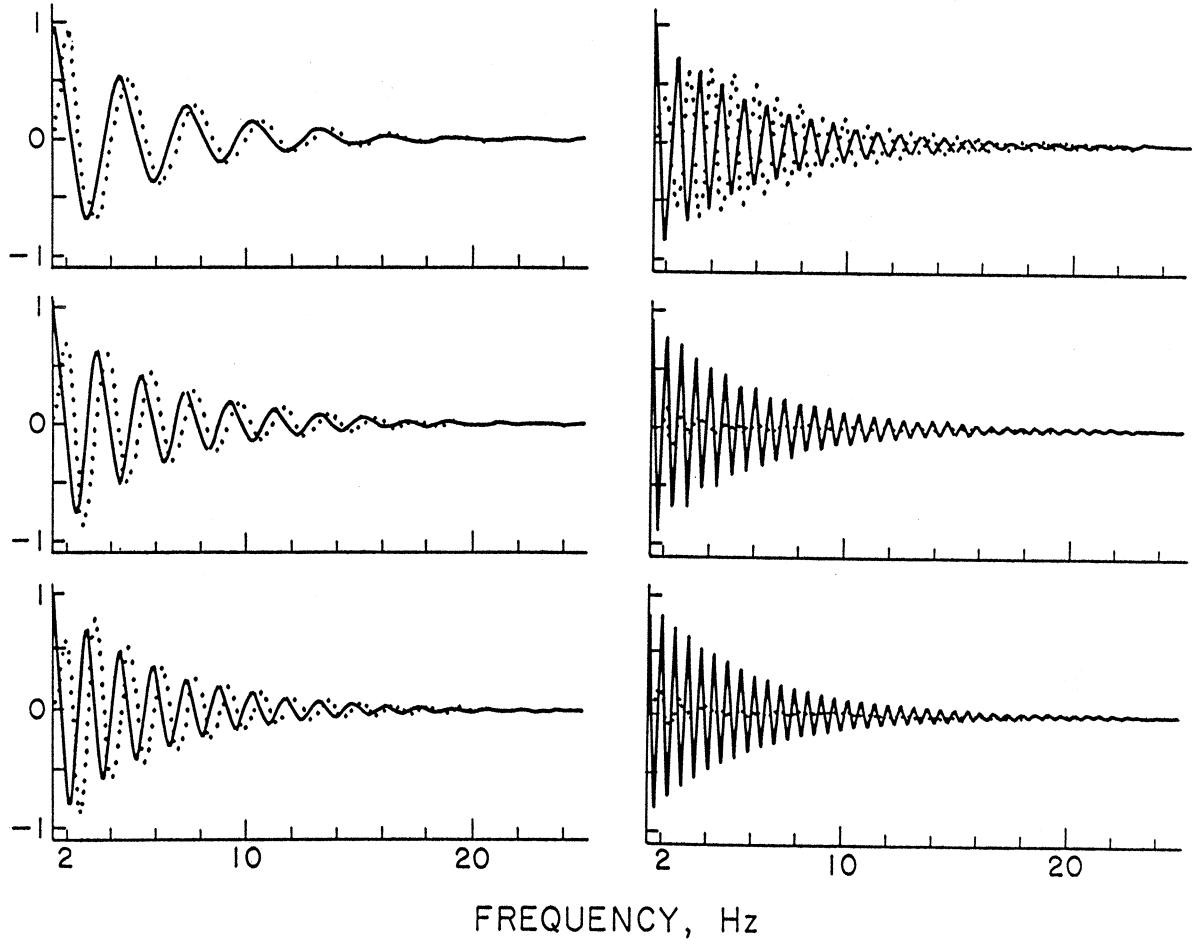

Figure II3 - 10 Input (solid lines) and output (dotted lines) decaying cosine functions filtered by the elliptic IIR filter.

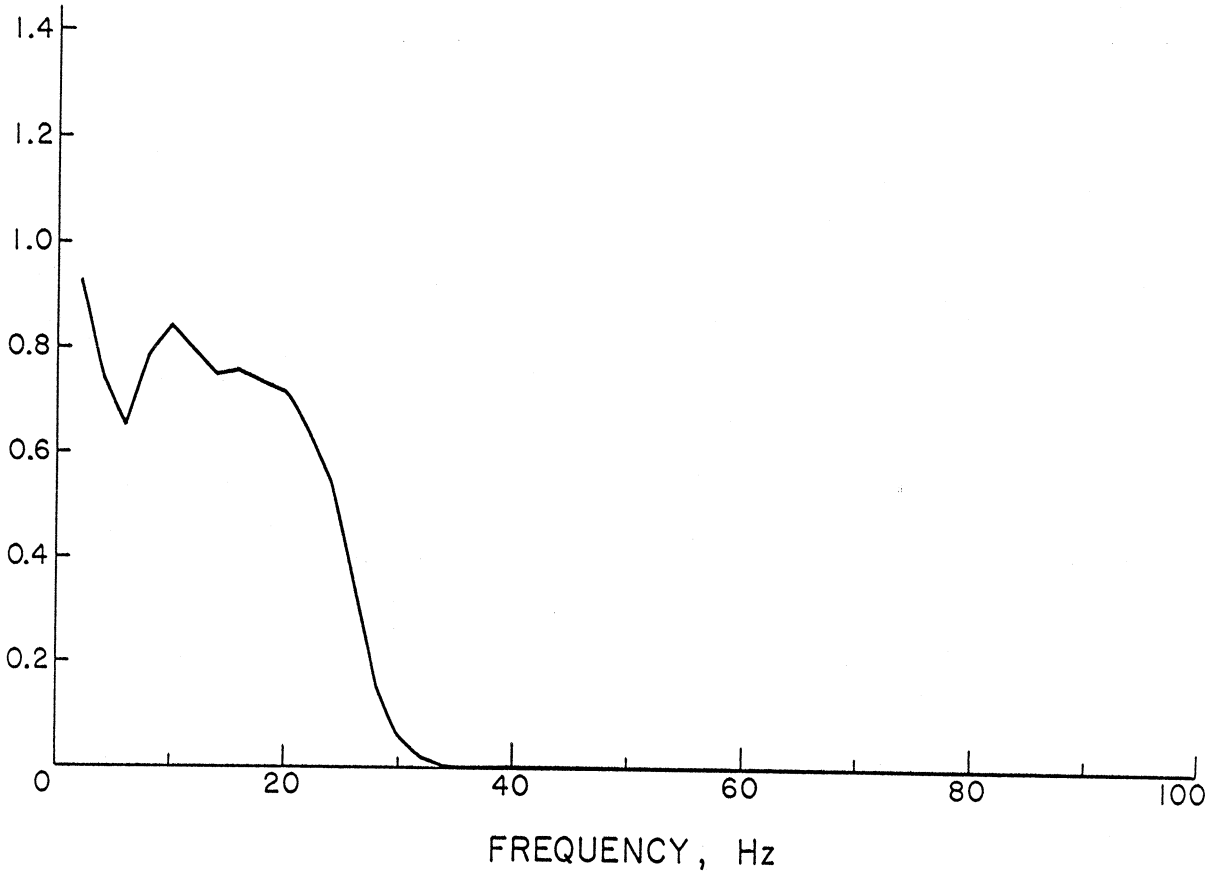

Figure II3 - 11 Transfer function amplitudes versus frequency (Hz) for data in Figure II3 - 10.

40 Hz. The output data resulting from the Ormsby filter again resemble the corresponding input data in the passband and have approximately zero amplitudes in the stopband.

Fig. $II3-9$ shows a plot of the numerical evaluation of the transfer function magnitude of the Ormsby filter versus frequency for this particular type of input data. It is computed as the ratio of the maximum output amplitude to that of the input at each frequency. Because of the special transient nature of the input, this may be used to measure the transient character, if any, of the Ormsby filter.

Fig. $II3-10$ shows the same plot of the exponentially decaying input cosine functions versus time and the corresponding output data filtered by an elliptic filter. As indicated earlier, the output data all have a phase shift relative to the input data. Being causal, the output data all start out with magnitudes close to 0, and take as much as half a cycle before picking up and being close to the input data. The output data thus do not pick up the early and large maxima. Fig. $II3-11$ shows a plot of the numerically calculated transfer function magnitude of the filter versus frequency for this particular type of input data. The transfer function starts out close to unity at low frequency, but then it decreases to .8 at about 5 Hz. It stays at around this magnitude till 20 Hz and then levels to zero at about 30 Hz.

In summary, two types of filters have been considered: Ormsby and Elliptic. The first type performs a perfect phase-distortionless transmission, and with the data in stored form, has both memory as well as anticipation terms. The second type filter gives a phase-distorted output. With decreasing magnitude input cosine function, the Ormsby filter shows a better performance than the elliptic filter.

$II3.4$ Design Criteria of a Low-pass Filter for Accelerograms

Two types of filters have been discussed: Ormsby and Elliptic. The first type is a symmetric ($h[k] = h[-k]$), nonrecursive digital filter which operates on equally spaced data ($x[n]$) with output ($y[n]$) given by

$$y[n] = \sum_k h[k]x[n-k] \qquad (II3.4.1)$$

and with a transfer function of the form

$$H(\omega) = h[0] + 2\sum_k h[k]\cos(k\omega T). \qquad (II3.4.2)$$

The filter performs a perfect phase-distortionless transmission. It has both memory as well as anticipation terms.

The second type is a recursive digital filter operating on equally spaced input data ($x[n]$) with output ($y[n]$) given by

$$y[n] = \sum_{k=1}^{L} a[k]y[n-k] + \sum_{k=0}^{K} b[k]x[n-k], \qquad (II3.4.3)$$

and a transfer function of the form:

$$H(\omega) = \frac{\sum_k b[k]\exp(-ik\omega T)}{1+\sum_k a[k]\exp(-ik\omega T)} \qquad (II3.4.4)$$

a rational function of $\exp(-i\omega T)$. Eq. ($II3.4.4$) shows that the filter by itself gives a phase-distorted output and, hence, a time reversal technique is needed to restore the phase of the input data. It has only memory terms and no anticipation terms.

Comparison of the performance of the two filters is an example of a more general comparison of two types of filters: recursive versus non- recursive filters. The Ormsby filter is a non-recursive filter that, for each n, responds only to values of $x[m]$ in the range ($x[n-N]$, $x[n+N]$). Non-recursive filters are thus also known as "Finite Impulse Response" (FIR) filters, and the elliptic filter used is an example of a "one-sided" physically realizable recursive filter. From its ability to produce, from one single impulse, effects which can extend indefinitely far into the future, it is also known as "Infinite Impulse Response" (IIR) filter.

Both types of filters have about the same flexibility to meet the various conditions. However, a "slow" transient character of the elliptic filter was illustrated above. At the beginning of time series, it takes time for an elliptic filter to "settle" down after a sudden change in input. The non-recursive Ormbsby filter, on the other hand, shows much smaller transient response. Because of such problems, and because of instabilities and phase shifts, recursive filters tend to be used in systems only where there are very long runs of data more or less stationary in character. Non-recursive filters, on the other hand, are simpler to understand, design, and use, and are more likely to be used in processing data which is more transient in nature, as in the case of earthquake engineering data, for example.

It is also noted that the elliptic IIR filter has ripples in the transfer function in both the passband and the stopband. Ripples are allowed in its design to achieve its optimality in the order of the filter. Earthquake engineering data processing requires the cascading sequence of many filters, i.e. one filter after another. Band-pass filtering is made of low- and high-pass filters, the instrument correction involves use of the differentiation filter twice, to get the first and second order derivatives, the integration involves use of integration and high-pass filters twice, to get velocity and displacement data. If the data passes through M such filters with ripple amplitudes $(1+\varepsilon)$ in the passband, then the resulting ripple peaks will be $(1+\varepsilon)^M$. Ripples in the passband are thus objectionable in data processing with many cascading filters. Ripples in the stopband are objectionable for the same reason. The input earthquake signal for data processing is often masked by instrument and digitization noise. After filtering out the noise, any small peaks that are left in the spectrum of the

signal might result from the original signal or from ripples in the stopband of the transfer functions used in the filtering process. This problem can, and should be, avoided by using a class of filters that vary smoothly throughout their pass-band.

It is with these considerations that the following guidelines are proposed for the design and improvement of new and/or existing low-, high- and band-pass filters to be used in earthquake engineering data processing:

(1) that the filter be of the form given by Eq. (*II*3.4.1), being a finite-impulse response (FIR) non-recursive filter with symmetric coefficients ($h[k] = h([-k])$, so that the transfer function is in the same form as Eq. (*II*3.4.2); this will ensure that the filter performs a perfect phase distortionless transmission;

(2) that the magnitude of the transfer function be free from ripples in both the pass and stop bands. The class of filters that vary smoothly should be used;

(3) that the Gibbs effects at the cutoff frequencies due to any form of truncation be minimized; the use of appropriate windowing technique and sharpening technique for smooth transition from the pass-band to the stop-band should be investigated.

*II*3.5 A Smooth FIR Lowpass Filter

Based on the design criteria proposed in the previous section, we consider the design of a class of lowpass filters that are monotone (vary smoothly) over the whole frequency band interval . The following approach, as described in Hamming (1977), has been adopted.

Given a symmetric ($h[k] = h[-k]$), nonrecursive digital filter that operates on equally spaced data ($x[n]$), the output, ($y[n]$), is computed by the formula:

$$y[n] = \sum_k h[k]x[n-k], \qquad (II3.5.1)$$

with the corresponding transfer function given by:

$$H(\omega) = h[0] + 2\sum_{k=1}^{K} h[k]\cos(k\omega). \qquad (II3.5.2)$$

Using the identity:

$$\cos(n\omega) = \sum_{k=0}^{n}(-1)^k C(n,2k)\cos^{n-2k}(\omega)(1-\cos^2(\omega))^k, \qquad (II3.5.3)$$

Eq. (*II*3.5.2) can be transformed into a polynomial in powers of $\cos(\omega)$, which, for suitable choice of coefficients, $b[k]$, takes the form:

$$H(\omega) = \sum_{k=0}^{K} b[k](\cos(\omega))^k = \sum_{k=0}^{K} b[k]t^k, \qquad (II3.5.4)$$

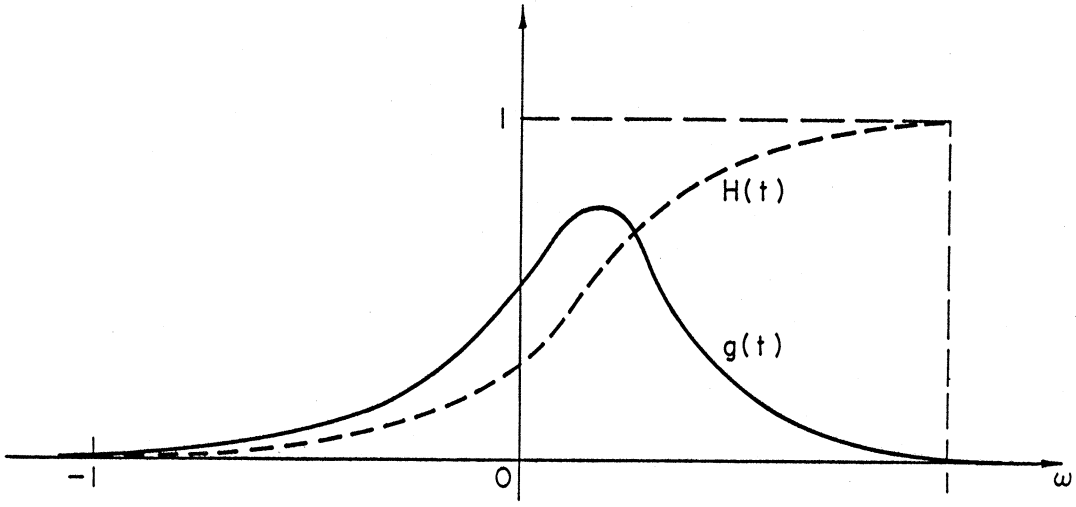

Figure II3 - 12 H(t) (equation II3.5.4) and g(t) (equation II3.5.5).

where $t = \cos(\omega)$. As ω goes from 0 to π, t goes from 1 to -1. The original low-pass filter, because of the reversal of the axis in the transform, now appears as a high-pass filter in the t variable (Fig. $II3-12$).

Consider the function,

$$g(t) = (1+t)^p(1-t)^q \qquad (II3.5.5)$$

with p and q as parameters (Fig. $II3-12$). It has a zero of order p at $t=-1$ and a zero of order q at $t=1$. Take

$$H(\omega) = \frac{\int_{-1}^{\cos\omega}(1+t)^p(1-t)^q dt}{\int_{-1}^{1}(1+t)^p(1-t)^q dt} \qquad (II3.5.6)$$

so that, after integration, $H(\omega)$ is a polynomial in $t=\cos\omega$ that has a $(p+l)$th-order zero at $\omega=\pi(t=-1)$ and the value 1 at $\omega=0(t=1)$, along with q derivatives (w.r.t. t) that are zero at $t=1$. From Eq. $(II3.5.5)$,

$$g'(t)=0 \quad \text{when} \quad t=\frac{p-q}{p+q} \qquad (II3.5.7)$$

which gives the inflection point of the function $H(t)$ in the t domain. Thus, to design a low-pass filter that passes the lower fraction $\alpha, 0<\alpha<1$, of the Nyquist interval $(0<\omega<\pi)$, set

$$\frac{p-q}{p+q} = t \simeq \cos\alpha\pi \quad \text{or} \quad \frac{p}{q} = \frac{1+\cos\alpha\pi}{1-\cos\alpha\pi} \qquad (II3.5.8)$$

which gives the ratio of p to q to be used. To get back the $h[k]$ coefficients, the transfer function $H(\omega)$ is transformed back to its Fourier series representation. A detailed description of the procedure is given in Hamming (1962). Fig. $II3-13$ shows the amplitudes, represented by solid lines of these filters versus frequency, ωT, at various cutoff frequencies in the range $0<\omega T<\pi$. Fig. $II3-14$ shows the same amplitudes in solid lines at logarithmic scale in units of dB. The order of the filter used is around 50. Often in the resulting design of the filter, a big portion of the higher order filter coefficients, $h[k]$, will be virtually so small that they can be taken to be zero. The order of the filter is thus reduced accordingly.

It is seen from Figs. $II3-13$ and $II3-14$ that the resulting filters, as represented by solid lines, all have a fairly wide transition band from 1 to 0. This transition band can be greatly reduced by a sharpening process to obtain a new filter from the old one as given by (Hamming, 1977):

$$H_0(\omega) = H_i^2(\omega)\ (3-2H_i(\omega)) \qquad (II3.5.9)$$

where

$H_i(\omega)$ is the original filter, and
$H_0(\omega)$ is the new output low-pass filter.

The new filter has the property that the small deviations from unity in the pass-band and the small deviations from zero in the stop-band are both squared, thus resulting in

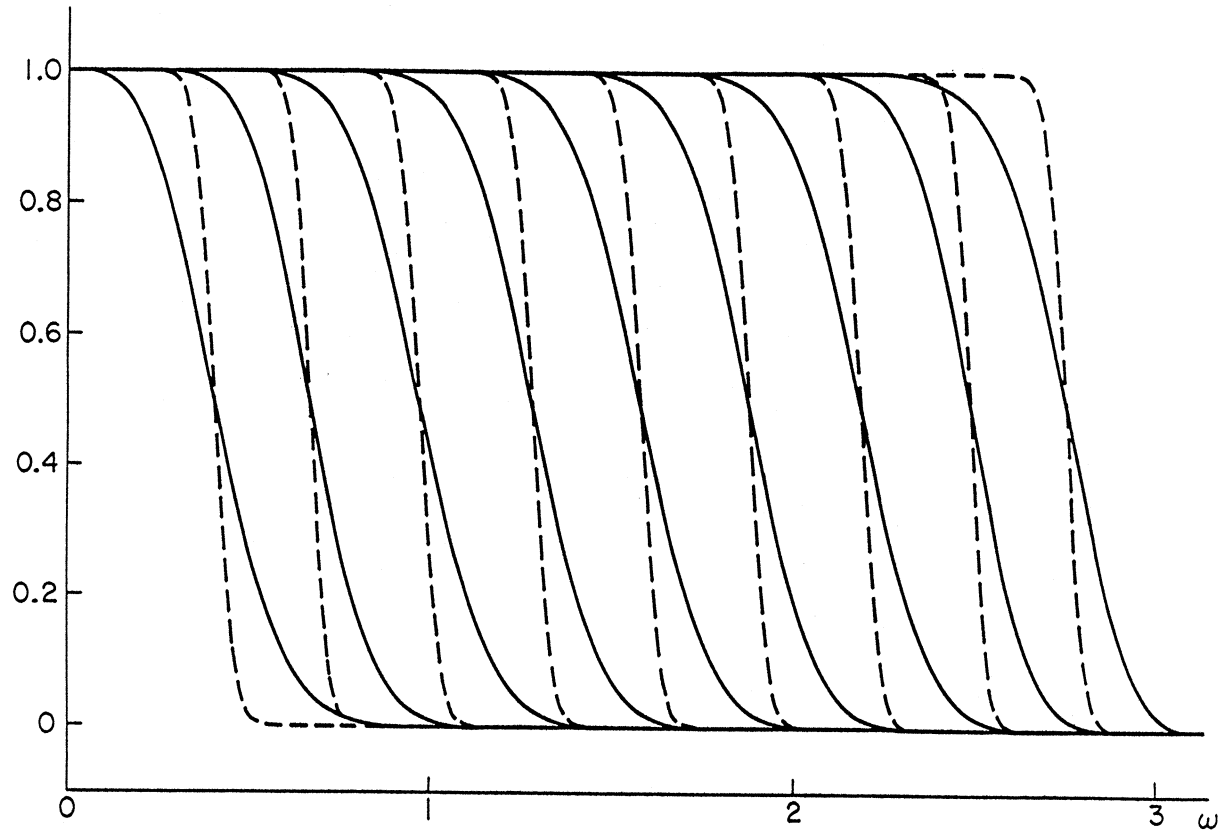

Figure II3 - 13 Smooth low-pass filters (solid lines) and their sharpened transition bands (dotted lines).

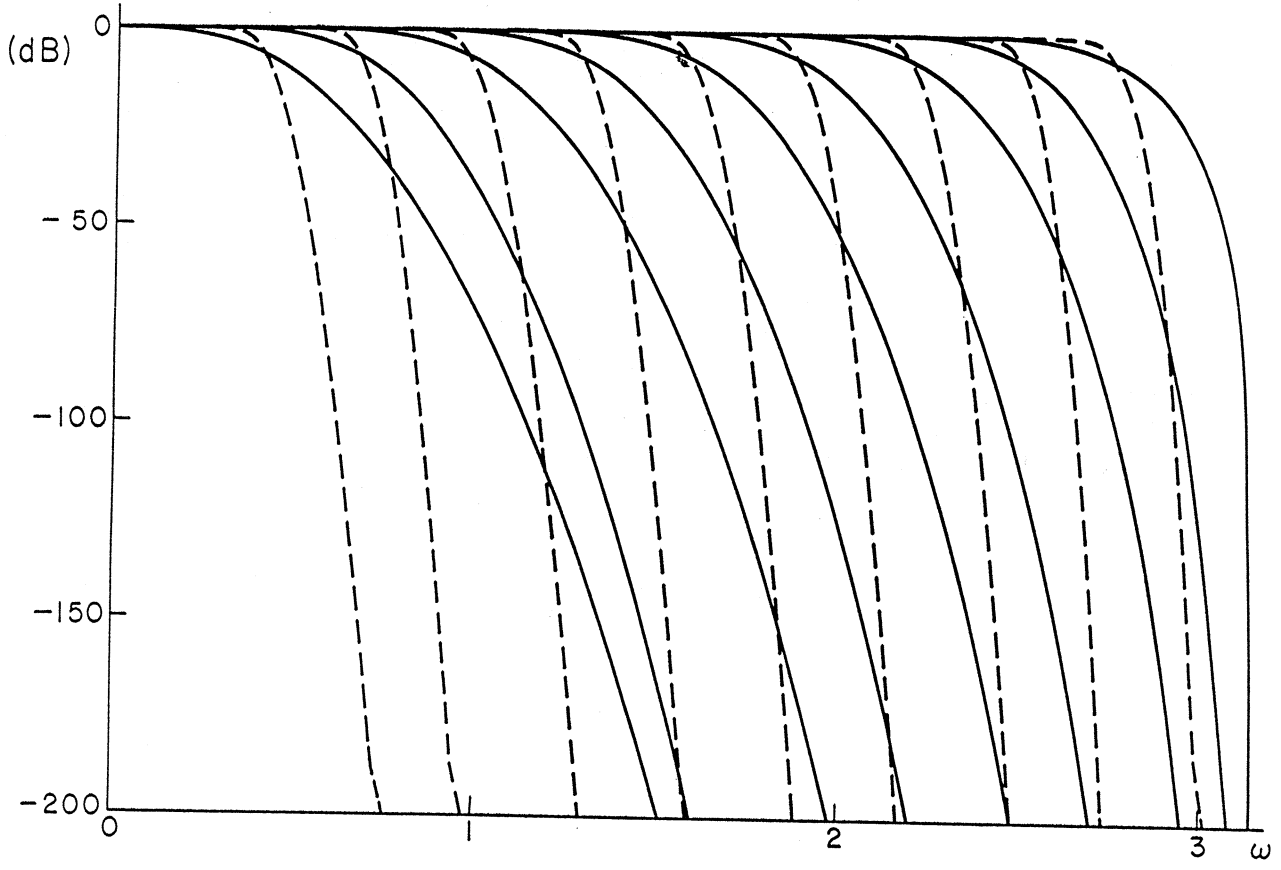

Figure II3 - 14 Smooth low-pass filters (solid lines) and their sharpened transition bands (dotted lines) on db amplitude scale.

great sharpening. Thus starting from a program or subroutine that designs the smooth low-pass filter, a new subroutine can be written to:

(a) process the signal once by the low-pass subroutine,

(b) double this output and subtract each output value from 3 times the corresponding input values, and

(c) finally pass this difference through the low-pass filter twice.

This will give a greatly sharpened filter of approximately three times the effective length. Fig. $II3-13$ shows plots of these transfer functions of the smooth low-pass filters. The solid lines are the original filters before they were sharpened by Eq. ($II3.5.9$) and the dashed lines give the corresponding sharpened filters. The dashed lines all have a much sharper, narrower transition band than the corresponding solid lines. Fig. $II3-14$ shows the same functions in logarithmic scale. Note that the magnitudes of the data in the stop-band are all < -200 dB.

Compared with the transfer function of the Ormsby filter (Fig. $II3-4$) this filter has much sharper and narrower transition zone around the cutoff frequency. The Gibbs effects, a result of the truncation of the Fourier series is not present in the smooth filters any more. Windowing is thus not necessary for the smooth filters.

*II*4 Data Processing for Volume II: (B) Instrument Correction

*II*4.1 Introduction

The transducer of a recording instrument usually records the relative displacement or relative velocity response of the instrument mass. Instrument correction is then the step that represents the transformation from the transducer relative displacement (or velocity) signal $x(t)$ to the input ground acceleration signal $a(t)$. For example, the dynamic equation of motion of the transducer as a single degree system is given by:

$$\ddot{x} + 2\zeta_0\omega_0\dot{x} + \omega_0^2 x = -a \qquad (II4.1.1)$$

where ω_0 is the natural frequency of the transducer, and ζ_0 is the fraction of critical damping.

With the displacement signal $x(t)$ sampled at equally spaced time intervals of T sec apart, the signal can then be represented as a sequence $(x[n])$, with

$$x[n] = x(nT) \qquad (II4.1.2)$$

for $n = 0, 1, 2, ...$ in the discrete domain. Instrument correction in the discrete domain then leads to numerical differentiation of the sequence $(x[n])$, once to get $(\dot{x}[n])$, and once more to get $(\ddot{x}[n])$, for use in the equation (following from Eq. $(II4.1.1)$)

$$a[n] = -(\ddot{x}[n] + 2\zeta_0\omega_0\dot{x}[n] + \omega_0^2 x[n]) \qquad (II4.1.3)$$

for $n = 0, 1, 2, ...$ Here $(a[n])$ represents the sequence of corrected acceleration data in digital form.

With many of the signals $x(t)$ available on analog films recorded by accelerographs, digital data $(x[n])$ were first obtained by digitizing the record manually. For example, some twenty years ago, all of the 1971 San Fernando Earthquake records have been digitized using a Benson-Lahner 099D data reducer unit. These records were then digitized on an unequal time basis, since this would lead to the best definition of the trace for a given number of data points. The average number of digitized points/second was about 20 to 30, in general, and up to about 30 to 50 in the most rapidly oscillating sections of the record. The computer software developed for data processing of strong-motion digitized accelerograms (Trifunac and Lee, 1973) interpolated the unequally spaced data to equally spaced data of 100 points/second. The central difference formulae for the first and second derivatives were used:

$$\begin{aligned} \dot{x}[n] &= (x[n+1] - x[n-1])/(2T) \\ \ddot{x}[n] &= (x[n+1] - 2x[n] + x[n-1])/(T^2). \end{aligned} \qquad (II4.14)$$

With data at equally spaced time intervals of 0.01 sec (100 pt/sec), these formulae are accurate up to about 15 Hz, the average sampling frequency of the hand digitized

data. No higher order differentiation formulae were thus required nor used for the hand digitized data in the early 70's. Since then, digital data are available from automatic digitization systems, where, for example, the data are automatically digitized at 200 (or more) points/sec using a Photodensitometer Photoscan P-1000 by Optronics International (Trifunac and Lee: 1979). Currently, using any inexpensive digital scanner, for example, interfaced with a PC, data can be digitized with a resolution of 600 points/inch, or over 200 points/sec, for typical analog records on 70 mm film.

*II*4.2 The Ideal Differentiating Formula

It is convenient to examine the numerical differentiating formulae in the frequency domain. This then becomes the problem of designing a filter to estimate the derivative of data given by a discrete sequence. The differentiating filter is to be designed as a linear time- invariant system, where the complex exponential functions $\exp(i\omega t)$ are eigenfunctions. The equation for the derivative:

$$\frac{d}{dt}(e^{i\omega t}) = i\omega e^{i\omega t} \qquad (II4.2.1)$$

gives the transfer function of the differentiating filter as (for $T = 1$):

$$H(\omega) = i\omega \qquad (II4.2.2)$$

for $-\pi \leq \omega \leq \pi$. The ideal differentiator with cutoff frequency, ω_c, has a transfer function similarly given by:

$$H_D(\omega) = \begin{cases} i\omega & |\omega| < \omega_c \\ 0 & \pi > |\omega| > \omega_c \end{cases}. \qquad (II4.2.3)$$

One general method of filter design is to examine its representation in terms of Fourier series,

$$H(\omega) = \sum h[n]e^{in\omega}. \qquad (II4.2.4)$$

Computing coefficients using the inverse Fourier series formula gives

$$b[k] = \frac{1}{\pi}\int_{-\pi}^{\pi} H(\omega)\sin k\omega d\omega = \frac{2}{\pi}\int_{0}^{\omega_c} i\omega \sin k\omega d\omega,$$

or

$$b[k] = \frac{2i}{\pi}\left(\frac{\sin k\omega_c}{k^2} - \frac{\omega_c \cos k\omega_c}{k}\right) \qquad (II4.2.5)$$

with the cutoff frequency $kc = \pi$. This gives

$$b[k] = \frac{-2i\cos \pi k}{k} = \frac{2i}{k}(-1)^{k+1} \qquad (II4.2.6)$$

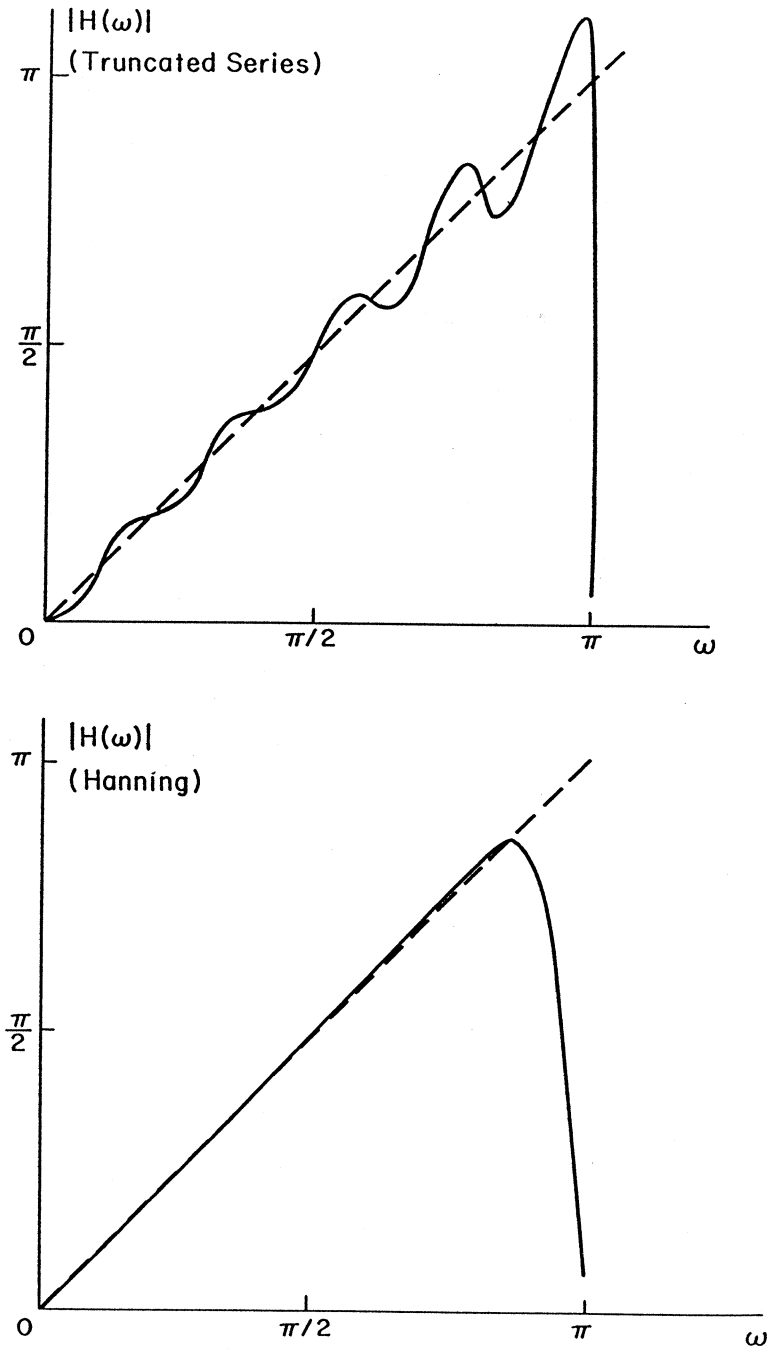

Figure II4 - 1 Transfer function amplitude for $k = 10$. (Top)

Figure II4 - 2 Transfer function amplitude for $k = 10$ with Hanning window. (Bottom)

We thus have an infinitely long sequence that must be truncated. Truncating the Fourier series will lead to Gibbs effect, and windowing is again necessary. Fig. $II4-1$ gives a plot of the transfer function amplitude in Eq. ($II4.2.2$) using K = 10 terms of the coefficients given by Eq. ($II4.2.6$), which shows the overshoot near the cutoff frequency, ω_c. Fig $II4-2$ gives a plot of the same function using windowing.

In the design of a digital differentiator, it is seen that for the filter to be purely imaginary, as in Eq. ($II4.2.2$) or Eq. ($II4.2.3$), the coefficients of the filter must have odd symmetry, that is

$$h[-k] = -h[k], \tag{$II4.2.7$}$$

for all k, so that

$$h[k](e^{ik\omega} - e^{-ik\omega}) = 2ih[k]\sin k\omega \tag{$II4.2.8$}$$

and the filter has the sine series representation. Thus with $x[n]$ denoting the digital derivative of $x[n]$, the differentiating formula should take the form

$$\dot{x}[n] = \sum_{-K}^{K} h[k]x[n-k] \tag{$II4.2.9$}$$

with $h[0] = 0$ and $h[-k] = -h[k]$, which will lead to the sine series

$$H(\omega) = 2i\sum_{1}^{K} h[k]\sin k\omega\ . \tag{$II4.2.10$}$$

($II4.2.9$) can be rewritten as

$$\dot{x}[n] = \sum_{1}^{K} h[-k](x[n+k] - x[n-k]), \tag{$II4.2.11$}$$

which is a linear combination of differences of symmetrically placed values of the function. In other words, Eq. ($II4.2.11$) can be considered as an n-th order central difference formula, one that will give a transfer function that is purely imaginary, as required, and can thus be designed to best approximate the ideal differentiator in Eq. ($II4.2.2$) or Eq. ($II4.2.3$).

$II4.3$ The Classical Differentiating Formulae

The classical 3-points' and 5-points' central difference formulae have transfer functions given by:

3 points ($K = 1$): $\quad H(\omega) = i\sin\omega T/T$

5 points ($K = 3$): $\quad H(\omega) = i(8\sin\omega T - \sin 2\omega T)/6T$ (II4.3.1)

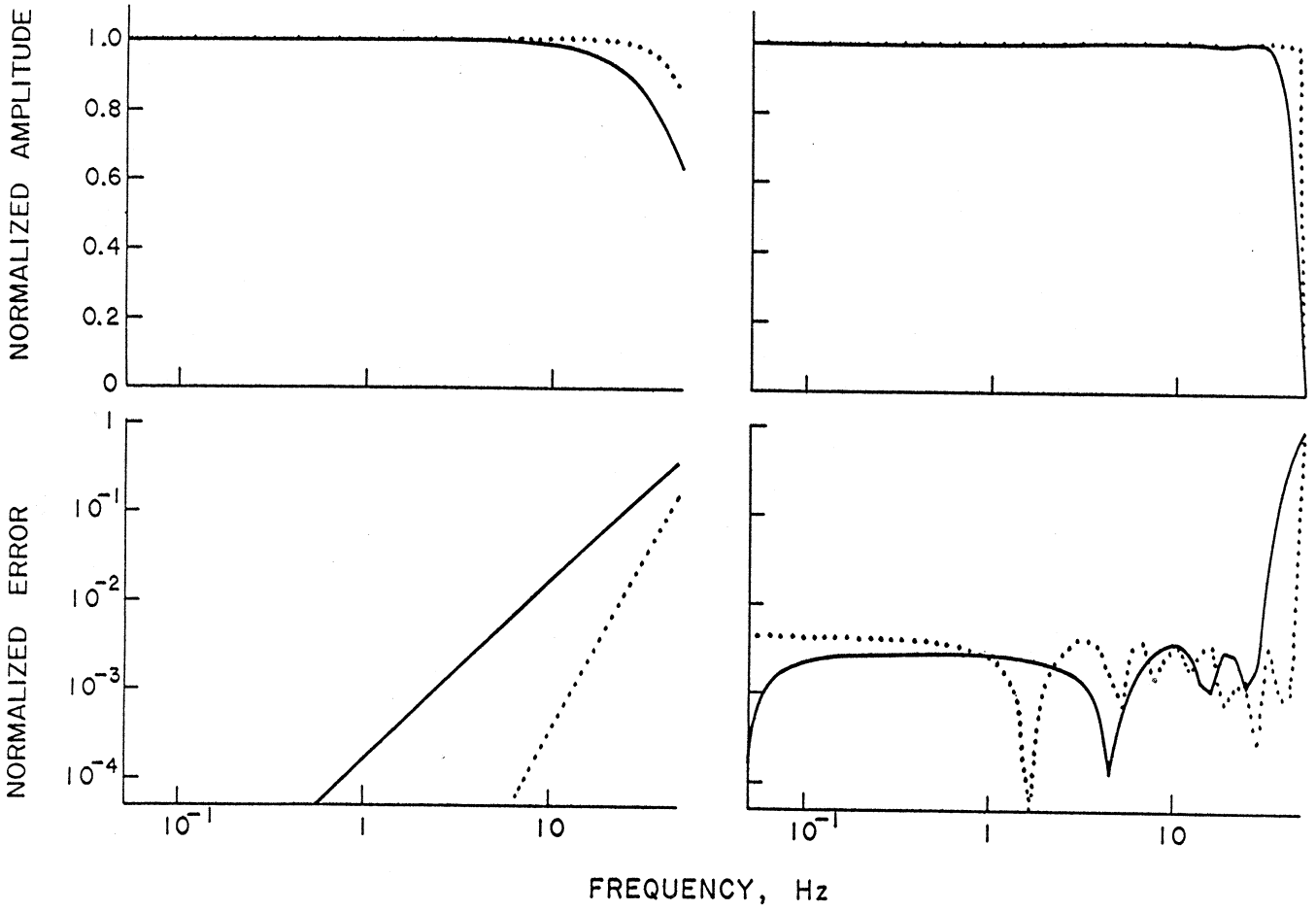

Figure II4 - 3 3-point (solid lines) and 5-point (dotted lines) transfer function $|H(\omega)/\omega|$ versus ω for $T = 0.005$ sec.

Figure II4 - 4 9-point (solid lines) and 31-point (dotted lines) transfer function amplitudes of $|H(\omega)/\omega|$, using FIR and $\Delta T = 0.01$.

With digitized data now available at 200 points/sec, or at time spacing of $T = .005$ sec, Fig. $II4-3$ shows a plot of the normalized transfer function amplitudes of $|H(\omega)/\omega|$ in Eq. ($II4.3.1$) versus frequency in Hz. The ideal transfer function will have a normalized amplitude of $|H(\omega)/\omega| = 1$ for all frequencies.

At 25 Hz, the lowpass cutoff frequency currently used in routine data processing (Trifunac and Lee, 1979), the 3- points' formula has a normalized magnitude of .8, while the 5-points' formula has magnitude of .98. Sunder (1980) proposed the use of 9-points' differentiating formulae obtained from the design of a Finite Impulse Response (FIR) filter with ripples. With data he proposed to be sampled at 100 points/sec, or a Nyquist frequency of 50 Hz, their normalized transfer function magnitudes versus frequencies are plotted in Fig. $II4-4$. At 25 Hz, both formulae have magnitudes close to 1, while at 50 Hz, the proposed Nyquist frequency, both have magnitudes decreasing rapidly to 0.

The question naturally arises, whether the 9-points or 31- points' FIR differentiating formulae proposed by Sunder (1980) should make any difference, if any, to the instrument correction step performed on the manually digitized data, for example, in the first 10 years of routine processing. Fig. $II4-3$ shows a plot of the logarithm of the normalized error amplitudes versus frequency, where

$$\varepsilon(\omega) = |H(\omega)/i\omega - 1.| \qquad (II4.3.2)$$

for the central difference 3-points' and 5-points' formulae. The magnitudes of the errors are significantly less than .01 for frequencies up to 10 Hz. Fig. $II4-4$ shows the same error amplitudes for the 9-points' and 31-points' FIR formulae. The magnitudes of the errors are systematically of order around .01 all through the range of frequencies considered. This is the result of allowing ripples in the design of the FIR filter, a fact which has already been discussed in section $II3.4$

Fig. $II4-5$ shows a plot of the average Fourier spectra versus period at M.M.I. levels of IV, VI, VIII, X and XII. It is obtained by empirical scaling of 186 strong-motion earthquake records (Trifunac and Lee, 1978). The data have been obtained by manual digitization of analog records obtained for earthquakes in the years from the 1933 through 1971. The plot shows that the Fourier amplitudes at periods $T < .05$ sec, or at frequencies $f > 20$ Hz, are less than 10% of the average amplitudes in the whole range of frequencies (.07 to 25 Hz). The previous three figures thus lead us to the conclusion that the different differentiating formulae will not lead to any significant change in the acceleration data that are based on old manual digitization of records between 1933 and 1971 .

Strong-motion data are now available at 200 points/sec or higher, or for Nyquist frequency of at least 100 Hz. Advances in the technology of designing strong-motion instruments may eventually lead to broadening the usable frequency range from the present value of 25 Hz to as high as 50 Hz. Thus, we need a differentiating formula that is accurate up to that range of frequency, or more generally, that has a transfer function that is accurate up to the variable cutoff frequency and decreases to zero beyond the cutoff frequency.

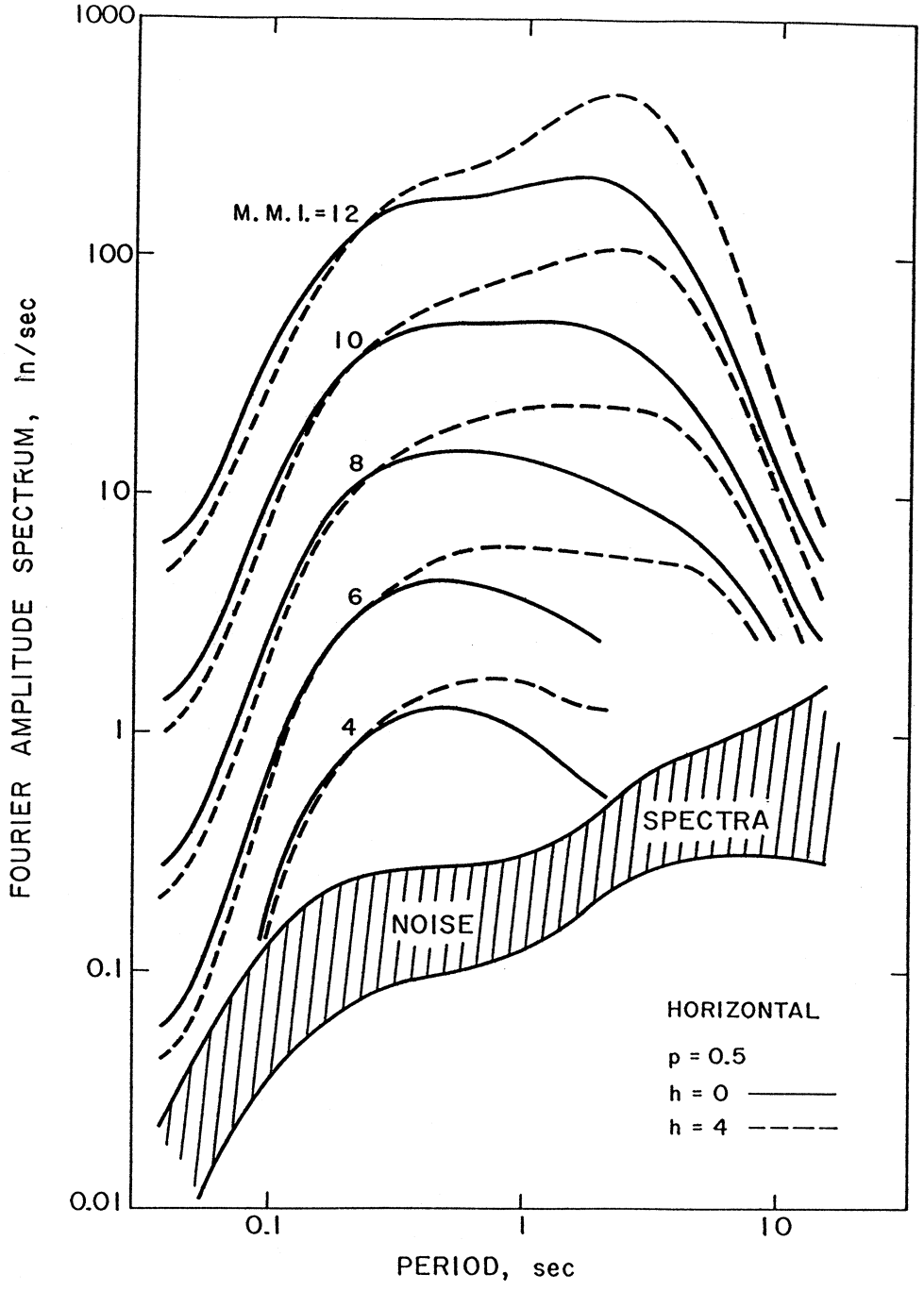

Figure II4 - 5 Average ($p = 0.5$) Fourier amplitude spectra versus period, for MMI levels IV, VI, VIII, X and XII. h is the depth of the sediments in km.

*II*4.4 Design Criteria for a Differentiation Formula

Based on the previous discussions, we need a differentiation formula that is accurate for data with frequencies up to the variable cutoff frequency, ω_L.

Let $\lambda = \omega_L/\omega_N$ be the ratio of the cutoff frequency to that of the Nyquist frequency, with $0 < \lambda < 1$. We propose the following criteria for the design of the differentiation filter:

(1) that the filter has the following input-output relationship:

$$\dot{x}[n] = \sum_{-K}^{K} c[k]x[n-k] = \sum_{1}^{K} c[-k](x[n+k] - x[n-k]) \qquad (II4.4.1)$$

where $K = K(\lambda)$ is the order of the filter. $c[k] = c[k,\lambda]$, k from $-K$ to K, will be the coefficients of the filter, all of which will depend on λ. The coefficients chosen will be asymmetric, or $c[0] = 0$, and $c[-k] = -c[k]$. Such a K-th order central difference type formula will give a transfer function that is purely imaginary:

$$H(\omega) = 2i \sum_{1}^{K} c[-k] \sin(k\omega) \qquad (II4.4.2)$$

as in the case of the ideal differentiator. Eq. (*II*4.4.3) guarantees that there will be no phase distortion from the filter.

(2) that the coefficients $c[k]$ be chosen so that the transfer functions vary smoothly and are close to that of the ideal differentiator in the pass-band, $0 \leq \omega \leq \omega_L$. No ripples should be present in the transfer function amplitudes in the pass-band, (section *II*3.4). The ratio of the normalized filter magnitude, $|H(\omega)/\omega|$, should approach unity tangentially at zero frequency. This will ensure that the error magnitude (Eq. *II*4.3.2) in the passband will vary smoothly from zero, at zero frequency, to an allowable limit, at the cutoff frequency. Suitable criteria for this limit may be stated as follows:

(3) that the normalized error magnitude of the differentiator within the pass-band, $\varepsilon(\omega)$, satisfies, say

$$|\varepsilon(\omega)| \leq 10^{-1} \qquad 0 \leq \omega \leq \omega_L \qquad (II4.4.3)$$

where from Eq. (*II*4.3.2)

$$\varepsilon(\omega) = \left| \frac{H(\omega)}{i\omega} - 1 \right| .$$

Based on the design criteria set above, we decided to design a class of differentiation filters that are monotone over the frequency band.

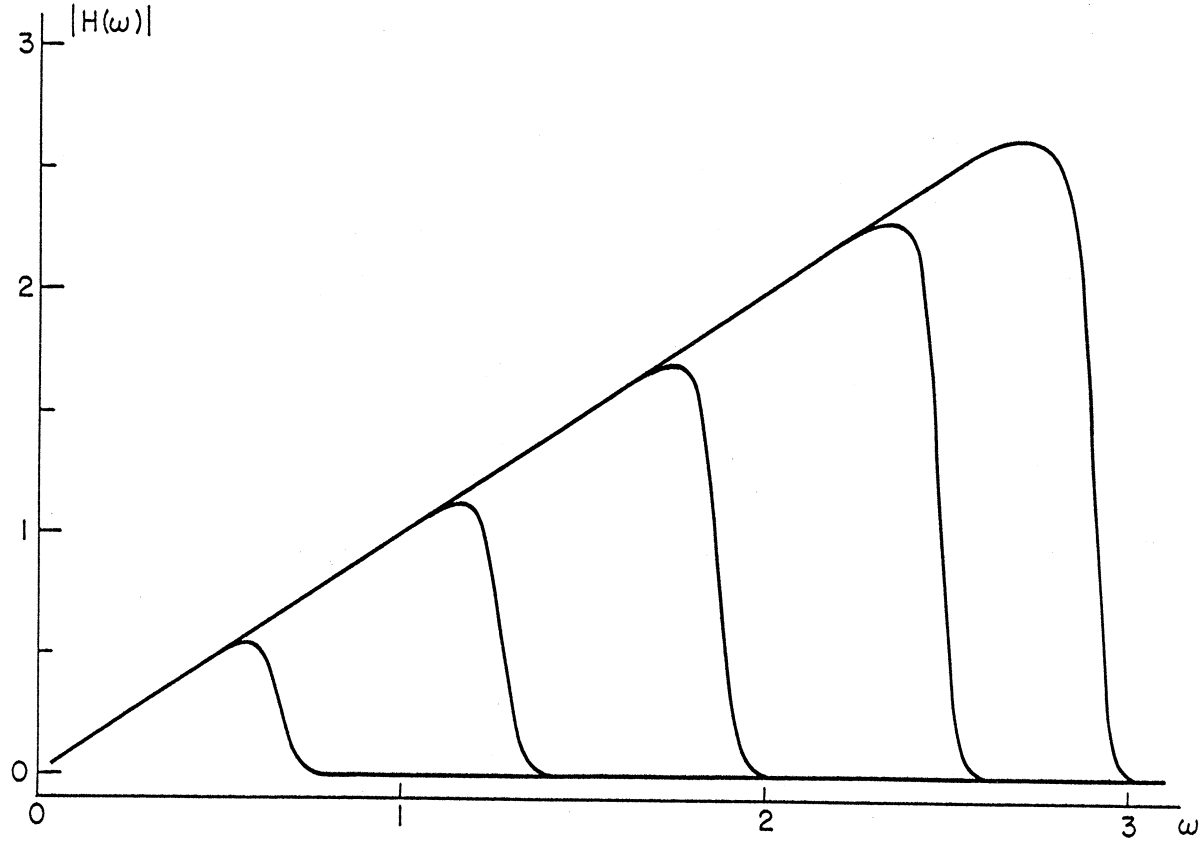

Figure II4 - 6 Differentiation filter amplitudes versus frequency (equation II4.4.7).

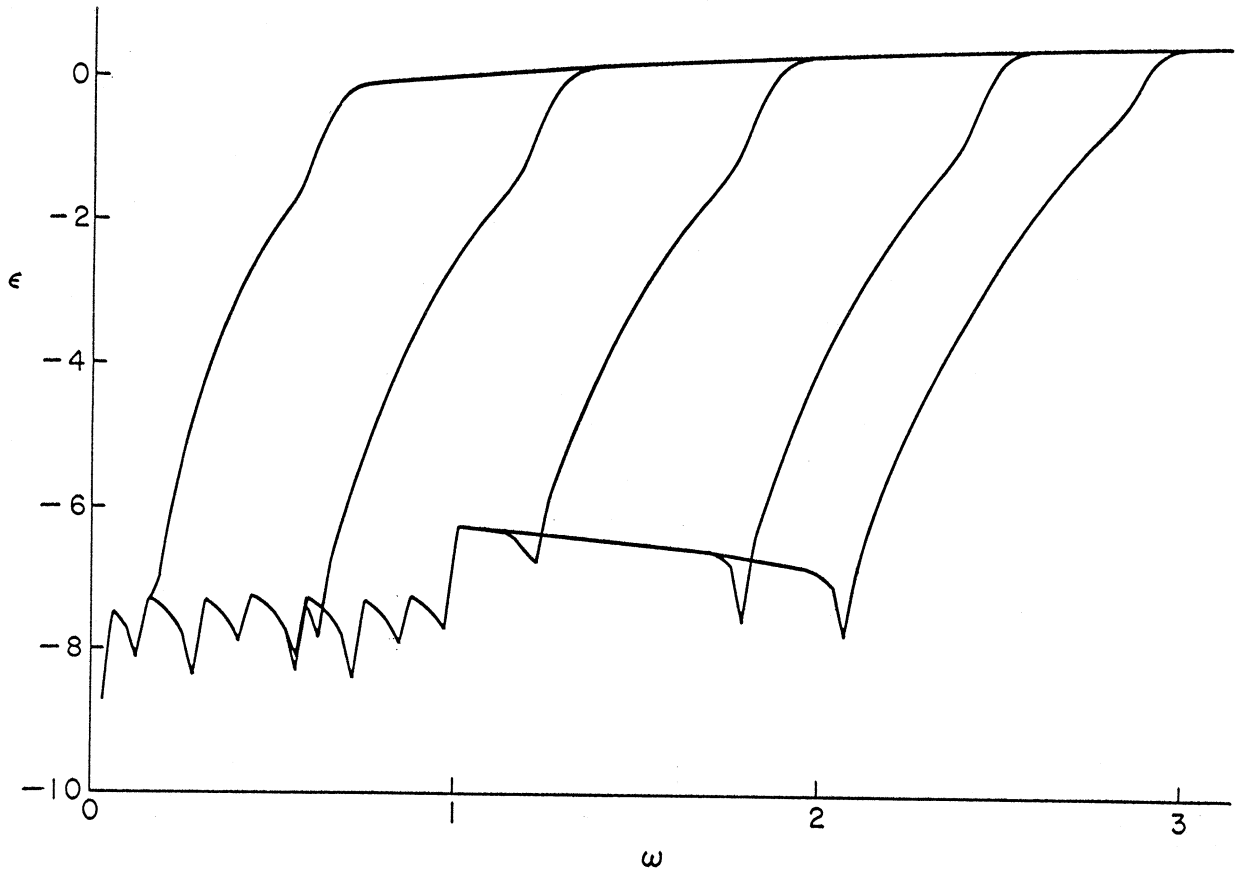

Figure II4 - 7 Normalized error magnitudes for differentiation filters in Figure II4 - 6.

Let $H_L(\omega)$ be the smooth nonrecursive low-pass filter given in section $II3.5$. It has the form

$$H_L(\omega) = b[0] + \sum_1^K b[k] \cos k\omega \simeq \begin{cases} 1 & 0 < \omega < \omega_L \\ 0 & \omega > \omega_L \end{cases} \qquad (II4.4.4)$$

Consider the function

$$H_L(\omega) = \sum_1^K c[k] \cos k\omega \qquad (II4.4.5)$$

whose coefficients $c[k]$ are defined by

$$c[0] = 0 \qquad c[k] = b[k]/(1 - b[0]), \qquad (II4.4.6)$$

so that the function $H_L(\omega)$ again approximates the ideal low-pass filter, with the only difference that it does not have a constant term, $c[0]$. Consider the differentiator filter, $H_D(\omega)$, given by

$$H_D(\omega) = \sum_1^N i\frac{c[k]}{k} \sin k\omega \qquad (II4.4.7)$$

This is obtained by integrating the "modified" smooth low-pass filter in Eq. $(II4.4.5)$ term by term w.r.t. ω and multiplying by i. This is a differentiation filter because the integral of the ideal low-pass filter w.r.t. ω

(ideal)

$$H_L(\omega) = \begin{cases} 1 & 0 < \omega < \omega_L \\ 0 & \omega > \omega_L \end{cases} \qquad (II4.4.8)$$

is the ideal differentiating filter:

(ideal)

$$H_D(\omega) = \begin{cases} i\omega & 0 < \omega < \omega_L \\ 0 & \omega > \omega_L \end{cases} \qquad (II4.4.9)$$

after multiplication by i.

The resulting differentiation filter, Eq. $(II4.4.7)$, is a smooth filter since it is derived from the smooth low-pass filter given in Section $II3.5$. Figure $II4-6$ shows a plot of the amplitudes versus frequencies for the function at various cutoff frequencies along the frequency band. Each of the functions approximates the ideal differentiator with slope 1 in its passband, and then slopes linearly to 0 from the cutoff frequency to the Nyquist frequency. After concatenation with their corresponding smooth low-pass filter, the amplitudes in the plot slope almost vertically to zero in the stop band. The normalized error magnitudes of the functions are given in Fig. $II4-7$. The functions used are all within the design criteria specified above.

*II*5 Data Processing for Volume II: (c) Baseline Correction and Noise-Free Frequency Band

*II*5.1 Introduction

Accelerograms low-pass filtered and corrected for instrument response are next baseline corrected by high-pass filtering. For all the records, an initial cutoff frequency of 0.07 Hz for the filter is first used. This corresponds to a cutoff period of approximately 14 sec, a sufficiently long period to cover a wide enough band of information for most strong-motion accelerograms (Trifunac et al., 1973). The final cutoff period or frequency band for each accelerogram will be determined separately from the signal- to-noise ratio of each component (Trifunac and Lee, 1979). This will be discussed in the second half of this chapter.

Prior to the introduction of the Automatic Record Digitization System (ARDS) (Trifunac and Lee, 1979), with data available only from hand digitization, the accelerogram data after instrument correction were then available at 50 points/sec, equally spaced at 0.02 seconds. The routine computer data processing then consisted of the following procedure for baseline correction (Trifunac, 1971):

(1) Prior to filtering the instrument corrected data, a straight zero acceleration baseline is least square fitted to the data to eliminate possible distortions caused by placing the photographic enlargement of the film negatives or a photocopy onto the digitization table.

(2) The data were next low-pass filtered by an equally weighted running mean filter with a window width of 0.04 sec (f = 2.5 Hz).

(3) The low-pass filtered data were decimated and only every tenth point was kept. The decimated data were then at 0.2 sec apart, or at 5 points/sec with a Nyquist frequency of 2.5 Hz. All long period components of periods over 10 sec were thus essentially undisturbed.

(4) The decimated data were then used as input to a low-pass Ormsby filter with cutoff frequency of 0.07 Hz. The resulting low-pass filtered data then represented the zero baseline data (Trifunac, 1971; Trifunac and Lee, 1979).

(5) The zero baseline data were interpolated to the original time spacing of 50 points/sec. Straight line interpolation was used.

(6) The baseline corrected data were obtained by subtracting the zero baseline data from the original data.

For data now available at 200 points/sec or more, or with a Nyquist frequency of at least 100 Hz at this stage, a high-pass cutoff frequency in the vicinity of .1 Hz will thus correspond to a ratio of 1 in 1000, or a very small fraction of the whole frequency band of the data. This is thus the problem of narrow band filtering or narrow band rejection.

*II*5.2 Narrow Band Filtering

The implementation of a narrow-band filter used to be one of the most difficult problems in digital filtering. This is because such narrow band filters inherently have sharp transitions in their frequency response, thus requiring sophisticated high-order designs to meet the desired frequency response specifications. Those filters usually require lengthy computation in their realizations. Rabiner and Crochiere (1975) showed that efficient implementation of narrow-band filtering by a digital filter can be realized using a sampling rate reduction (decimation) followed by a sampling rate increase (interpolation). Such decimation and interpolation processes can be efficiently implemented using finite impulse response (FIR) digital filters.

The proposed new procedure can be shown to have the following properties:

(1) The computation (in terms of multiplications per sample) needed to implement the filter is greatly reduced from that required for a standard direct form implementation for an equivalent finite impulse response (FIR) digital filter.

(2) The computation is comparable to that required for optimum (elliptic infinite impulse response (IIR) filters in a cascade realization.

(3) The phase response can be set to be linear or even zero.

(4) The roundoff noise generated in computing the output can be significantly less than that of a standard direct form FIR implementation.

(5) The coefficient sensitivity problems can be less severe than those for standard direct form FIR implementations.

*II*5.3 Multi-Stage Decimation and Interpolation

For data sampled at 100 to 200 points/sec, a multi-stage (2 or 3) decimation-interpolation for narrow-band FIR filtering has been found to be efficient (Crochiere and Rabiner, 1975). The general procedure for N such stages is as shown in Fig. $II5-1$.

At the i-th stage of decimation, let the input signal have a sampling interval of T_i sec, and the output decimated signal have a sampling rate of $T_{i+1} = MT_i$ sec. The input signal is first low-pass filtered giving the signal $w[n]$. This is done to avoid aliasing at the larger sampling interval MT_i. The sampling rate reduction is then achieved by forming a new sequence ($y[n]$) by extracting every M-th sample of $w[n]$. A block diagram of this stage is given in Fig. $II5-2$.

The process of interpolating the input signal at the i-th stage of interpolation is similar, as shown in Fig. $II5-3$, where the sampling rate is increased by an integer ratio L, or equivalently, the sampling interval reduced by a factor $1/L$, so that $T_{i+l} = T_i/L$. This is done by first inserting $(L-1)$ zero-valued samples between each sample of $y[n]$.

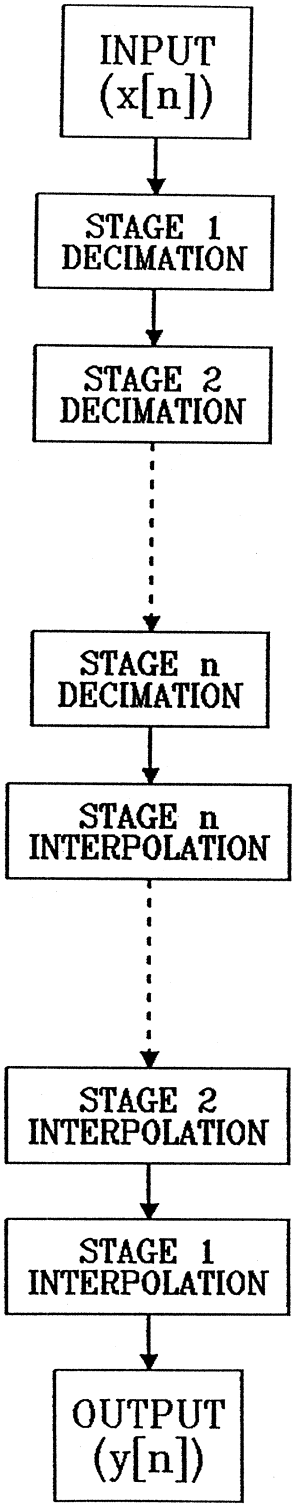
INPUT
(x[n])
STAGE 1
DECIMATION
STAGE 2
DECIMATION
STAGE n
DECIMATION
STAGE n
INTERPOLATION
STAGE 2
INTERPOLATION
STAGE 1
INTERPOLATION
OUTPUT
(y[n])

Figure II5 - 1

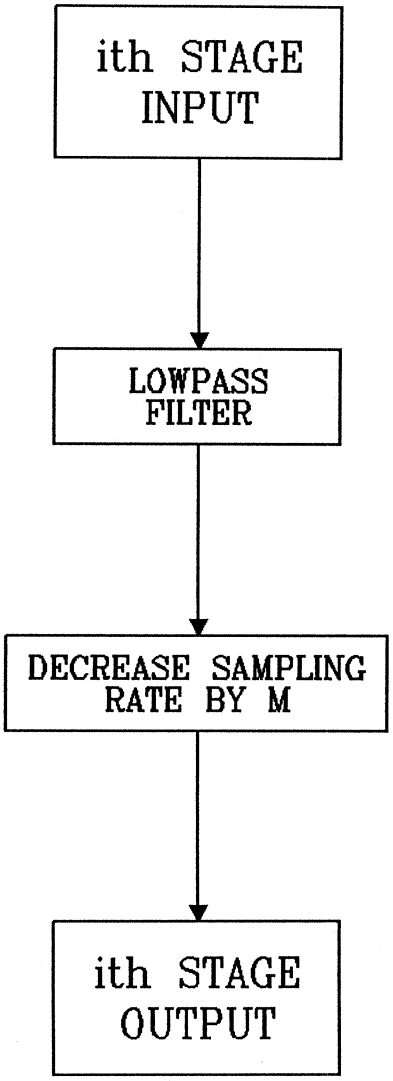

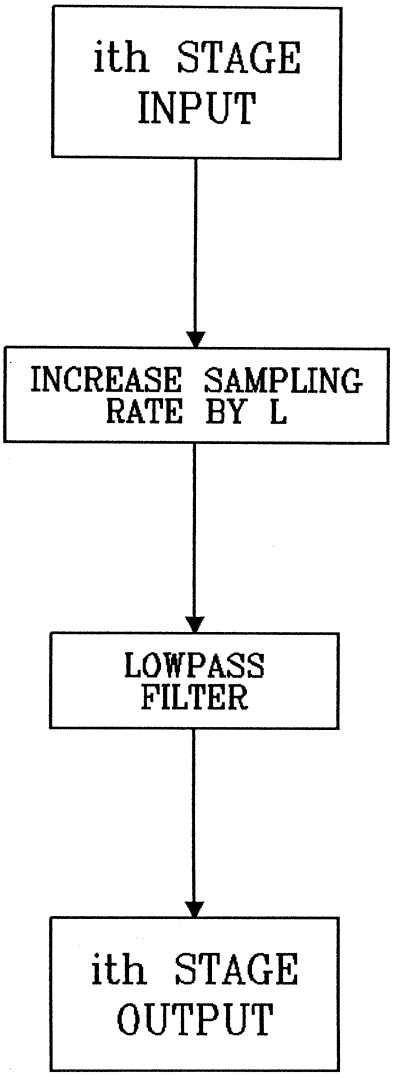

Figure II5 - 2 (Left)
Figure II5 - 3 (Right)

This will create a signal $w[n]$ having frequency component with period identical to the original sampling period.

The next step is to eliminate these periodic components and retain only the pass-band frequencies by an appropriate low-pass interpolation filter. The implementation of such filter will be discussed in more detail in the next section. The resulting output signal is then the desired interpolated signal with sampling rate $T_{i+1} = T_i/L$.

Note that the implementation of such interpolators and decimators involves the use of digital filters in which the input and output sampling rates are different. One of the important considerations in the implementation of such sampling rate changing systems is the choice of the appropriate type of low-pass filters (Rabiner and Gold, 1975). For this type of system, significant savings in computation can be obtained by using a FIR non-recursive filter in a direct form implementation. Such saving in computation is due to the observation that for FIR decimators only one out of each M output samples needs to be calculated, while for FIR interpolators, (L-1) out of every L samples of the input are zero-valued, and thus do not affect the computation. These facts cannot be exploited using the corresponding recursive IIR filters.

As mentioned above, the design of interpolation filters involves the use of low-pass digital filters. Such filters can be designed in a variety of ways, as described in Lee (1989) for example, using window designs, equiripple designs, smooth designs, etc. The FIR nonrecursive interpolation filter turns out to be the most efficient, as described in the previous section. The filter used here is one designed by Oetken et al. (1975). It is one in which the mean square criterion is used.

This is applied to a computer program for the design of an interpolation filter in which the sampling rate is increased by an integer factor of L. The resulting filter design allows the original input samples to pass through the interpolator unchanged and it interpolates $(L-1)$ sample values in between each pair of original samples in such a way that the mean square error between these samples and their ideal values is minimized. The ideal values are the theoretical values predicted by the sampling theorem. The input signal is assumed to be band limited, which is always the case for the low-passed equally spaced accelerogram data.

The original input sample ($x[n]$), given at the original sampling rate, is first converted to one of the new sampling rates (w[n) as follows:

$$w[n] = \begin{cases} x[n], & \text{n = kL} \\ 0, & \text{otherwise} \end{cases} \qquad (II5.3.1)$$

$w[n]$ is obtained from $x[n]$ by inserting $(L-1)$ zeros between adjacent samples of the input sample data. Assuming the degree of the filter to be $2LN$, the output of the filter $y[n]$, will be

$$y[n] = \sum_j h[j]w[n-j] \qquad (II5.3.2)$$

will create a signal w[n] having frequency component with period identical to the original sampling period.

The next step is to eliminate these periodic components and retain only the pass-band frequencies by an appropriate low-pass interpolation filter. The implementation of such filter will be discussed in more detail in the next section. The resulting output signal is then the desired interpolated signal with sampling rate $T_{i+1} = T_i/L$.

Note that the implementation of such interpolators and decimators involves the use of digital filters in which the input and output sampling rates are different. One of the important considerations in the implementation of such sampling rate changing systems is the choice of the appropriate type of low-pass filters (Rabiner and Gold, 1975). For this type of system, significant savings in computation can be obtained by using a FIR non-recursive filter in a direct form implementation. Such saving in computation is due to the observation that for FIR decimators only one out of each M output samples needs to be calculated, while for FIR interpolators, (L-1) out of every L samples of the input are zero-valued, and thus do not affect the computation. These facts cannot be exploited using the corresponding recursive IIR filters.

As mentioned above, the design of interpolation filters involves the use of low-pass digital filters. Such filters can be designed in a variety of ways, as described in Lee (1989) for example, using window designs, equiripple designs, smooth designs, etc. The FIR nonrecursive interpolation filter turns out to be the most efficient, as described in the previous section. The filter used here is one designed by Oetken et al (1975). It is one in which the mean square criterion is used.

This is applied to a computer program for the design of an interpolation filter in which the sampling rate is increased by an integer factor of L. The resulting filter design allows the original input samples to pass through the interpolator unchanged and it interpolates $(L-1)$ sample values in between each pair of original samples in such a way that the mean square error between these samples and their ideal values is minimized. The ideal values are the theoretical values predicted by the sampling theorem. The input signal is assumed to be band limited, which is always the case for the low-passed equally spaced accelerogram data.

The original input sample ($x[n]$) given at the original sampling rate is first converted to one of the new sampling rates (w[n) as follows:

$$w[n] = \begin{cases} x[n], & \text{n = kL} \\ 0, & \text{otherwise} \end{cases} \qquad (II5.3.1)$$

$w[n]$ is obtained from $x[n]$ by inserting (L - 1) zeros between adjacent samples of the input sample data. Assuming the degree of the filter to be 2LN, the output of the filter $y[n]$, will be

$$y[n] = \sum_j h[j]w[n-j] \qquad (II5.3.2)$$

where $h[j]$ is the impulse response of the filter. Since $w[n] = 0$ for $n \neq kL$ according to Eq. (II5.3.1), for $n = kL$,

$$y[kL] = \sum_j h[jL]x[(k-j)L] \qquad (II5.3.3)$$

and for $n = kL + i$, with i = 1,2,3,...,L - 1,

$$y[kL] = \sum_j h[jL + i]x[(k-j)L] \qquad (II5.3.4)$$

which means that for $n = kL$, $y[n]$ will be calculated using only $2N + 1$ samples of $x[n]$ and $h[n]$ and if $n \neq kL$, only $2N$ samples of both sequences will be used.

Examples of the use of the filter to input samples of sine functions at various sampling rates are shown in Fig. $II5-4$, where the original sample points are represented by "0" and the output data are plotted as solid lines. Note that the characteristics of the interpolation filter enable the interpolated data to fill in missing peaks predicted by the sampling theorem that are not present in the original sample.

II5.4 The Determination of Cutoff Frequency Band

Having determined and established the use of proper decimation and interpolation filters for baseline correction, we turn to the problem of the determination of the "right" or appropriate cutoff frequency band. As mentioned at the beginning of this chapter, when the routine data processing scheme was first developed, all digitized data were band-pass filtered in the frequency band from 0.07 Hz to 25 Hz (Trifunac, 1971) so that the digitization and processing noise outside the frequency band can be eliminated. The choice of 0.07 Hz and 25 Hz was then based on a detailed study of digitization error characteristics of the digitization system available at that time (Trifunac et al., 1973). These limits then and now do not necessarily apply to records digitized elsewhere with different digitization equipment and processing machines. It is also the case that accelerograms with smaller amplitudes may have a more restricted frequency band within which the signal-to-noise ratio is greater than one.

In the early stage of routine processing, it becomes clear that the optimum band-pass frequency would have to vary from one record to another, if one were to eliminate all significant noise from the digitized data. With routine processing of all data in the band 0.07 Hz to 25 Hz, it was known that many records with small amplitudes, recorded during small to intermediate earthquakes and at intermediate to large distances, will still have a considerable content of digitization and processing noise, especially for periods longer than 1 to 2 seconds. Trifunac (1977) presented an analysis of the first 186 ground motion records, in which he established the frequency bands beyond which the data may be affected by digitization and processing noise.

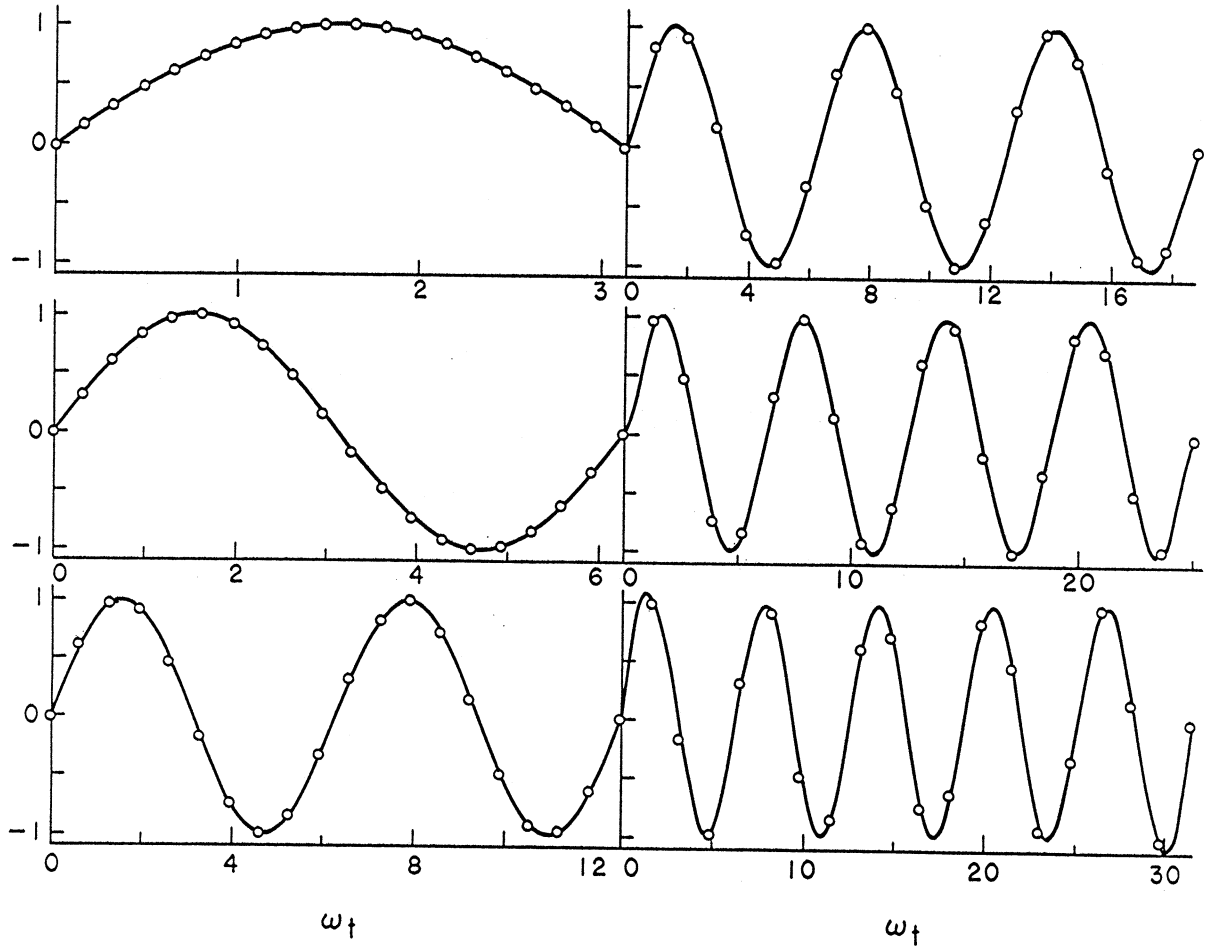

Figure II5 - 4 Interpolation filter (solid lines) and original sample points (small circles).

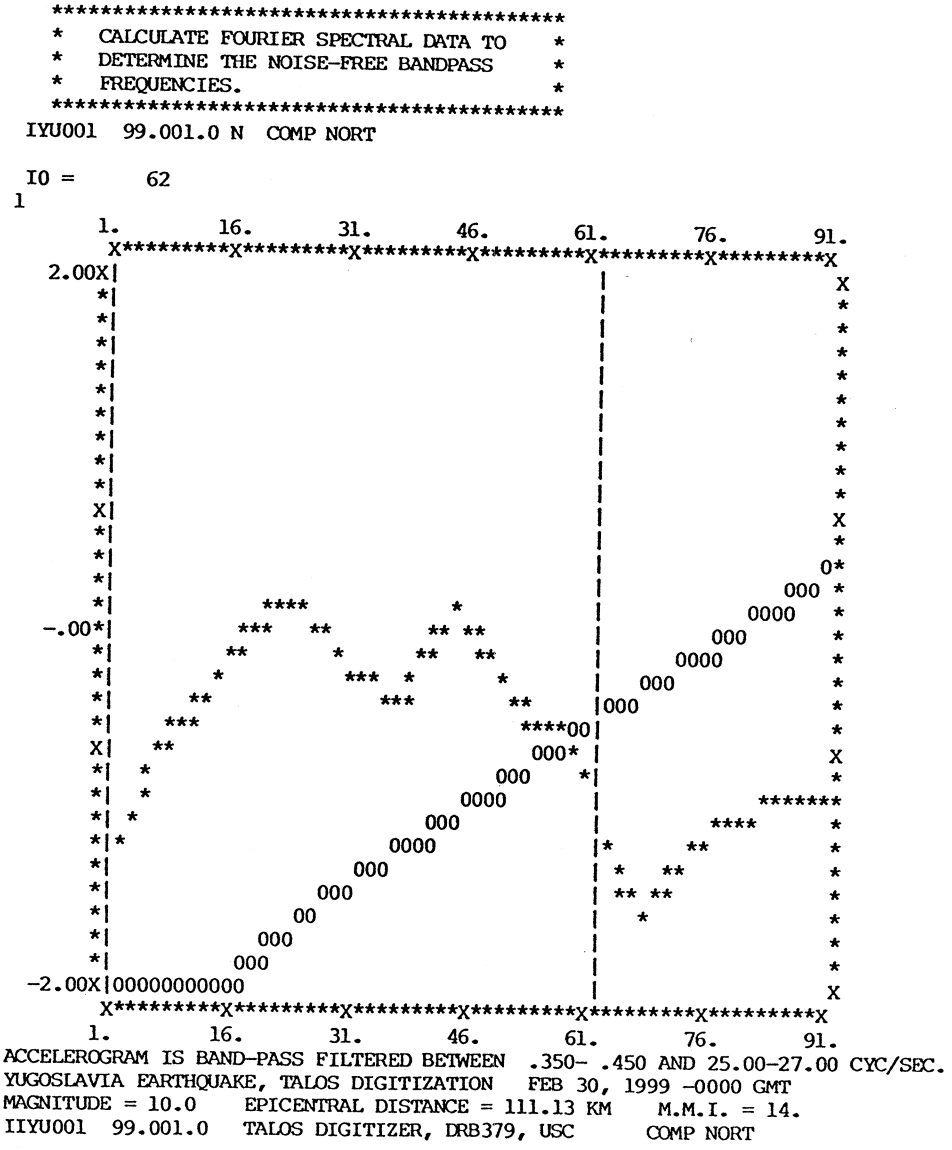

Figure II5 - 5 Selection of long period cut-off for chosen signal-to-noise ratio equal to 1. The horizontal axis, labeled by 1 through 91, shows 91 periods along $\log_{10} T$ axis and with $T(1) = 0.04$ sec and $T(91) = 15$ sec. The vertical amplitude scale corresponds to $\log_{10} |F(T)|$ in in/sec.

Trifunac and Lee (1978) considered a batch of 186 records which correspond to uniformly processes earthquake ground accelerations in the Western United States of America for the period from 1933 to 1971. These were refiltered with band-pass frequencies predetermined by visual inspection to maximize the signal-to-noise ratio within the band. Of the 186 records or 558 components considered, 69% were originally processed with standard 15 sec (0.07 Hz) cutoff, and the remaining 31% with the 8 sec (.125 Hz) cutoff. As a result of the above procedure, as much as 50% of the records routinely filtered at 15 sec were refiltered with a shorter long period cutoff ranging from 1 to 15 sec. Similarly, about 12% of the records, routinely filtered at 8 sec were refiltered with cutoff periods ranging from 1 to 8 sec.

It is also found in many cases, that the signal-to-noise ratio at the high frequency (short period) end also becomes small for many accelerograms which were recorded during small earthquakes and/or at greater epicentral distances. For the current Automatic Digitization using PC, an estimate of the digitization noise was presented in Part I of this work.

It might appear difficult at present, as it was in the late 60's through the 80's, to select an optimum long period cutoff for a standard routine data processing scheme. No such one cutoff period for all records can be selected to satisfy the requirements of all future analyses which will or need to use the corrected strong-motion accelerograms. It becomes clear, however, that in the routine data processing scheme, a step has to be included to have a computer subroutine determine automatically the frequency band that is as free from noise as possible, and a subsequent step to refilter the data at this new cutoff frequency band. The resulting strong-motion acceleration data from routine processing will now have a variable cutoff frequency band that normally depends on the amplitudes of the strong-motion, which in turn depend on the magnitudes of the earthquake, the local geology and epicentral distance of the site from the source.

Fig. $II5-5$ shows an example of the current computer output at the step where the Fourier amplitudes of the input acceleration are calculated and compared with those of the digitization noise of the same length. A simple line-printer plot shows the automatic determination of the cutoff period, which in this case is shorter than the usual 15 sec cutoff period. Here, the x-axis is labeled from 1 to 91 and represents the 91 periods from 0.04 sec to 15 sec, which are roughly uniformly distributed along the logarithmic scale. The vertical axis is for $\log_{10}|F(T)|$ and with units of inches/second.

*II*6 Data Processing for Volume II: (D) Corrected Velocity and Displacement

*II*6.1 Introduction

With the digital acceleration data band-pass filtered and instrument corrected, integration is the next step of data processing to complete the calculation of the velocity and displacement curves. The calculation of the velocity and displacement data from an accelerogram is not a trivial matter (Hudson, 1970). Early in the 1960's, a number of studies of the best way of carrying out this integration have been made (Hudson, 1963; Berg, 1963; Brady, 1966; Amin and Ang, 1966; Schiff and Bogdanoff, 1967). In the 1970's, most methods employed digital computations and certain correction techniques for long period errors resulting from integration (Trifunac and Lee, 1973).

Hudson (1970) listed several important reasons for the computation of velocity and displacement data with reasonable accuracy. Edwards and Northwood (1959) and Neumann (1958) showed that for blast loading the single best descriptive number related to structural damage is the maximum ground velocity. Neumann (1959) also showed that the maximum ground velocity can be correlated approximately with the Modified Mercalli Intensity Scale, a scale commonly used to give a round measure of the damage associated with strong earthquakes. In a similar fashion, the ground displacement data also has practical application because of the direct relationship between ground displacements and the strain to which large structures such as dams and underground pipelines might be subjected.

*II*6.2 Digital Integration

The data processing program developed originally for the manually digitized data (Trifunac and Lee, 1973) used the trapezoidal rule of integration,

$$y[n+1] = y[n] + .5T(x[n] + x[n+1]) \qquad (II6.2.1)$$

with $(x[n])$ representing the input and $(y[n])$ the output digital data. T is the equally spaced sampling time of the sequence in seconds. Since y occurs on both sides of this equation, this is a recursive filter.

Again, as in the case of differentiation formulae (Section *II*4.1), with data originally interpolated to 100 points/sec, the trapezoidal rule is good for data up to frequencies of about 15 Hz. We again examine the numerical integration formulae in the frequency domain, which then becomes the problem of designing a filter to estimate the integral of digital data. The integration filter is to be designed as a linear time-invariant system, where the complex exponential functions, $\exp(i\omega t)$, are again eigenfunctions (Section *II*4.2). The equation for the integral

$$\int \exp(i\omega t)\,dt = \frac{1}{i\omega}\exp(i\omega t), \qquad (II6.2.2)$$

gives the transfer function of the integration filter as (for T=1)

$$H(\omega) = \frac{1}{i\omega} \qquad (II6.2.3)$$

for $-\pi \leq \omega \leq \pi$. The ideal integrator with cutoff frequency, ω_c, has a transfer function similarly given by

$$H_I(\omega) = \begin{cases} \frac{1}{i\omega} & |\omega| < \omega_c \\ 0 & \omega_c < |\omega| < \pi \end{cases} \qquad (II6.2.4)$$

Note from Eqs. (*II*6.2.3) and (*II*6.2.4) that the phase of the integration filter is $-\pi/2$. The filter corresponding to the trapezoidal rule, Eq. (*II*6.2.1), by assuming the input $x(t)$ as $e^{i\omega t}$ and the corresponding output $y(t)$ as $H(\omega)e^{i\omega t}$, has a transfer function

$$H(\omega) = \frac{1}{2}\frac{(e^{i\omega}+1)}{(e^{i\omega}-1)} = \frac{\cos\frac{\omega}{2}}{2i\sin\frac{\omega}{2}}, \qquad (II6.2.5)$$

which approaches $\frac{1}{i\omega}$ as $\omega \to 0$, but gradually decreases to zero as $\omega \to \pi$, the Nyquist frequency. This means that, like most common integration formulae, the frequency response function of the integrator will not differ significantly from the ideal response at frequencies much less than the Nyquist frequency. If the input to an integrator is band limited to frequencies less than the Nyquist frequency, the theory shows that it should be able to integrate the function exactly. Exact integration will, however, require the entire input time history. Integration formulae with a finite number of filter weights should, therefore, be designed to have a frequency response within the passband frequency, as close to the ideal one as possible.

Sunder (1980) proposed the use of an integration formula (Schussler-Iber) of the form:

$$y[n+1] = y[n] + \left(\frac{T}{3}\right)\sum_{k=0}^{7} b[k]x[n+1-k], \qquad (II6.2.6)$$

with $b[k] = b[7-k]$. The phase of the corresponding filter, however, is not $-\pi/2$, unlike the case of the ideal integrator. Hence, the use of this filter will produce a phase distorted output, which is objectionable for data processing in earthquake engineering.

*II*6.3 Design Criteria for a Digital Integrator

To choose an appropriate integration formula, let $y(t)$ be the integral of a function $x(t)$:

$$y(t) = \int_0^t x(u)du \qquad (II6.3.1)$$

where $x(t) = 0$ for $t < 0$, and $t \geq (N-1)T$. The function $x(t)$ is sampled at equally spaced intervals of T sec, $\{x[n]\}$, with $x[n] = x(nT)$, $n = 0, 1, 2, \ldots$ Integrating the function in steps of T seconds, we can write

$$y[n+1] = y[n] = + \int_{nT}^{(n+1)T} x(t)dt \qquad (II6.3.2)$$

The portion of the function $x(t)$ for $nT \leq t \leq (n+1)T$ can be reconstructed, say, from the sequence $\{x[n+k]\}$, for k from $-K+1$ to $+K$, using some form of reconstruction formula,

$$x(t) = \sum_{k=-K+1}^{K} x[n+k]h(t-(n-k)T), \qquad (II6.3.3)$$

where $h(t)$ is the impulse response of the reconstruction filter. Note that when $K = \infty$, the Whittaker reconstruction filter will be one such filter.

Substituting Eq. $(II6.3.3)$ into Eq. $(II6.3.2)$ gives

$$y[n+1] = y[n] + \sum_{k=-K+1}^{K} b[k]x[n+k], \qquad (II6.3.4)$$

where

$$b[k] = \int_0^T h(t+kT)dt. \qquad (II6.3.5)$$

To ensure that the corresponding filter has a phase shift of $-\pi/2$, we need

$$b[k] = b[-k+1] \qquad (II6.3.6)$$

for $k = 1$ to K, so that

$$y[n+1] = y[n] + \sum_{k=1}^{K} b[k](x[n+k] + x[n-k+1]). \qquad (II6.3.7)$$

Choosing $x(t)$ as $e^{i\omega t}$ and $H(\omega)e^{i\omega t}$, the transfer function of the filter is given by

$$\begin{aligned} H(\omega) &= \frac{\sum_{k=1}^{K} b[k](e^{ik\omega} + e^{-i(k-1)\omega})}{e^{i\omega} - 1} \\ &= \sum_{k=1}^{K} \frac{b[k]\cos(k-\frac{1}{2})\omega}{i\sin\frac{\omega}{2}} \end{aligned} \qquad (II6.3.8)$$

which shows that this filter indeed has the right phase of $-\pi/2$. Note that trapezoidal rule is a special case of this with $K = 1$ and $b[1] = .5$ $(T = 1)$.

As in the case of differentiation, we propose the use of the integration filter that is accurate for data of frequencies up to the pre-determined variable cutoff frequency, ω_L. Again, let $\lambda = \omega_L/\omega_N$, be the ratio of the cutoff frequency to that of the Nyquist frequency. With $0 < \lambda < 1$, we propose the following criteria for the design of the integration filter:

(1) That the filter be of the form as in Eq. (*II*6.3.4)

$$y[n+1] = y[n] + \sum_{k=-K+1}^{K} b[k]x[n+k]$$

where $K = K(\lambda)$, the order of the filter, $b[k] = b[k,\lambda]$, $k = -K+1$ to K, and the coefficients of the filter, will all depend on λ. The coefficients will satisfy $b[k] = b[-k+1]$, for $k = l, 2, 3, ..., K$, so that the phase of the filter will be $-\pi/2$, as in the case of the ideal integrator. This will ensure no phase distortion.

(2) That the coefficients $b[k] = b[k,\ \lambda]$ be chosen so that the resulting filter, Eq. (*II*6.3.8), will be as close to the ideal one as possible, within the passband of the frequency bandwidth.

(3) That the filter be as smooth as possible, the magnitude of the transfer function should be free from ripples in both the pass- and stop-band.

(4) That the amplitude ratio |design filter/ideal filter| should approach 1 as $\omega \rightarrow 0$, so that both have the same tangency at $\omega = 0$.

With appropriate digital integration performed on the acceleration data to get the velocity data, the computed velocity data is next high pass filtered using the same procedure with the same cutoff as in the case of the acceleration data. This is performed to eliminate any long period error resulting from the integration and resulting from the uncertainties involved in estimating the initial velocity of ground motion (Hudson, et al., 1971). The same baseline correction is carried out for the displacement data obtained from integrating the velocity data. Thus, the final step of Volume II data processing is now completed.

*II*6.4 Volume II Output File: *V2X0001.DAT*

The corrected acceleration, velocity and displacement data are written onto a disk file. The set-up of one disk file of the Volume II *V2X0001.DAT* (say), is as follows:

Volume II Disk File
(one file per one acceleration component)

Each file has:

(1) heading data of alphanumeric type;

(2) heading data of integer type;

(3) heading data of floating point type;

(4) corrected acceleration points equally spaced at 50 pts/sec;

(5) Velocity points equally spaced at 50pts/sec;

(6) Displacement points equally spaced at 50 pts/sec; and

(7) EOF

The detailed description and a sample of the heading data set are given in the following section.

Line Number	Heading Data Array (CORTIL(i),I=I1,I2) I1-I2	Description
1	1-40	Volume II MAIN title
2-14	41-560	Same as (CORTIL(I),I=1,520) in the line no. 1-13 of Vol. I heading data
15	561-600	Frequency limits for the band-pass filtering
16	601-640	No. of corrected acceleration data
17	641-680	Time spacing of interpolated data
18	681-720	Value & time of peak acceleration
19	721-760	Value & time of peak velocity
20	761-800	Value & time of peak displacement
21	801-840	Initial velocity G displacement
22,23	841-920	Earthquake title; same as line no.8
24,25	921-1000	Volume II earthquake title
	ICOR(I) I	
26	1-20	Same as IR(1)-IR(20) of line no.14 in Volume I heading data
27	21-30	Same as IR(21)-IR(30) of line no.15 in Volume I heading data
	31-40	Blank
28	41-50	Blank
	51	NDATAB, same as NDATA,ICOR(28)
	52	NDATA2, same as NDATA,ICOR(28)
	53	NDATAA, no. of corrected data of acceleration
	54	NSKIP1, no. of points to be skipped in the SMU decimation process
	55	NSKIP2, no. of points to be skipped in the BAS decimation process
	56	IPRO, no. of points in the digital

		filter in BAS filtering process
	57	NITR, no. of iterations used in the BAS filtering process
	58	IEXP, defined in the BAS comment cards
	59	NLINEl, no. of letters in the earthquake title (used by the plotting subroutine)
	60	NLINE2, no. of letters in the second earthquake title (used by subroutine TRILOT)
29	61	NSKVEL, no. of velocity data to be skipped in the decimation process
	62	NSKDIS, no. of displacement data to be skipped in the decimation process
	63	NSKV, no. of velocity data to be skipped in the plotting process
	64	MDATV, no, of velocity data
	65	NSKD, no. of displacement data to be skipped in the plotting process
	66	NDATD, no. of displacement data
30	67-80	Blank
	81-100	Blank
	FCOR(I) I	
31	1-5	Same as FR(1)-FR(5) in line no.15 of Volume I heading data
	6-10	0.0
32-3S	11-50	0.0
36	51	SCALEl, scaling factor for converting coordinates
	52	SCALE2, scaling factor for convering input from G/10 to cm/sec^2
	53	DDTl , time interval for equally spaced input data for Instrument Correction
	54	TMXl , duration of uncorrected data
	55	WN0, natural frequency of the instrument
	56	SCALl , scaling factors for the time coordinates
	57	SCAL2, scaling factors for the acceleration coordinates
	58	FN2, roll-off termination frequency for Ormsby low-pass filter in cps
	59	DF2, roll-off width for low-pass filter in cps
	60	TMX2, maximum value of the time coordinate for plotting
37	61	DDT2, time spacing of interpolated acceleration data
	62	FNl , roll-off termination frequency for Ormsby low-pass filter in cps
	63	DFl, roll-off width for Ormsby low-

		pass filter
	64	TBEG, initial time, usually 0.0 (set in Volume II Main Program).
	65	TVAL(l), time of peak acceleration in sec
	66	PVAL(l), value of Feak accelerationin cm/sec2
	67	TVAL(2), time of peak velocity in sec
	68	PVAL(2), value of peak velocity in cm/sec
	69	TVAL(3), time of peak displacement in sec
	70	PVAL(3), value of peak displacement in cm
38	71	v_ϕ, initial velocity
	72	BANDl, filter (high-pass) roll-off frequency in cps
	73	BAND2, filter (low-pass) roll-off frequency in cps
	74	DTV, time spacing of velocity data used in calculating weights of high-pass filters
	75	DDIS, time spacing of displacement data used in calculating weights of high-parr filters
	76	x_0, initial displacement
	77	TLVAL(2), time of peak velocity in sec in the plotting process
	78	PLVAL(2), value of peak velocity in cm/sec in the plotting process
	79	TLVAL(3), time of peak displacement in sec in the plotting process
	80	PLVAL(3), value of peak displacement in cm in the plotting process
39,40	81-100	0.0

The corrected acceleration, velocity and displacement for each component of an earthquake record are also plotted to appropriate scales by the Volume II Plotting Program, (Fig. $II6-1$) and printed out by the Volume II Printing Program (Fig. $II6-2$). Details concerning identification and peak values of acceleration, velocity, and displacement are given at the top of each plot. The first line gives the name, date, and time of occurrence of the earthquake. The second line is comprised of identification labels, the observation station and component processed. The third line gives the band-pass filtering values (Fig. $II6-1$).

It will be observed that, contrary to general practice, the y-axis is marked positive downwards. Since the accelerograph registers the negative of the true acceleration, it is necessary to either invert the recorded accelerogram about the x-axis or change the positive

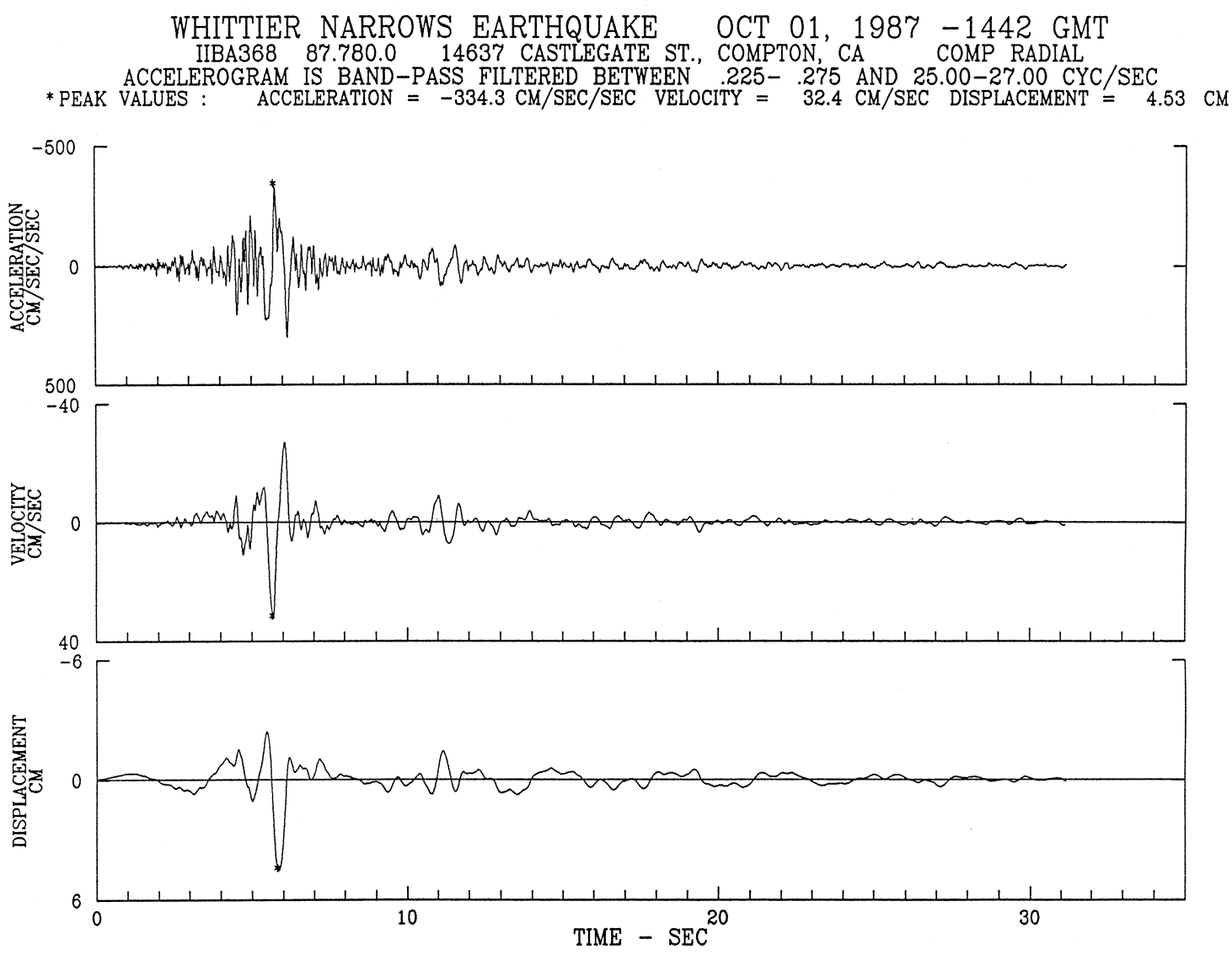
WHITTIER NARROWS EARTHQUAKE OCT 01, 1987 -1442 GMT
IIBA368 87.780.0 14637 CASTLEGATE ST., COMPTON, CA COMP RADIAL
ACCELEROGRAM IS BAND-PASS FILTERED BETWEEN .225- .275 AND 25.00-27.00 CYC/SEC
*PEAK VALUES : ACCELERATION = -334.3 CM/SEC/SEC VELOCITY = 32.4 CM/SEC DISPLACEMENT = 4.53 CM
-500
ACCELERATION CM/SEC/SEC
0
500
-40
VELOCITY CM/SEC
0
40
-6
DISPLACEMENT CM
0
6
0
10
20
30
TIME - SEC

Figure II6 - 1

IIBA368 87.780.0 WHITTIER NARROWS EARTHQUAKE OCT 01, 1987 -1442 GMT EPICENTER 34 03 29N, 118 04 12W
STATION USC# 0078 14637 CASTLEGATE ST., COMPTON, CA COMP RADIAL 33 53 57N, 118 11 47W

INSTR PERIOD = .040 SEC DAMPING = .577 ACCELEROGRAM IS BAND-PASS FILTERED BETWEEN .225- .275 AND 25.00-27.00 CYC/SEC

PEAK VALUES: ACCELERATION = -334.29 CM/SEC/SEC VELOCITY = 32.41 CM/SEC DISPLACEMENT = 4.53 CM
AT 5.74 SEC AT 5.68 SEC AT 5.84 SEC

INITIAL VELOCITY = .2160 CMS/SEC; INITIAL DISPLACEMENT = -.0120 CMS

1559 INSTRUMENT AND BASELINE CORRECTED ACCELERATION DATA IN MM/SEC/SEC, AT EQUALLY-SPACED INTERVALS OF .020 SEC.

-8	16	14	7	0	1	-8	-15	-4	2	0	43	7	-21	-25	-29	8	-5	2	35
22	27	-7	-42	4	-14	4	18	-3	15	-30	-19	-4	-13	28	32	-3	-14	-7	-66
-44	13	-13	-11	65	82	38	-19	-13	1	-17	-28	-17	52	96	-19	-88	-57	-74	-45
64	3	46	20	76	78	-40	-79	67	114	-21	-139	-64	63	-80	-103	-63	-12	132	173
-97	88	110	-134	-131	-74	-62	-120	-32	121	91	-166	25	-11	-123	132	14	-19	394	309
-321	-289	113	-60	-191	-30	-77	12	71	-123	-171	71	54	-104	-139	-78	4	291	211	-19
26	146	196	-52	-236	-159	-21	-93	-314	-397	-327	125	456	235	23	336	607	190	-465	-425
-3	-69	-427	-245	25	300	303	64	49	77	-119	-3	346	287	-160	-122	-197	-688	-516	-204
-131	-221	74	473	200	-19	357	578	191	-236	-266	-401	-348	-54	-14	-328	-207	-49	-58	157
404	193	44	95	69	-54	-277	-23	716	599	-352	-824	-568	-270	94	250	241	249	240	422
182	-437	-434	-184	-160	197	486	277	211	378	729	811	308	-624	-874	-208	630	436	-96	-268
-899	-1275	-1098	-1038	-947	-148	1343	2044	1983	1455	733	-308	-285	693	1080	1038	521	-974	-1182	-192
-180	-1105	-1478	-431	1561	1583	1033	104	-1328	-2102	-1776	-1306	-990	-82	821	461	-991	-1493	-1035	231
1239	910	-212	-583	-498	-797	-729	-66	-88	-419	613	1876	2213	2254	2259	2156	2179	2198	2038	1401
853	748	816	637	48	-1207	-2723	-3343	-3181	-2689	-2007	-1245	-607	-789	-1466	-1981	-2005	-1532	-1390	-1461
-1226	-790	-252	117	566	1409	2372	2907	2991	2559	1696	971	760	377	-184	-463	-672	-987	-1202	-926
-204	203	-252	-500	-38	622	897	866	593	286	-338	-893	-703	-39	318	178	237	763	1030	619
-54	-376	-696	-806	-658	-688	-785	-217	331	8	-570	-851	-789	-183	590	745	535	318	570	989
902	139	-308	-98	213	362	455	298	-76	-337	-428	-523	-136	431	316	90	-137	-411	-316	-196
-180	-244	-340	-92	194	117	-177	-433	-274	149	322	234	229	361	347	84	-59	-167	-334	-226
60	21	109	320	68	-181	-51	23	83	75	34	136	36	-122	-117	-261	-60	273	103	-118
-34	52	69	132	121	103	73	42	83	-104	-389	-380	-183	-35	59	182	32	-76	-70	-135
-58	-40	-201	118	436	116	-329	-160	138	193	155	213	223	14	-281	-314	-19	307	427	192
-34	151	306	102	-210	-386	-405	-237	-229	-438	-482	-402	-312	-188	-146	-207	-76	235	353	275
171	188	253	254	221	356	449	350	91	-149	-96	95	28	-87	-129	-278	-432	-453	-319	-137
-14	-3	3	-5	52	88	-80	-221	-197	-95	100	81	-66	-61	39	69	29	12	191	414
533	555	523	421	218	-68	-243	-225	-189	-125	14	67	90	194	163	-178	-480	-532	-489	-582
-685	-715	-654	-497	-248	-122	-144	-188	-265	-300	-181	141	462	702	855	824	706	723	811	750
561	389	359	413	319	153	88	65	-35	-98	-103	-155	-275	-322	-284	-383	-591	-739	-816	-873
-784	-565	-385	-179	86	273	412	610	742	724	610	368	93	-56	-135	-132	-163	-230	-74	212
204	6	-37	5	10	-27	-109	-198	-106	-5	-36	-54	13	179	353	407	330	268	242	161
119	177	119	-177	-366	-369	-349	-237	-96	-71	-67	39	159	217	195	146	97	95	188	300
336	350	307	116	-152	-329	-435	-436	-366	-218	-116	-178	-127	8	52	7	-76	-154	-149	-81
64	168	153	209	274	245	149	75	-2	-41	-18	-1	-46	-130	-180	-234	-297	-321	-229	-19
94	33	-38	14	90	44	12	57	21	-133	-212	-259	-304	-296	-262	-168	13	167	241	284
283	216	147	86	-15	-41	-8	7	25	33	21	38	75	51	-31	-99	-65	42	48	-32
-46	1	5	-34	-89	-129	-131	-77	-2	105	260	341	269	157	4	-126	-92	-32	14	17
-12	-42	-14	55	47	-73	-220	-254	-202	-62	101	46	-86	-135	-116	-68	10	60	62	45
47	85	53	-61	-111	-21	112	212	274	230	77	-47	-33	-69	-186	-142	-10	72	114	94
78	98	47	35	45	-10	8	75	81	0	-123	-219	-242	-252	-275	-261	-220	-160	-97	-46

Figure II6 - 2

-27	-37	-16	6	30	45	80	99	81	120	227	285	231	93	24	11	22	20	32	69
88	67	24	45	114	129	82	-71	-173	-204	-246	-300	-330	-250	-148	-104	-72	-50	-26	-45
-45	27	123	155	134	107	104	148	144	37	-79	-92	-14	34	-3	-42	-43	-3	102	153
126	130	124	139	169	161	143	142	88	15	33	32	-2	-49	-138	-190	-197	-178	-113	-117
-190	-246	-271	-231	-148	-109	-110	-105	-71	1	109	135	97	59	68	117	188	228	188	123
106	71	44	70	134	213	233	126	-33	-121	-118	-164	-209	-163	-84	-30	8	42	65	75
73	62	39	25	53	96	97	32	-20	-16	3	30	83	139	82	22	-46	-112	-141	-136
-104	-109	-121	-77	-27	2	15	30	42	15	-65	-153	-160	-106	-48	33	82	78	137	213
243	230	186	182	227	268	287	242	131	44	-41	-125	-182	-254	-293	-230	-143	-108	-75	-40
-25	-50	-45	15	65	77	22	-11	33	44	-22	-112	-126	-115	-112	-56	-9	-63	-83	3
83	87	66	67	100	103	50	-33	-95	-120	-91	-55	-49	-90	-135	-79	4	13	-24	-20
43	104	140	114	60	35	58	108	97	34	48	58	13	10	-13	-88	-153	-162	-148	-157
-111	-29	-38	-75	-45	-15	-37	-74	-84	-76	-73	-105	-116	-84	-2	45	30	-7	-13	9
58	97	103	114	135	138	118	78	35	32	61	61	55	72	106	126	110	47	-42	-106
-128	-132	-113	-74	-49	-1	42	17	-29	-71	-91	-112	-109	-75	-60	-40	-18	-6	17	73
149	191	181	136	91	43	-25	-93	-100	-82	-86	-109	-84	23	125	150	119	84	76	91
64	13	-6	-13	-13	-1	-3	-14	-14	-7	-3	-28	-17	35	30	-11	-25	-45	-30	-15
29	59	65	36	7	37	91	81	11	-32	-21	-19	-32	-10	-7	-4	37	9	-39	-25
-6	-26	-61	-73	-44	-31	-37	-57	-83	-89	-46	-20	-19	1	47	85	87	59	51	45
41	5	-36	-20	-11	-28	-45	-47	-20	-2	13	15	19	4	26	74	55	27	32	15
-49	-80	-49	-29	-52	-66	-68	-60	-37	-50	-73	-54	14	67	40	-2	10	34	26	2
10	5	5	41	46	60	95	71	-15	-20	21	-22	-96	-78	-31	-10	-23	-49	-76	-84
-53	-27	-35	-20	38	79	78	76	68	49	43	75	106	113	79	32	25	15	3	2
14	-13	-67	-78	-78	-86	-120	-160	-165	-114	-51	-30	-18	-14	-38	-35	9	22	12	36
69	87	77	50	22	14	32	49	55	37	36	49	57	49	31	29	20	15	10	-3
-13	-26	-53	-78	-79	-55	-40	-25	6	26	37	25	29	65	48	-8	-41	-54	-72	-106
-141	-155	-135	-120	-82	4	85	82	59	77	111	102	79	73	38	-6	-16	-20	-19	-12
9	1	12	52	88	104	95	77	59	20	-19	-66	-89	-99	-98	-111	-134	-164	-154	-114
-100	-109	-104	-72	-54	-46	-18	28	58	62	40	44	66	44	35	48	80	84	61	33
45	65	67	81	48	7	2	7	17	5	19	8	-20	-41	-53	-45	-37	-27	-34	-52
-53	-36	-1	23	40	48	30	-11	-5	9	39	58	42	27	22	33	34	17	-18	-19
7	26	25	11	15	28	36	39	22	1	22	27	-45	-100	-105	-80	-69	-62	-32	-6
21	7	-14	-25	-37	-25	-10	8	11	8	-17	-35	-35	-6	21	38	45	34	23	22
29	39	55	90	92	73	57	11	-36	-38	-53	-67	-63	-79	-112	-114	-99	-96	-72	-54
-32	-11	-18	-18	-22	-10	14	40	81	97	130	140	147	128	72	32	7	-8	-2	13
-2	-11	5	7	-8	-7	-2	-15	-20	-35	-30	-44	-42	0	6	-14	-18	-16	-26	-30
-2	-3	-40	-69	-59	-22	14	33	26	13	30	25	-9	-5	16	25	18	11	29	15
3	-5	6	14	13	11	23	32	41	69	92	80	71	65	38	6	-15	-38	-53	

780 INSTRUMENT AND BASELINE CORRECTED VELOCITY DATA IN MM/SEC, AT EQUALLY-SPACED INTERVALS OF .040 SEC.

2	2	2	2	2	2	2	2	1	1	2	2	1	1	2	2	1	1	2	2
0	0	1	3	4	3	3	5	5	2	1	3	5	7	6	9	6	6	3	4
8	10	7	4	1	4	2	2	3	7	14	7	5	2	2	-1	0	-3	-6	2
4	9	8	2	-3	-17	-13	-4	9	14	1	-5	-14	-4	0	1	3	11	4	-17
-27	-32	-20	-15	1	-4	-18	-23	-32	-36	-30	-22	-19	-22	-18	-3	-29	-39	-31	-21
-9	-20	-30	-23	-10	6	33	15	8	22	7	-39	-80	-79	-5	52	50	72	109	83
66	27	20	77	77	4	-50	-53	-45	-95	-88	-59	-77	-105	-115	-117	-51	39	127	213
270	302	324	274	148	43	-8	-44	-118	-182	-238	-268	-262	-204	-92	6	50	64	46	8
-24	-25	-38	-16	16	24	-4	-8	1	29	51	36	7	-22	-30	-33	-63	-69	-43	-25
9	18	15	29	38	27	10	21	24	11	2	-8	-11	-9	-22	-18	-8	5	9	2
-5	-3	5	2	2	5	9	5	-2	4	3	4	9	13	16	11	-2	-4	1	-1
-5	-8	-3	1	-4	3	12	12	3	13	21	28	31	18	7	-9	-24	-32	-38	-30

Figure II6 - 2 (cont.)

```
-19  -11   -1   14   26    23   25   23   12   -4    -10  -10   -9   -8  -15   -17  -15  -17  -14  -12
  4   25   41   40   31    27   29   35   28    8    -16  -44  -63  -70  -78   -88  -83  -56  -25    5
 33   50   64   71   72    69   61   48   31    2    -32  -55  -63  -53  -30    -2   11    9    3   -5

  0    2    1   -1   -8   -10  -12   -5    9   19     26   31   25   10    0    -3   -2    6   11   15
 26   39   43   30   13     4   -2   -3   -3   -9    -11   -6    3   12   15    14   14    9    0  -12
-14  -12  -11   -9   -7   -12  -22  -33  -38  -32    -21  -12   -8   -9   -8    -7   -5   -3   -5   -4
 -4   -4   -5   -9  -12    -7    6   12    9    9      9    9   10    8   -1    -3   -2   -6   -8   -6
 -3    0   -2   -2    7    15   15   11    7   10     13   17   19   19   22    21   13    3   -7  -13

-15  -17  -16  -14  -11    -5    5    9   10   10     13   15   17   22   19    11   -1  -11  -16  -18
-20  -19  -14   -9   -4    -3   -6   -6   -8   -8     -2    2    8   14   18    20   20   17   10    3
 -3  -13  -22  -27  -31   -31  -27  -24  -20  -12     -6   -4   -1    7   11     7    0   -7   -8   -7
 -4   -2   -1    2    4     3    4    8    9    5      0   -5   -8   -8   -7    -7  -13  -17  -16  -12
 -4    5   13   23   32    34   29   19   11    6      5    3    4    6    7     8    4    0   -3   -5

 -4   -1    2    6    5     1   -1   -5   -8   -7     -7   -3    1    3    7     9   11   12    9    3
 -3   -5   -7   -8  -11   -14  -17  -20  -19  -19    -18  -14  -10   -4   -1     1    3    6   11   12
  9    4    0    0    1    -2   -6   -9  -11  -11     -8   -1    4    5    2    -1   -5   -5    1    4
  7    8    7    7    6     6    5    6    5    4      3    5    6    8   10     9    8    8    8    8
  7    5    3    1   -2    -5   -6   -6   -3    0      2    2    1    0   -2    -2   -2   -1    1    3

  3    0   -1   -4   -6    -8  -10   -8   -7   -6     -6   -5   -4   -1    1     1    0   -2   -3   -5
 -8   -9   -9   -6   -3    -1    2    7    9    9     10    9    6    3   -3    -7   -8   -9  -10   -9
 -7   -4   -2   -1    2     3    5    7    9    9      9    8    6    4    3     4    5    7    7    5
  1   -5   -9   -9   -6    -3    2    4    4    4      3    4    6   10   13    14   11    7    3   -3
 -8  -12  -15  -17  -16   -14  -12  -10   -8   -5     -3   -1    2    3    3     4    4    2    0   -1

 -3   -4   -3   -2   -2    -1    1    2    3    4      3    4    5    6    7     8    8    5    1   -1
 -1   -1   -2   -3   -3    -3   -4   -4   -3   -1      0    1    5    7    8     6    4    0   -4   -8
-10  -10  -11  -12  -10    -6    0    5    6    6      6    6    6    6    5     4    2    2    1    0
  0   -1   -3   -4   -3    -2   -2   -2   -1    0      0    0    1    1    2     5    8   11   11    9
```

```
      312  INSTRUMENT AND BASELINE CORRECTED DISPLACEMENT DATA IN  .10*MM,   AT EQUALLY-SPACED INTERVALS OF    .100  SEC.

 -1   -3   -5   -8  -12   -15  -18  -22  -24  -29    -29  -30  -30  -29  -24   -19  -16   -8   -5   -1
  8   18   22   24   27    40   41   37   51   51     55   67   62   41   40    27   -2  -19  -32  -56

-76  -96 -107  -84  -68  -115 -139  -78   11   43    106   63  -13  -85 -198  -225  -38  267  448  432
268    9 -111  -60  -40   -67  -60  -56  -31    0    -23  -78 -101  -81  -44   -23   -5   -8  -22  -23

-18  -16  -11   -4    0     6   21   20   19   12     11   19   29   54   61    34    1  -10    9   30
 29   17    2  -16  -28    -2   30   60   71   22    -55 -129 -132  -80  -10    46   54   -2  -37  -30

-31  -31  -38  -47  -32    -6   -3   -4   11   48     66   63   56   52   64    75   67   54   45   21
-12  -24  -33  -37  -41   -46  -55  -49  -40  -30    -28  -31  -37  -38  -33   -19  -10    7   28   39

 28   12    0    5   16    32   50   47   30   14      8    3   -3    2   19    39   45   32    3  -22
-34  -36  -26  -26  -32   -32  -28  -21  -14  -19    -25  -38  -49  -42  -13    13   21   25   31   34

 30   29   33   30   22    19   25   35   38   32     22    3  -16  -30  -32   -28  -18  -14  -14  -21
-32  -32  -29  -33  -29   -22  -15   -9   -5    0     10   18   25   30   29    23   22   23   21   19

 21   21   15    6   -1    -6   -6   -6  -11  -20    -24  -20  -11   -3   -4   -12  -21  -24  -23  -17
 -8    0    3    9   15    10    3    5    9   13     25   35   33   20    4    -8  -14  -14  -11   -8

 -9  -13  -14  -13  -10    -5    1    8    8    7      4    1   -1    2    9    12    6   -5  -15  -14
 -8   -3    2    4    5     2   -2   -4   -6   -6     -5    3
```

Figure II6 - 2 (cont.)

direction of the y-axis. Since investigators are often familiar with typical accelerograms in the form as registered by the instrument, it is preferred to label the y-axis suitably and retain the familiar appearance of the accelerograms.

In the old Volume II reports, the corrected accelerogram was printed out at equal time intervals of 0.02 seconds. Fig. *II*6 – 2 shows the identification labels and the beginning of the printout for the component plotted in Fig. *II*6 – 1. For each component in a record, the identification labels are given in the first line, together with the latitude and longitude of the earthquake. In the second line, the station number of the observation station, as well as its latitude and longitude, are given for the convenience of those who would like to work on seismic waves. The accelerograph characteristics used for instrument correction are also given in each case.

The data can be printed out in integer form with units of mm/sec^2, so as to utilize the printing space more efficiently. There are 20 successive values of acceleration at 0.02 sec intervals, printed along each row with blank spaces after every set of 5 entries for easy reading. Similarly, at the end of 10 lines, one row is skipped before printing the succeeding values. The velocity data are next printed out in integer form with units of mm/sec. There are 20 successive values of velocity at 0.04 sec intervals printed along each row with blank spaces after every set of five entries for easy reading. One row is skipped at the end of every five lines. Similarly, the displacement data can next be printed in units of mm with 20 successive values per line at 0.10 sec intervals. One row is skipped at the end of every two lines. This printing is performed by the Volume II Printing program which reads a Volume II disk file.

Since the initial values of velocity and displacement are given, with the corresponding acceleration data, it is possible to compute the velocity and displacement curves if numerical values are desired. However, it must be remembered that the integrated curves so obtained might need further filtering to eliminate minor long period errors resulting from small errors in the initial values. This question is discussed in greater detail in Hudson, et al., (1971).

*II*7 Data Processing for Volume III: Response and Fourier Spectra

*II*7.1 Introduction: Single-Degree-of-Freedom System

The calculation of Response Spectra of earthquake strong ground motions continues to be the main tool for preliminary design of many earthquake resistant structures. The spectra have also been used in studies of the wave amplification properties of the ground since the spectra contain valuable information about the characteristics of the ground motion. Spectra have also been used as a guide in the dynamic considerations of earthquake resistant code provisions. In view of these important applications of spectral data, and the availability of vast amount of recorded strong-motion earthquake accelerations, an efficient algorithm for the calculation of response spectra is useful.

The calculation of Response Spectra involves a single degree-of-freedom system, which can be thought of as a one story structure. For acceleration $a(t)$ of the base of this structure, the differential equation of motion may be written as

$$m\ddot{x} + c\dot{x} + kx = -ma \qquad (II7.1.1)$$

where $x = x(t)$ is the relative displacement between the structure and its base, m is the mass, c the constant damping coefficient, and k the spring constant of the system. The nonhomogeneous term, $-ma$, represents the inertial force applied to the system. Introducing the natural frequency ω and the fraction of critical damping ς as

$$\omega_0 = \sqrt{k/m} \qquad (II7.1.2)$$

$$\varsigma = \frac{c}{2m\omega_0}, \qquad (II7.1.3)$$

Eq. (*II*7.1.1) can be written as:

$$\ddot{x} + 2\omega_0\dot{x} + \omega_0^2 x = -a \qquad (II7.1.4)$$

For any general acceleration of the base $a(t)$, the relative displacement $x(t)$ is given by the Duhamel convolution integral assuming zero initial conditions:

$$x(t) = \frac{-1}{\omega_0\sqrt{1-\varsigma^2}} \int_0^t a(\tau) \exp(-\varsigma\omega_0(t-\tau)) \times \sin\omega_0\sqrt{1-\varsigma^2}(t-\tau)d\tau \qquad (II7.1.5)$$

The exact relative velocity $\dot{x}(t)$ follows from Eq. (*II*7.1.5) as

$$\dot{x}(t) = \frac{-1}{\sqrt{1-\varsigma^2}} \int_0^t a(\tau) \exp[-\varsigma\omega_0(t-\tau)] \times \cos(\omega_0\sqrt{1-\varsigma^2}(t-\tau) + \delta)d\tau \qquad (II7.1.6)$$

with

$$\delta = \tan^{-1}(\varsigma/\sqrt{1-\varsigma^2}). \qquad (II7.1.7)$$

The absolute acceleration $\ddot{y}(t) = \ddot{x}(t) + a(t)$ of the system is given by

$$\ddot{y} = -(2\omega_0\varsigma\dot{x} + \omega_0^2 x) \qquad (II7.1.8)$$

or

$$\ddot{y} = \frac{\omega_0}{\sqrt{1-\varsigma^2}} \int_0^t a(\tau) \exp[-\varsigma\omega_0(t-\tau)] \times \sin(\omega_0\sqrt{1-\varsigma^2}(t-\tau) + 2\delta)d\tau \qquad (II7.1.9)$$

For engineering applications, the maximum absolute values of the quantities $x(t)$, $\dot{x}(t)$ and $\ddot{y}(t)$ experienced during the earthquake response are of primary importance. These quantities are defined by

$$\begin{aligned} \text{SD} &\equiv \max\{|x(t)|\} \\ \text{SV} &\equiv \max\{|\dot{x}(t)|\} \\ \text{SA} &\equiv \max\{|\ddot{y}(t)|\} \end{aligned} \qquad (II7.1.10)$$

In typical engineering structures, the fraction of critical damping, ς, is small. Therefore, in Eq. (*II*7.1.6) and Eq. (*II*7.1.7)

$$\sqrt{1-\varsigma^2} \approx 1 \quad \text{and} \quad \delta \approx 0. \qquad (II7.1.11)$$

Furthermore, in Eq. (*II*7.1.6), if the cosine term is replaced by a sine term, the following approximate relationships between SD, SV and SA in Eq. (II7.1.10) exist:

$$\begin{aligned} SV &\approx \omega_0 SD \\ SA &\approx \omega_0 SV. \end{aligned} \qquad (II7.1.12)$$

For earthquake-like excitations these approximations can be made plausible (Hudson, 1962). For engineering applications, it is often convenient to define the following approximations:

$$\begin{aligned} \text{Pseudo relative velocity, PSV} &= \omega_0 \text{SD} \\ \text{Pseudo absolute accelerations, PSA} &= \omega_0^2 \text{SD}. \end{aligned} \qquad (II7.1.12)$$

Because of their relationship, SD, PSV and PSA can be conveniently plotted on a common tripartite logarithmic plot.

*II*7.2 The Original Algorithm

Starting from the corrected accelerogram data available at equally spaced time intervals of T = .02 sec, an approach based on the exact analytical solution of the Duhamel

convolution integral, Eq. (*II*7.1.5), for successive linear segments of the excitation was used to calculate the Volume III Response Spectra (Trifunac and Lee, 1973). This approach and its accuracy were described in detail by Nigam and Jennings (1968). A summary of the method formerly used in Routine Processing is described here.

For the input acceleration $a(t)$ used in Eq. (*II*7.1.4), consider the time interval $[nT,(n+1)T]$. Here, $a(t)$ is given by a linear segment joining $a[n]$ and $a[n+1]$, and Eq. (*II*7.1.4) becomes

$$\ddot{x}+2\omega_0\varsigma x+\omega_0^2 x=-a[n]-\frac{\Delta a}{\Delta t}(t-nT) \qquad (II7.2.1)$$

with

$$\frac{\Delta a}{\Delta t}=\frac{a[n+1]-a[n]}{T}$$

and

$$nT\le t\le (n+t)T \qquad (II7.2.2)$$

The solution of Eq. (*II*7.2.1) within the time interval $[nT,(n+1)T]$ is

$$\begin{aligned} x(t)=&\exp[-\varsigma\omega_0(t-nT)][C_1\sin\omega_1(t-nT)\\ &+C_2\cos\omega_1(t-nT)]+\Big(-a[n]\omega_0+2\varsigma\frac{\Delta a}{\Delta t}\\ &-\frac{\Delta a}{\Delta t}(t-nT)\omega_0\Big)/\,\omega_0^3 \end{aligned} \qquad (II7.2.3)$$

where

$$\omega_1=\omega_0\sqrt{1-\varsigma^2} \qquad (II7.2.4)$$

$$C_1=\frac{1}{\omega_1}\left(\varsigma\omega_0 x[n]+\dot{x}[n]-\frac{2\varsigma^2-1}{\omega_0^2}\frac{\Delta a}{\Delta t}+\frac{\varsigma}{\omega_0}a[n]\right) \qquad (II7.2.5)$$

$$C_2=x[n]-\frac{2\varsigma}{\omega_0^2}\frac{\Delta a}{\Delta t}+\frac{a[n]}{\omega_0^2} \qquad (II7.2.6)$$

Substituting C_1 and C_2 into Eq. (II7.2.3) and setting $t=(n+1)T$ leads to the recursive relation for $x[n]$ and $x[n]$ given by

$$\begin{pmatrix} x[n+1]\\ \dot{x}[n+1]\end{pmatrix}=\mathbf{A}\begin{pmatrix} x[n]\\ \dot{x}[n]\end{pmatrix}+\mathbf{B}\begin{pmatrix} a[n]\\ a[n+1]\end{pmatrix} \qquad (II7.2.7)$$

where $\mathbf{A}=\mathbf{A}(\varsigma,\omega_0,T),\mathbf{B}=\mathbf{B}(\varsigma,\omega_0,T)$ are 2 by 2 matrices whose elements are given by

$$\begin{aligned} a_{11}=&\exp(-\varsigma\omega_0 T)\Big(\frac{\varsigma}{\sqrt{1-\varsigma^2}}\sin\omega_1 T+\cos\omega_1 T\Big)\\ a_{12}=&\frac{\exp(-\varsigma\omega_0 T)}{\omega_1}\sin\omega_1 T\\ a_{21}=&-\frac{\omega_0}{\sqrt{1-\varsigma^2}}\exp(-\varsigma\omega_0 T)\sin\omega_1 T\\ a_{22}=&\exp(-\varsigma\omega_0 T)\Big(\cos\omega_1 T-\frac{\varsigma}{\sqrt{1-\varsigma^2}}\sin\omega_1 T\Big) \end{aligned} \qquad (II7.2.8)$$

and

$$
\begin{aligned}
b_{11} &= \exp(-\varsigma\omega_0 T)\Big[\Big(\frac{2\varsigma^2-1}{\omega_0^2 T}+\frac{\varsigma}{\omega_0}\Big)\frac{\sin\omega_1 T}{\omega_1} \\
&\quad + \Big(\frac{2\varsigma}{\omega_0^3 T}+\frac{1}{\omega_0^3}\Big)\cos\omega_1 T\Big] - \frac{2\varsigma}{\omega_0^3 T} \\
b_{12} &= -\exp(-\varsigma\omega_0 T)\Big[\Big(\frac{2\varsigma^2-1}{\omega_0^2 T}\Big)\frac{\sin\omega_1 T}{\omega_1} \\
&\quad + \frac{2\varsigma}{\omega_0^3 T}\cos\omega_1 T\Big] - \frac{1}{\omega_0^2}+\frac{2\varsigma}{\omega_0^3 T} \\
b_{21} &= \exp(-\varsigma\omega_0 T)\Big[\Big(\frac{2\varsigma^2-1}{\omega_0^2 T}+\frac{\varsigma}{\omega_0}\Big) \\
&\quad \times\Big(\cos\omega_1 T - \frac{\varsigma}{\sqrt{1-\varsigma^2}}\sin\omega_1 T\Big) - \Big(\frac{2\varsigma}{\omega_0^3 T}+\frac{1}{\omega_0^2}\Big) \\
&\quad \times(\omega_1\sin\omega_1 T + \varsigma\omega_0\cos\omega_1 T)\Big] + \frac{1}{\omega_0^2 T} \\
b_{22} &= -\exp(-\varsigma\omega_0 T)\Big[\frac{2\varsigma^2-1}{\omega_0^2 T}\Big(\cos\omega_1 T - \\
&\quad - \frac{\varsigma}{\sqrt{1-\varsigma^2}}\sin\omega_1 T\Big) - \frac{2\varsigma}{\omega_0^3 T}(\omega_1\sin\omega_1 T \\
&\quad + \varsigma\omega_0\cos\omega_1 T)\Big] - \frac{1}{\omega_0^2 T}
\end{aligned}
\qquad (II7.2.9)
$$

Eq. ($II7.2.7$) gives a recursive iteration method of computing $\{x[n+1],\ \dot{x}[n+1]\}$ from $\{x[n],\ \dot{x}[n]\}$ and $\{a[n],\ a[n+1]\}$, starting from $x[0] = \dot{x}[0] = 0$, zero initial conditions.

$II7.3$. Digital Simulation of a Continuous System

Lee (1984), using the digital impulse invariant and step invariant simulation of a continuous system, derived a fast algorithm for calculating the responses $x(t)$ and $\dot{x}(t)$, with only 2 multiplications and 3 additions at each iteration step. Recently, Lee (1990) updated and improved this algorithm to compute simultaneously $x(t)$, $\dot{x}(t)$ and $\ddot{x}(t)$ with 2 multiplications and 4 additions.

The following is a brief summary of the methods presented in Lee (1984, 1990). Starting with the input acceleration data, $a(t), t \geq 0$, the relative displacement response data, $x(t), t \geq 0$, can be considered as an output of a continuous system. In terms of the Laplace transform, it takes the form

$$X(s) = H_0(s)A(s), \qquad (II7.3.1)$$

with

$$H_0(s) = \frac{-1}{(s+\alpha)^2 + \beta^2}, \qquad (II7.3.2)$$

with $\alpha = \omega_0\varsigma$ and $\beta = \omega_0\sqrt{1-\varsigma^2}$. $A(s)$ and $X(s)$ respectively are the Laplace transforms of the input, $a(t)$, and output, $x(t)$, functions, and $H_0(s)$ is the corresponding displacement transfer function.

With the input acceleration data available in digital form $\{a[n] : n \geq 0\}$, sampled equally spaced at T seconds apart, the output displacement can also be calculated at the same sampling rate of T seconds and be of the form $\{x[n] : n \geq 0\}$. The corresponding z-transforms for the input and output digital data are, respectively

$$A[z] = \sum_{n=0}^{\infty} a[n]z^{-n}, \quad \text{and}$$
$$X[z] = \sum_{n=0}^{\infty} x[n]z^{-n}, \qquad (II7.3.3)$$

and are related by

$$X(z) = H_0[z]A[z], \qquad (II7.3.4)$$

with $H_0[z]$ representing the digital system function, corresponding to the continuous transfer function $H_0(s)$ in Eq. (II7.3.2). When the input $a[n]$ assumes the equally spaced sampled values $a(nT)$ of $a(t)$, the resulting output $x[n]$ will simulate the sampled values $x(nT)$ of $x(t)$. Such methods of digital simulations have been available for a long time, and further details can be found in many references (Gold and Radar, 1969; Stearns, 1975; Papoulis, 1977). The general method can be summarized as follows:

(1) Let the desired transfer function be $H(s)$. Start with an invariant input function, $i(t)$, find its Laplace transform, $I(s)$, and z-transform, $I[z]$.

(2) Calculate the continuous output function, $g(t)$, as the inverse Laplace transform of $H(s)I(s)$, i.e. $g(t) = \mathcal{L}^{-1}[H(s)I(s)]$.

(3) With T the input sampling rate in seconds, define the corresponding sequence $g[n] = g(nT)$, $n \geq 0$, and the z-transform $G[z]$ of $\{g[n] : n \geq 0\}$ as $G[z] = \sum_{n=0}^{\infty} g[n]z^{-n}$.

(4) The invariant digital simulation is then $H[z] = \frac{G[z]}{I[z]}$.

A sufficient condition for the above procedure to give accurate simulation is that the input digital data be bandlimitted (Papoulis, 1977). For the case of input acceleration data, the routine computer processing of strong-motion accelerograms has the data bandpass filtered at or within the frequency band 0.07-25 Hz. Since the input acceleration data used for the response calculation are thus always bandlimitted, simulation with good desired accuracy can be successfully achieved.

*II*7.4 The Updated Fast Algorithm

Using digital simulation, Lee (1990) derived an algorithm for the simultaneous calculation of relative displacement, $x(t)$, velocity, $\dot{x}(t)$ and acceleration, $\ddot{x}(t)$. The digital system functions used for the calculation of $x(t)$, $\dot{x}(t)$ and $\ddot{x}(t)$ will be

$$\bar{H}_0[z] = \frac{-\gamma_0 a_0 T z}{z^2 - bz + c}, \qquad (II7.4.1)$$

for relative displacement, using the LSQ (least-squares) adjusted impulse invariant digital simulation,

$$\bar{H}_1[z] = \frac{-\gamma_1 a_0 z^{\frac{1}{2}}(z-1)}{z^2 - bz + c}, \qquad (II7.4.2)$$

for relative velocity, using the LSQ and phase adjusted step invariant digital simulation, and

$$\bar{H}_2[z] = \frac{-\gamma_2 a_0 (z-1)^2}{T(z^2 - bz + c)}, \qquad (II7.4.3)$$

for relative acceleration, using the DC-adjusted ramp invariant digital simulation. Each of these simulators has a common term in the denominator which corresponds to the characteristic equation of the digital system:

$$z^2 - bz + c = 0, \qquad (II7.4.4)$$

with $b = 2e^{-\alpha T}\cos\beta T$, and $c = e^{-2\alpha T}$. The corresponding numerator terms increase in the order or power of z and also in the number of terms from $\bar{H}_0[z]$ to $\bar{H}_2[z]$. Setting $z = e^{sT}$, Eq. $(II7.4.4)$ has two roots given by

$$s = \omega_0(-\varsigma \pm i\sqrt{1-\varsigma^2}), \qquad (II7.4.5)$$

which are identical to the roots of the characteristic equation of the corresponding continuous transfer function:

$$(s+\alpha)^2 + \beta^2 = 0, \quad \text{or} \quad s^2 + 2\omega_0\varsigma s + \omega_0^2 = 0, \qquad (II7.4.6)$$

so that all three system functions in Eq. $(II7.6.1)$ to $(II7.6.3)$ have the same characteristics as the corresponding continuous transfer functions that they simulate.

The digital output sequences $\{x[n]\}$, $\{\dot{x}[n]\}$ and $\{\ddot{x}[n]\}$ have recursive relations respectively given by

$$\begin{aligned} x[n+1] &= bx[n] - cx[n-1] - \gamma_0 a_0 T a[n], \\ \dot{x}[n+1] &= b\dot{x}[n] - cx[n-1] - \gamma_1 a_0 (a[n] - a[n-1]), \quad \text{and} \\ \ddot{x}[n+1] &= b\ddot{x}[n] - cx[n-1] - \gamma_2 a_0 (a[n] - 2a[n] + a[n-1]), \end{aligned} \qquad (II7.4.7)$$

with appropriate prescribed initial values for each of these sequences. Note that the term $\dot{x}[n]$, unlike $x[n]$ and $\ddot{x}[n]$, represents the relative velocity at time $t = (n - \frac{1}{2})T$, not at time

$t = nT$. The linearity of all these recursive relations suggests the following modification of the algorithm. Consider, instead, the following three digital invariant functions

$$\begin{aligned}
\tilde{H}_0[z] &= \frac{-z}{z^2 - bz + c}, \\
\tilde{H}_1[z] &= \frac{-z^{\frac{1}{2}}(z-1)}{z^2 - bz + c}, \qquad \text{and} \\
\tilde{H}_2[z] &= \frac{-(z-1)^2}{T(z^2 - bz + c)},
\end{aligned} \tag{II7.4.8}$$

each differing from the corresponding simulation functions by removal of all the constant factors in the numerator. These constant scaling factors can be applied at each step of the iterations respectively to $x[n], \dot{x}[n]$ and $\ddot{x}[n]$, or equivalently, by linearity, applied to all the terms of the sequence at the end of the iteration. The cumulative round-off error from digital computation is directly proportional to the number of multiplications at each iteration step . To keep this a minimum, each iteration step thus should have the least possible number of multiplications and hence the scaling constants are not included in the system functions in Eq. (*II*7.4.8). Let the corresponding digital output sequences be defined as $\{u[n]\}$, $\{\dot{u}[n]\}$ and $\{\ddot{u}[n]\}$ respectively. They are related to the original digital sequences by

$$\begin{aligned}
u[n] &= x[n]/(\gamma_0 a_0 T), \\
\dot{u}[n] &= \dot{x}[n]/(\gamma_1 a_0), \quad \text{and} \\
\ddot{u}[n] &= \ddot{x}[n]T/(\gamma_1 a_0),
\end{aligned} \tag{II7.4.9}$$

and the corresponding recursive relations, using Eq. (*II*7.4.8), become

$$\begin{aligned}
u[n+1] &= bu[n] - cu[n-1] - a[n], \\
\dot{u}[n+1] &= b\dot{u}[n] - c\dot{u}[n-1] - (a[n] - a[n-1]), \quad \text{and} \\
\ddot{u}[n+1] &= b\ddot{u}[n] - c\ddot{u}[n-1] - (a[n+1] - 2a[n] + a[n-1]),
\end{aligned} \tag{II7.4.10}$$

with appropriate initial values for each of the three sequences. The first two recursive relations in Eq. (*II*7.4.10) are identical to those given in the earlier algorithm (Lee, 1984). Another simplification is now possible. Using the linearity of the recursive relations, or by induction on n, it can be shown that the recursive relations in Eq. (*II*7.4.10) are equivalent to the following:

$$\begin{aligned}
u[n+1] &= bu[n] - cu[n-1] - a[n], \\
\dot{u}[n+1] &= u[n+1] - u[n], \quad \text{and} \\
\ddot{u}[n+1] &= \dot{u}[n+1] - \dot{u}[n].
\end{aligned} \tag{II7.4.11}$$

It should be noted that the transformation from Eqs. (*II*7.4.10) to (*II*7.4.11) is possible only because the scaling constants present in the numerators of the system functions $\bar{H}_0[z]$, $\bar{H}_1[z]$ and $\bar{H}_2[z]$ in Eqs. (*II*7.4.1) to (*II*7.4.3) are removed and not included at each step of the iteration. From Eq. (*II*7.4.11), each step of iteration now requires only

two multiplications and four subtractions. The multiplications are performed only to the relative displacement sequence $\{u[n]\}$, using the scale factors b and c which remain constant throughout the steps of the iteration for an oscillator of given natural frequency ω_0 and fraction of critical damping ς.

There is another advantage in not doing the scaling during the iteration steps. For some engineering applications, it is only the maximum absolute values of the relative responses experienced during the earthquake that is of importance and need to be kept. Under such circumstances, when only these maximum values are needed, the scaling need to be performed just on the maximum amplitudes, and not on all the amplitudes at each iteration step or at the end of the iteration. In particular, because of the relationship between SD, PSV and PSA, as shown in Eq. (II7.1.3), the PSV value can be conveniently plotted on a tripartite logarithmic plot from which all three quantities can be identified. In such a case, only the relative displacement response $\{x[n]\}$ will need to be calculated, using just the first recursive relation in Eq. (II7.4.1). There will then be needed only 2 multiplications and 2 additions at each iteration step.

For the case of zero damping, $\varsigma = 0$, $c = e^{-2\alpha T} = 1$, so that the recursion relations from Eq. (II7.4.11) become,

$$\begin{aligned} u[n+1] &= bu[n] - u[n-1] - a[n], \\ \dot{u}[n+1] &= u[n+1] - u[n], \quad \text{and}. \\ \ddot{u}[n+1] &= \dot{u}[n+1] - \dot{u}[n] \end{aligned} \qquad (II7.4.12)$$

This requires only 1 multiplication and 4 subtractions, thus resulting in additional savings in the total number of multiplications required. This has already been noted in the earlier algorithm of Lee (1984).

II7.5 Volume III Output File: $V3X0001.DAT$

The spectral amplitudes are stored on a disk file, V3X0001.DAT as follows:

Volume III File
(one file per one acceleration component)

Each file has:

(1) heading data of alphanumeric type;

(2) heading data of integer type;

(3) heading data of floating point type;

(4) response values and times of maximum responses for 91 periods and five damping ratios (acceleration, velocity, displacement, and pseudo velocity response amplitudes)

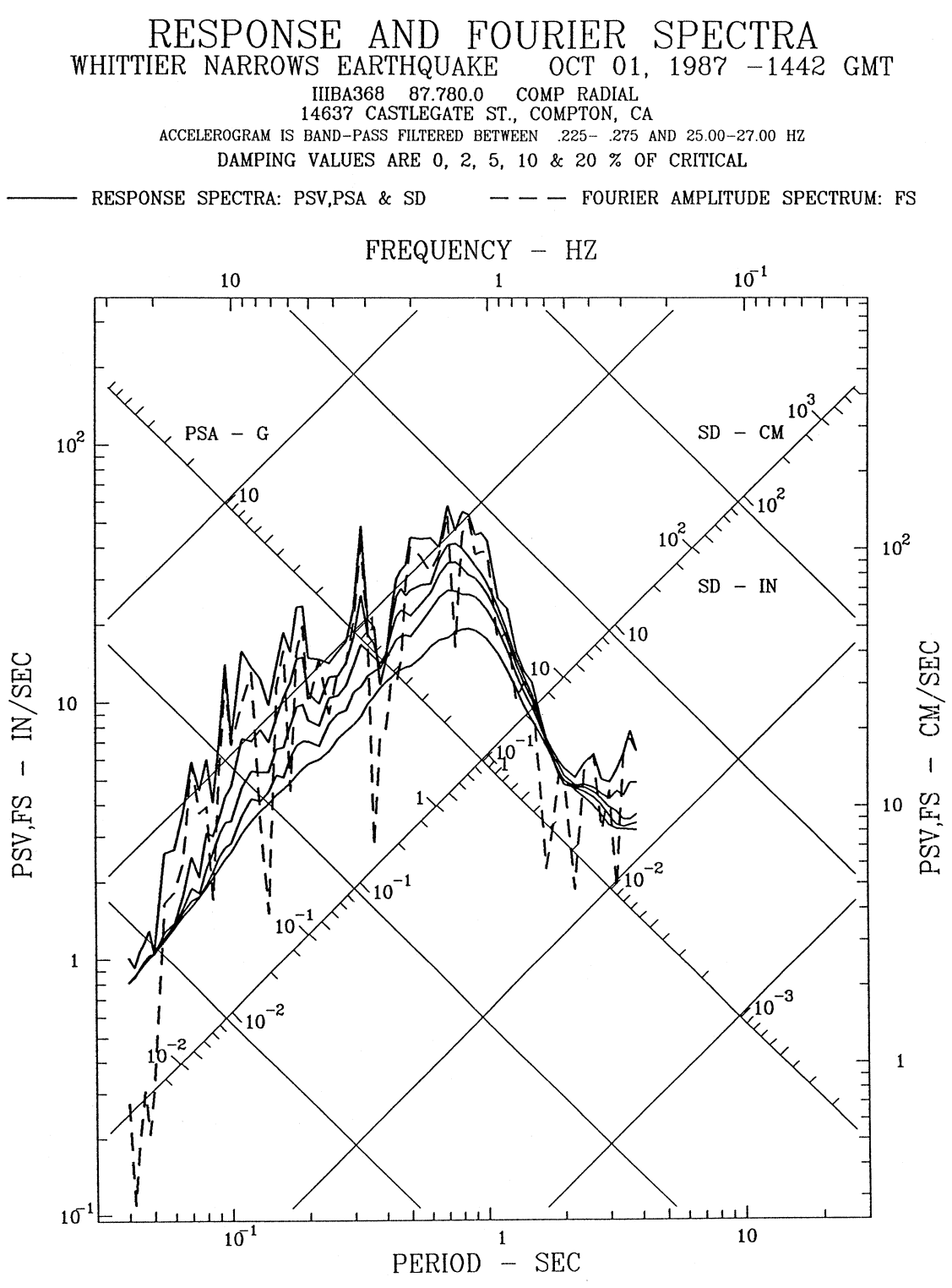
RESPONSE AND FOURIER SPECTRA
WHITTIER NARROWS EARTHQUAKE OCT 01, 1987 -1442 GMT
IIIBA368 87.780.0 COMP RADIAL
14637 CASTLEGATE ST., COMPTON, CA
ACCELEROGRAM IS BAND-PASS FILTERED BETWEEN .225- .275 AND 25.00-27.00 HZ
DAMPING VALUES ARE 0, 2, 5, 10 & 20 % OF CRITICAL
RESPONSE SPECTRA: PSV,PSA & SD
FOURIER AMPLITUDE SPECTRUM: FS
FREQUENCY - HZ
PERIOD - SEC
PSV,FS - IN/SEC
PSV,FS - CM/SEC
PSA - G
SD - CM
SD - IN

Figure II7 - 1

WHITTIER NARROWS EARTHQUAKE OCT 01, 1987 -1442 GMT

IIIBA368 87.780.0 14637 CASTLEGATE ST., COMPTON, CA COMP RADIAL

THE UNITS USED ARE SEC FOR PRD, IN/SEC FOR FS, SV AND PSV, IN FOR SD AND G FOR SA

	DAMPING = 0 %					DAMPING = 2 %				DAMPING = 5 %				DAMPING = 10 %				DAMPING = 20 %			
PRD	FS	SD	SV	SA	PSV	SD	SV	SA	PSV	SD	SV	SA	PSV	SD	SV	SA	PSV	SD	SV	SA	PSV
.040	276-3	648-5	357-3	107-5	102-2	521-5	232-3	863-6	818-3	516-5	180-3	856-6	811-3	517-5	171-3	857-6	811-3	519-5	170-3	864-6	816-3
.042	110-3	619-5	247-3	931-6	926-3	568-5	224-3	854-6	850-3	571-5	194-3	860-6	855-3	573-5	187-3	865-6	858-3	577-5	188-3	871-6	863-3
.044	199-3	752-5	357-3	103-5	107-2	641-5	241-3	878-6	916-3	639-5	218-3	877-6	912-3	637-5	205-3	876-6	909-3	638-5	208-3	878-6	912-3
.046	308-3	855-5	442-3	107-5	117-2	722-5	306-3	906-6	987-3	710-5	256-3	891-6	969-3	705-5	229-3	887-6	962-3	704-5	230-3	886-6	962-3
.048	208-3	991-5	480-3	114-5	130-2	795-5	306-3	916-6	104-2	782-5	292-3	902-6	102-2	776-5	259-3	896-6	102-2	774-5	253-3	895-6	101-2
.050	326-3	846-5	437-3	898-6	106-2	834-5	418-3	884-6	105-2	842-5	350-3	894-6	106-2	840-5	292-3	894-6	106-2	838-5	275-3	895-6	105-2
.055	166-2	226-4	207-2	198-5	258-2	113-4	724-3	991-6	129-2	107-4	495-3	943-6	122-2	105-4	366-3	928-6	121-2	104-4	335-3	923-6	119-2
.060	183-2	254-4	228-2	187-5	266-2	133-4	744-3	983-6	140-2	132-4	589-3	973-6	138-2	130-4	474-3	964-6	136-2	128-4	391-3	951-6	134-2
.065	236-2	385-4	281-2	242-5	373-2	183-4	113-2	115-5	177-2	164-4	867-3	104-5	159-2	159-4	656-3	101-5	154-2	153-4	499-3	980-6	148-2
.070	590-2	658-4	577-2	356-5	590-2	278-4	186-2	151-5	249-2	211-4	114-2	116-5	189-2	190-4	833-3	104-5	170-2	180-4	658-3	996-6	161-2
.075	370-2	546-4	396-2	257-5	458-2	249-4	147-2	118-5	208-2	216-4	119-2	104-5	181-2	210-4	103-2	100-5	176-2	209-4	830-3	102-5	175-2
.080	394-2	768-4	481-2	318-5	603-2	394-4	208-2	165-5	309-2	286-4	151-2	121-5	225-2	249-4	129-2	104-5	196-2	243-4	103-2	104-5	191-2
.085	170-2	555-4	310-2	203-5	410-2	407-4	233-2	151-5	301-2	350-4	188-2	132-5	259-2	295-4	160-2	114-5	218-2	281-4	122-2	107-5	208-2
.090	566-2	103-3	683-2	338-5	722-2	510-4	283-2	169-5	356-2	436-4	234-2	145-5	304-2	358-4	191-2	122-5	250-2	323-4	138-2	110-5	226-2
.095	121-1	213-3	137-1	627-5	141-1	653-4	393-2	193-5	432-2	516-4	279-2	153-5	341-2	411-4	209-2	126-5	272-2	370-4	148-2	113-5	245-2
.100	684-2	115-3	696-2	305-5	722-2	755-4	452-2	203-5	474-2	548-4	314-2	149-5	344-2	450-4	222-2	128-5	283-2	414-4	156-2	117-5	260-2
.110	981-2	278-3	155-1	610-5	159-1	126-3	564-2	280-5	722-2	823-4	406-2	188-5	470-2	634-4	281-2	144-5	362-2	540-4	171-2	125-5	308-2
.120	131-1	263-3	133-1	485-5	138-1	135-3	594-2	249-5	707-2	104-3	430-2	197-5	543-2	808-4	300-2	155-5	423-2	659-4	199-2	130-5	345-2
.130	341-2	256-3	108-1	402-5	124-1	163-3	629-2	256-5	787-2	111-3	468-2	176-5	537-2	856-4	325-2	138-5	414-2	783-4	216-2	130-5	378-2
.140	151-2	218-3	782-2	295-5	978-2	156-3	664-2	214-5	701-2	120-3	524-2	167-5	538-2	101-3	372-2	139-5	451-2	903-4	245-2	131-5	405-2
.150	114-1	329-3	136-1	387-5	138-1	208-3	655-2	247-5	871-2	157-3	485-2	186-5	658-2	125-3	412-2	151-5	524-2	105-3	272-2	132-5	439-2
.160	159-1	476-3	174-1	493-5	187-1	269-3	922-2	279-5	105-1	170-3	631-2	180-5	669-2	131-3	468-2	140-5	513-2	118-3	299-2	130-5	463-2
.170	454-2	425-3	141-1	390-5	157-1	324-3	110-1	298-5	120-1	220-3	796-2	205-5	815-2	166-3	534-2	160-5	613-2	133-3	347-2	130-5	490-2
.180	158-1	669-3	229-1	548-5	234-1	423-3	133-1	347-5	148-1	276-3	932-2	231-5	965-2	195-3	604-2	168-5	682-2	151-3	376-2	132-5	526-2
.190	198-1	710-3	223-1	522-5	235-1	452-3	135-1	333-5	150-1	297-3	966-2	223-5	983-2	213-3	642-2	161-5	705-2	168-3	396-2	132-5	554-2
.200	987-2	473-3	147-1	313-5	149-1	348-3	112-1	236-5	109-1	270-3	840-2	185-5	847-2	224-3	590-2	155-5	704-2	184-3	393-2	132-5	579-2
.220	147-1	515-3	144-1	282-5	147-1	347-3	826-2	190-5	990-2	284-3	595-2	156-5	811-2	237-3	506-2	138-5	676-2	210-3	390-2	127-5	601-2
.240	902-2	541-3	121-1	249-5	142-1	479-3	103-1	222-5	126-1	398-3	816-2	187-5	104-1	316-3	594-2	152-5	827-2	247-3	399-2	123-5	645-2
.260	131-1	652-3	148-1	256-5	157-1	526-3	116-1	207-5	127-1	440-3	901-2	178-5	106-1	376-3	693-2	153-5	908-2	299-3	472-2	127-5	724-2
.280	141-1	767-3	166-1	259-5	172-1	634-3	111-1	217-5	142-1	521-3	849-2	181-5	117-1	414-3	757-2	149-5	929-2	345-3	546-2	130-5	773-2
.300	206-1	110-2	203-1	323-5	230-1	856-3	155-1	255-5	179-1	665-3	122-1	199-5	139-1	524-3	910-2	159-5	110-1	392-3	600-2	128-5	820-2
.320	414-1	246-2	480-1	638-5	484-1	132-2	260-1	346-5	259-1	854-3	160-1	227-5	168-1	587-3	102-1	159-5	115-1	449-3	646-2	127-5	882-2
.340	191-1	113-2	206-1	259-5	209-1	994-3	170-1	230-5	184-1	854-3	133-1	198-5	158-1	688-3	965-2	164-5	127-1	536-3	659-2	135-5	990-2
.360	274-2	112-2	157-1	230-5	196-1	966-3	129-1	198-5	169-1	856-3	109-1	180-5	149-1	757-3	875-2	162-5	132-1	608-3	699-2	138-5	106-1
.380	729-2	711-3	124-1	131-5	118-1	816-3	106-1	151-5	135-1	858-3	958-2	159-5	142-1	826-3	903-2	158-5	137-1	689-3	793-2	141-5	114-1
.400	772-2	913-3	120-1	151-5	144-1	954-3	110-1	159-5	150-1	977-3	105-1	164-5	153-1	935-3	100-1	160-5	147-1	767-3	882-2	142-5	120-1
.420	120-1	149-2	182-1	223-5	222-1	136-2	157-1	206-5	204-1	124-2	130-1	189-5	186-1	108-2	117-1	169-5	161-1	838-3	984-2	141-5	125-1
.440	118-1	210-2	253-1	288-5	300-1	180-2	203-1	248-5	256-1	151-2	165-1	210-5	215-1	123-2	137-1	175-5	175-1	919-3	109-1	141-5	131-1
.460	148-1	239-2	281-1	300-5	327-1	202-2	231-1	253-5	275-1	166-2	190-1	213-5	227-1	132-2	152-1	174-5	181-1	980-3	117-1	139-5	134-1
.480	293-1	261-2	341-1	300-5	342-1	198-2	255-1	228-5	259-1	169-2	192-1	198-5	222-1	139-2	157-1	166-5	182-1	105-2	123-1	134-5	137-1
.500	405-1	348-2	429-1	369-5	437-1	216-2	282-1	231-5	272-1	171-2	214-1	183-5	215-1	143-2	162-1	157-5	180-1	110-2	127-1	130-5	138-1
.550	366-1	378-2	434-1	332-5	432-1	249-2	293-1	220-5	285-1	210-2	249-1	186-5	240-1	178-2	201-1	162-5	203-1	131-2	137-1	128-5	149-1
.600	320-1	416-2	437-1	307-5	436-1	274-2	300-1	203-5	287-1	254-2	268-1	189-5	266-1	218-2	218-1	167-5	228-1	157-2	154-1	131-5	165-1
.650	378-1	416-2	417-1	261-5	402-1	372-2	364-1	234-5	359-1	324-2	306-1	207-5	314-1	263-2	240-1	172-5	254-1	181-2	182-1	129-5	175-1
.700	543-1	648-2	577-1	350-5	581-1	455-2	400-1	247-5	409-1	386-2	341-1	211-5	347-1	302-2	282-1	170-5	271-1	198-2	207-1	122-5	178-1

Figure II7 - 2

IIIBA368 87.780.0 14637 CASTLEGATE ST., COMPTON, CA COMP RADIAL

THE UNITS USED ARE SEC FOR PRD, IN/SEC FOR FS, SV AND PSV, IN FOR SD AND G FOR SA

		DAMPING = 0 %				DAMPING = 2 %				DAMPING = 5 %				DAMPING = 10 %				DAMPING = 20 %			
PRD	FS	SD	SV	SA	PSV	SD	SV	SA	PSV	SD	SV	SA	PSV	SD	SV	SA	PSV	SD	SV	SA	PSV
.75	164-1	557-2	463-1	263-5	467-1	495-2	422-1	234-5	414-1	417-2	371-1	199-5	349-1	320-2	304-1	157-5	269-1	223-2	219-1	114-5	187-1
.80	458-1	700-2	550-1	290-5	550-1	502-2	425-1	209-5	394-1	422-2	372-1	177-5	332-1	332-2	307-1	142-5	260-1	244-2	223-1	111-5	192-1
.85	516-1	721-2	530-1	265-5	533-1	496-2	409-1	183-5	367-1	421-2	360-1	157-5	311-1	352-2	298-1	134-5	261-1	260-2	219-1	106-5	192-1
.90	375-1	640-2	452-1	209-5	447-1	486-2	373-1	160-5	339-1	433-2	331-1	144-5	302-1	364-2	279-1	124-5	254-1	271-2	209-1	991-6	189-1
.95	384-1	690-2	458-1	203-5	457-1	477-2	326-1	141-5	316-1	430-2	294-1	129-5	284-1	366-2	252-1	113-5	242-1	277-2	196-1	919-6	183-1
1.00	383-1	678-2	426-1	180-5	426-1	458-2	284-1	122-5	288-1	416-2	260-1	113-5	261-1	361-2	227-1	101-5	227-1	279-2	181-1	844-6	175-1
1.10	173-1	440-2	277-1	963-6	251-1	407-2	264-1	897-6	233-1	378-2	246-1	847-6	216-1	336-2	219-1	781-6	192-1	271-2	176-1	701-6	155-1
1.20	188-1	439-2	254-1	808-6	230-1	357-2	245-1	661-6	187-1	335-2	230-1	630-6	175-1	304-2	210-1	601-6	159-1	255-2	174-1	574-6	133-1
1.30	101-1	325-2	234-1	510-6	157-1	307-2	226-1	483-6	148-1	289-2	215-1	464-6	140-1	267-2	197-1	454-6	129-1	234-2	169-1	466-6	113-1
1.40	121-1	293-2	211-1	397-6	132-1	279-2	205-1	379-6	125-1	263-2	196-1	367-6	118-1	243-2	184-1	364-6	109-1	214-2	162-1	382-6	959-2
1.50	111-1	286-2	184-1	337-6	120-1	256-2	181-1	303-6	107-1	244-2	177-1	296-6	102-1	227-2	170-1	301-6	952-2	203-2	155-1	329-6	852-2
1.60	508-2	231-2	177-1	239-6	905-2	225-2	172-1	235-6	885-2	218-2	165-1	234-6	858-2	209-2	157-1	247-6	821-2	193-2	148-1	286-6	758-2
1.70	224-2	196-2	168-1	180-6	724-2	195-2	164-1	180-6	719-2	193-2	159-1	184-6	714-2	190-2	150-1	203-6	703-2	182-2	142-1	249-6	674-2
1.80	320-2	186-2	158-1	152-6	649-2	178-2	155-1	147-6	622-2	171-2	152-1	147-6	596-2	173-2	145-1	168-6	604-2	172-2	137-1	219-6	600-2
1.90	524-2	179-2	149-1	131-6	592-2	173-2	147-1	128-6	571-2	164-2	145-1	126-6	542-2	159-2	140-1	142-6	525-2	163-2	134-1	194-6	539-2
2.00	499-2	176-2	141-1	117-6	553-2	165-2	140-1	111-6	519-2	158-2	139-1	110-6	496-2	153-2	136-1	124-6	480-2	158-2	131-1	174-6	497-2
2.20	186-2	179-2	130-1	982-7	512-2	167-2	130-1	929-7	477-2	165-2	130-1	970-7	471-2	163-2	128-1	110-6	464-2	160-2	128-1	148-6	456-2
2.40	567-2	223-2	129-1	103-6	583-2	183-2	129-1	856-7	480-2	178-2	129-1	884-7	466-2	171-2	128-1	991-7	449-2	162-2	127-1	132-6	425-2
2.60	624-2	261-2	132-1	102-6	630-2	193-2	132-1	767-7	466-2	186-2	131-1	790-7	449-2	177-2	129-1	888-7	426-2	164-2	127-1	118-6	395-2
2.80	315-2	224-2	136-1	756-7	502-2	196-2	135-1	671-7	440-2	188-2	133-1	692-7	421-2	177-2	131-1	788-7	396-2	162-2	128-1	106-6	364-2
3.00	456-2	234-2	138-1	690-7	491-2	201-2	137-1	596-7	421-2	186-2	135-1	594-7	391-2	172-2	132-1	692-7	361-2	158-2	128-1	958-7	331-2
3.20	187-2	279-2	140-1	722-7	548-2	230-2	138-1	599-7	452-2	191-2	136-1	511-7	376-2	170-2	133-1	608-7	333-2	163-2	129-1	885-7	320-2
3.40	635-2	344-2	140-1	788-7	635-2	235-2	139-1	544-7	435-2	189-2	137-1	473-7	350-2	177-2	134-1	586-7	326-2	172-2	129-1	838-7	319-2
3.60	723-2	443-2	140-1	907-7	774-2	280-2	138-1	574-7	489-2	200-2	136-1	463-7	350-2	191-2	133-1	565-7	333-2	182-2	128-1	797-7	318-2
3.80	647-2	395-2	138-1	725-7	653-2	296-2	137-1	544-7	489-2	221-2	135-1	450-7	365-2	205-2	132-1	545-7	338-2	192-2	128-1	760-7	317-2

Figure II7 - 2 (cont.)

For each acceleration component, a plot showing response spectra and two pages of the tables containing most of the spectral ordinates are obtained. The plot is that of the Pseudo Relative Velocity response spectrum, PSV, together with the relative displacement spectrum, SD, and the Pseudo Acceleration spectrum, PSA, in the tripartite logarithmic plot versus period (Fig. *II*7−1). This convenient plot is made possible by the relationships between PSV, SD and PSA. The units labeled are in/sec and cm/sec for PSV, in and cm for SD, and g for PSA. The name of the earthquake, the instrument location, band-pass filtering parameters, and the damping values appear in the descriptive titles. The five continuous line plots correspond to damping values of 0, 2, 5, 10, and 20% of critical. These curves will usually be free of any confusion with the zero damped curve having the largest ordinates. The dashed curve on this plot is the Fourier amplitude spectrum, FS, calculated at the same periods as for the PSV spectra.

The two pages of tables (Fig. *II*7 − 2) contain values of the ordinates for the above plots. After the titles, these are arranged in columns, the periods (PER), Fourier amplitude spectrum (FS), and then sets of four columns containing SD, SV, SA, and PSV for all of the five damping values. The units are indicated and each value is followed by a multiplication power of 10, e.g., 731-1 is 73.1.

*II*7.6 Conclusion: Batch Model Data Processing on PC

Batch mode data processing on PC involves efficient execution of the Volume I, II and III data processing programs with minimal user's iteration and the least possible amount of required input from the user. The existing Volume I processing stage requires the input of data on the earthquake, the station and the accelerogram information for each component of each record, a step which is often repeated unnecessarily in routine processing of records from the same earthquake or station. It is thus appropriate to set up an information file for earthquake, "EQUAKE.INFO," say, and similarly one for the existing stations, "STATION.INFO," to be used with all the necessary information on files. Processing the Volume I stage will then involve only referring to the appropriate earthquake and system reference numbers each time. This will enable batch mode Volume I processing.

With the use of appropriate filters for low-pass filtering, instrument and baseline correction, the automatic determination of the cutoff frequencies for band-pass filtering and the use of appropriate integration filter, all described in detail in the previous chapters, the batch mode Volume II processing on PC is now fully developed. Currently, the Volume III processing is also available in batch mode on PC. This will thus allow one batch job for successive Volume I, II and III processing and will provide an efficient procedure for data processing of a large data load.

The results of this work, we hope, should be of value for the engineering community. Our aim has been to provide a set of guidelines for different steps in automatic digitization and data processing, for the design and efficient use of the necessary filters and an efficient prototype for digitization and data processing of a large data load. The low cost of the

modern hardware components means that desktop automatic digitization and processing of strong-motion accelerograms can be realized in every engineer's office!

ACKNOWLEDGEMENTS

We are indebted to Ms. E. Novikova for her numerous contributions to this work. She tested many of our new routines and suggested numerous improvements to increase the efficiency of operator interaction during TV program. Ms. Novikova and Dr. Todorovska critically read the manuscript and offered many useful suggestions and improvements. For all these contributions, we are most grateful.

REFERENCES

Alford, J.L., G.W. Housner and R. R. Martel (1951). Spectrum Analysis of Strong Motion Earthquakes. EERL, Calif. Inst. of Tech., Pasadena, California.

Amin, M., and A.H.S. Ang (1966). A Non-Stationary Stochastic Model for Strong- Motion Earthquakes. Structural Research Series No. 306, Univ. of Illinois, Urbana, Illinois.

Anders, E.B., J. Johnson, A.D. Lasaine, P.W. Spikes and J.T. Taylor (1964). Digital Filters. NASA Contr. Rep. CR-136, USA.

Berg, G.V. (1963). A Study of Error in Response Spectrum Analysis, Primeras Jornadas Chilenas de Sismologia and Ingenieria Antisismica, Vol. I. Asociacion Chilena de Sismologia and Ingenieria Antisismica, Santiago, Chile.

Biot, M.A. (1941). Mechanical Analyzer for the Prediction of Earthquake Stresses. Bull. Seism. Soc. Amer., **31**, 151-171.

Brady, A.G. (1966). Studies of Response to Earthquake Ground Motion. EERL, Calif. Inst. of Tech., Pasadena, California.

Edwards, A.T. and T.D. Northwood (1959). Experimental Blasting Studies on Structures. Ottawa: Hydro-Electric Power Commission of Ontario and National Research Council, Canada.

Gold, B. and C.M. Rader (1975). Digital Processing of Signals. McGraw Hill, New York, New York.

Hamming, R.W. (1962). Numerical Methods for Scientists and Engineers. McGraw-Hill, New York, New York.

Hamming, R.W. (1977). Digital Filters. Prentice Hall, New Jersey.

Housner, G.W. (1947). Ground Displacement Computed from Strong-Motion Accelerograms. Bull. Seism. Soc. Amer., **37**, 299-305.

Hudson, D.E. (1963). The measurement of Ground Motion of Destructive Earthquakes. Bull. Seism. Soc. Amer., **53(2)**, 419-437.

Hudson, D.E. (1970). Ground Motion Measurements, Earthquake Engineering, R.L. Wiegel Coordinating Editor, Chapter 6. Prentice Hall, Inc., Englewood Cliffs, New Jersey.

Hudson, D.E. (1984). Golden Anniversary Workshop on Strong Motion Seismology, March 30-31, 1983, Dept. of Civil Eng., Univ. of Southern California, Los Angeles, California.

Hudson, D.E., N.C. Nigam and M.D. Trifunac (1969). Analysis of Strong Motion Accelerograph Records. Fourth World Conf. on Earthquake Eng., Santiago, Chile.

Hudson, D.E., M.D. Trifunac, A.G. Brady and A. Vijayaraghavan (1971), Strong Motion Earthquake Accelerograms, II, Corrected Acceleration and Integrated Velocity and Displacement Curves. EERL 71-50, Calif. Inst. of Tech., Pasadena, California.

Hudson, D.E., M.D. Trifunac and A.G. Brady (1972). Analyses of Strong Motion Earthquake Accelerograms. Response Spectra, Vol. III, Part A, EERL 72-80, Calif. Inst. of Tech., Pasadena, California.

Lee, V.W. (1984). A New Fast Algorithm for the Calculation of Response of a Single-Degree-of-Freedom System to Arbitrary Load in Time. Int. J. Soil Dynamics and Earthquake Eng., **3(4)**, 191-199.

Lee, V.W. (1989). Recent Developments on Data Processing of Strong-Motion Accelerograms: Interpolation of Uniform and Non-Uniform Sampling from Digitized Data. Int. J. Soil Dynamics and Earthquake Eng., **8(4)**, 202-212.

Lee, V.W. (1990). Efficient Algorithm for Computing Displacement, Velocity, and Acceleration Responses of an Oscillator for arbitrary Ground Motion. Int. J. Soil Dynamics and Earthquake Eng., **9(6)**, 288-300.

Lee, V.W. and M.D. Trifunac (1982). EQINFOS (The strong-Motion Earthquake Data Information System). Dept. of Civil Eng., Report No. CE 82-01 , Univ. of Southern California, Los Angeles, California.

Lee, V.W. and M.D. Trifunac (1984). Current Developments in Data Processing of Strong Motion Accelerograms. Report No. CE 84-01, Dept. of Civil Eng., Univ. Southern California, Los Angeles California.

Neumann, F. (1958). Damaging Earthquake and Blast Vibrations, The Trend in Engineering, Seattle: University of Washington.

Neumann, F. (1959). Seismological Aspects of the Earthquake Engineering Problem. Proc. of the 3rd Northwest Conference of Structural Engineering, State College of Washington.

Nigam, N.C. and Jennings, P.C., (1969). Calculation of Response Spectra from Strong-Motion Earthquake Records. Bull. Seism. Soc. Amer., **59**, 909-922.

Oetken, G., T.W. Parks and H.W. Schyster (1975). New Results in the Design of Digital Interpolators. IEEE Trans. on Acoustics, Speech and Signal Processing, Vol. ASSP-23, No. 3, 301-309.

Oppenheim, A.V. and R.W. Schafer (1975). Digital Signal Processing. Prentice Hall, New Jersey.

Papoulis, A. (1977). Signal Analysis. McGraw Hill, New York.

Rabiner, L.R. and R.E. Chochiere (1975). A Novel Implementation for Narrow- Band FIR Digital Filters. IEEE Trans. on Acoustics, Speech and Signal Processing, Vol. ASSP-23, No. 5, 457-464.

Rabiner, L.R. and B. Gold (1975). Theory and Application of Digital Signal Processing. Prentice Hall, New Jersey.

Schiff, A., and J.L. Bogdanof (1967). Analysis of Current Methods of Interpreting Strong Motion Accelerograms. Bull. Seism. Soc. Amer., **57(5)**, 857-874.

Stearns, S.D. (1975). Digital Signal Analysis. Hayden Book Company, New Jersey.

Sunder, S.S. (1980). On the Standard Processing of Strong-Motion Earthquake Signals. Ph.D. Thesis, Research Report R80-38, School of Engineering, Mass. Inst. of Tech., Cambridge, Mass.

Trifunac, M.D. (1971). Zero Baseline Correction of Strong-Motion Accelerograms. Bull. Seism. Soc. Amer., **61**, 1201-1211 .

Trifunac, M.D. (1972). A Note on Correction of Strong- Motion Accelerograms for Instrument Response. Bull. Seism. Soc. Amer., **62**, 401-409.

Trifunac, M.D. (1973). Analysis of Strong Earthquake Ground Motion for Prediction of Response Spectra. Int. J. of Earthquake Eng. and Struct. Dynamics, **2(1)**, 59-69.

Trifunac, M.D. (1977). Uniformly Processed Strong Earthquake Ground Accelerations in the Western United States of America for the Period from 1933 to 1971 : Pseudo

Relative Velocity Spectra and Processing Noise. Dept. of Civil Eng., Report No. CE 77-04, Univ. of Southern California, Los Angeles, California.

Trifunac, M.D. and J.G. Anderson (1978). Preliminary Models for Scaling Relative Velocity Spectra. Dept. of Civil Eng. Report No. 78-05, Univ. Southern California, Los Angeles, California.

Trifunac, M.D. and D.E. Hudson (1970). Laboratory Evaluation and Instrument Corrections of Strong Motion Accelerographs. EERL 70-04, Calif. Inst. of Tech., Pasadena, California.

Trifunac, M.D., and V.W. Lee (1973). Routine Computer Processing of Strong Motion Accelerograms. Earthquake Eng. Res. Lab., EERl 73-03, Calif. Inst. of Tech., Pasadena, California.

Trifunac, M.D., and V.W. Lee (1974). A Note on the Accuracy of Computed Ground Displacements from Strong Motion Accelerograms. Bull. Seism. Soc. Amer., **64**, 1209-1219.

Trifunac, M.D., and V.W. Lee (1978). Uniformly Processed Strong Earthquake Ground Accelerations in the Western United States of America for the Period from 1933 to 1971: Corrected Acceleration, Velocity and Displacement Curves. Dept. of Civil Engr., Report No. CE 78-01, Univ. of Southern California, Los Angeles, California.

Trifunac, M.D. and V.W. Lee (1979). Automatic Digitization and Processing of Strong Motion Accelerograms, I and II. Dept. of Civil Eng., Report No. 79-15, Univ. of Southern California, Los Angeles, California.

Trifunac, M.D., F.E. Udwadia and A.G. Brady (1971). High Frequency Errors and Instrument Corrections of Strong Motion Accelerograms. Earthquake Eng. Res. Lab., EERL 71-05, Calif. Inst. of Tech., Pasadena.

Trifunac, M.D., F.E. Udwadia and A.G. Brady (1973). Analysis of Errors in Digitized Strong Motion Accelerograms. Bull. Seism. Soc. Amer., **63**, 157-187.